Fall 2011

# Wireless sensor network for health monitoring

Jin Soo Choi
*New Jersey Institute of Technology*

# Copyright Warning & Restrictions

The copyright law of the United States (Title 17, United States Code) governs the making of photocopies or other reproductions of copyrighted material.

Under certain conditions specified in the law, libraries and archives are authorized to furnish a photocopy or other reproduction. One of these specified conditions is that the photocopy or reproduction is not to be "used for any purpose other than private study, scholarship, or research." If a, user makes a request for, or later uses, a photocopy or reproduction for purposes in excess of "fair use" that user may be liable for copyright infringement,

This institution reserves the right to refuse to accept a copying order if, in its judgment, fulfillment of the order would involve violation of copyright law.

Please Note: The author retains the copyright while the New Jersey Institute of Technology reserves the right to distribute this thesis or dissertation

Printing note: If you do not wish to print this page, then select "Pages from: first page # to: last page #" on the print dialog screen

## ABSTRACT

## WIRELESS SENSOR NETWORK FOR HEALTH MONITORING

**by**
**Jin Soo Choi**

Wireless Sensor Network (WSN) is becoming a significant enabling technology for a wide variety of applications. Recent advances in WSN have facilitated the realization of pervasive health monitoring for both homecare and hospital environments. Current technological advances in sensors, power-efficient integrated circuits, and wireless communication have allowed the development of miniature, lightweight, low-cost, and smart physiological sensor nodes. These nodes are capable of sensing, processing, and communicating one or more vital signs. Furthermore, they can be used in wireless personal area networks (WPANs) or wireless body sensor networks (WBSNs) for health monitoring. Many studies were performed and/or are under way in order to develop flexible, reliable, secure, real-time, and power-efficient WBSNs suitable for healthcare applications. To efficiently control and monitor a patient's status as well as to reduce the cost of power and maintenance, IEEE 802.15.4/ZigBee, a communication standard for low-power wireless communication, is developed as a new efficient technology in health monitoring systems. The main contribution of this dissertation is to provide a modeling, analysis, and design framework for WSN health

monitoring systems. This dissertation describes the applications of wireless sensor networks in the healthcare area and discusses the related issues and challenges. The main goal of this study is to evaluate the acceptance of the current wireless standard for enabling WSNs for healthcare monitoring in real environment. Its focus is on IEEE 802.15.4/ZigBee protocols combined with hardware and software platforms. Especially, it focuses on Carrier Sense Multiple Access with Collision Avoidance mechanism (CSMA/CA) algorithms for reliable communication in multiple accessing networks. The performance analysis metrics are established through measured data and mathematical analysis.

This dissertation evaluates the network performance of the IEEE 802.15.4 un-slotted CSMA/CA mechanism for different parameter settings through analytical modeling and simulation. For this protocol, a Markov chain model is used to derive the analytical expression of normalized packet transmission, reliability, channel access delay, and energy consumption. This model is used to describe the stochastic behavior of random access and deterministic behavior of IEEE 802.15.4 CSMA/CA. By using it, the different aspects of health monitoring can be analyzed. The sound transmission of heart beat with other smaller data packet transmission is studied. The obtained theoretical analysis and simulation results can be used to estimate and design the high performance health monitoring systems.

# WIRELESS SENSOR NETWORK FOR HEALTH MONITORING

**by**
**Jin Soo Choi**

**A Dissertation**
**Submitted to the Faculty of**
**New Jersey Institute of Technology**
**in Partial Fulfillment of the Requirements for the Degree of**
**Doctor of Philosophy in Electrical Engineering**

**Department of Electrical and Computer Engineering**

**January 2012**

.

**APPROVAL PAGE**

**WIRELESS SENSOR NETWORK FOR HEALTH MONITORING**

**Jin Soo Choi**

---

Dr. Mengchu Zhou, Dissertation Advisor — Date
Professor of Electrical and Computer Engineering, NJIT

---

Dr. William N. Carr, Committee Member — Date
Professor Emeritus of Electrical and Computer Engineering, NJIT

---

Dr. Sui-hoi E. Hou, Committee Member — Date
Associate Professor of Electrical and Computer Engineering, NJIT

---

Dr. Yun-Qing Shi, Committee Member — Date
Professor of Electrical and Computer Engineering, NJIT

---

Dr. Zhiming Ji, Committee Member — Date
Associate Professor of Mechanical and Industrial Engineering, NJIT

## BIOGRAPHICAL SKETCH

**Author:** Jin Soo Choi

**Degree:** Doctor of Philosophy

**Date:** January 2012

**Undergraduate and Graduate Education:**

- Doctor of Philosophy in Electrical Engineering,
  New Jersey Institute of Technology, Newark, NJ, 2012

- Master of Science in Electrical Engineering,
  New Jersey Institute of Technology, Newark, NJ, 2003

- Bachelor of Science in Electrical Engineering,
  Hannam University, Daejon, Republic of Korea, 2000

**Major:** Electrical Engineering

**Presentations and Publications:**

Jin Soo Choi and Mengchu Zhou, "Recent Advances in Wireless Sensor Networks for Health Monitoring," International Journal of Intelligent Control and Systems, Vol. 15, No. 4, pp. 49-58, December 2010.

Jin Soo Choi and Mengchu Zhou, "Performance analysis of ZigBee-based body sensor networks," IEEE International Conference on Systems Man and Cybernetics (SMC), Istanbul, Turkey, pp. 2427-2433, October 2010.

Jin Soo Choi and Mengchu Zhou, “Design Issue in ZigBee-based Sensor Network for Healthcare Applications,” IEEE International Conference on Networking, Sensing and Control, Beijing, China, ID:ICNSC12-98), April 11-14, 2012.

Jin Soo Choi and William N. Carr, “Biomedical auscultation monitoring system,” 4th Annual New Jersey Biomedical Engineering Showcase, NJ, March 2007.

Ravindra N.M., Preethi Ganapathy and Jin Soo Choi, “Energy gap-refractive index relations in semiconductors – An overview,” An International Research Journal– Infrared Physics and Technology, Volume 50, Issue 1, pp. 21-29, March 2007.

To my beloved family

## ACKNOWLEDGEMENT

I would like to express my sincere appreciation to my advisor, Dr. MengChu Zhou, for his constant help, encouragement, guidance, patience and support through this dissertation research. His unique view points and wide knowledge stimulate many ideas presented in this dissertation.

I would like to express my great appreciation to my committee members Professor William N. Carr, Professor Sui-hoi E Hou, Professor Zhiming Ji and Professor Yun-Qing Shi for reviewing my dissertation and sharing their time and expertise.

I would also like to thank my friends and colleagues in the Discrete Event System Laboratory for their assistance, collaboration and friendship.

I wish to thank the Office of Graduate Studies for their help. I also thank the faculty and staff of the Department of Electrical and Computer Engineering and the Office of International Students and Faculty for their kind support.

Finally, my sincere gratitude goes to my parents, my wife, Jeong Min Lee and my daughter and son, Ashley and Ryan whose endless love and encouragement enabled me to complete this work.

## TABLE OF CONTENTS


| Chapter | Page |
|---|---|
| 1 INTRODUCTION……..……. | 1 |
| 1.1 Background and Motivation ……..……..... | 1 |
| 1.2 Goal and Objective of this Dissertation …….. | 2 |
| 1.3 Organization of this Dissertation …… | 3 |
| 2 OVERVIEW OF WIRELESS SENSOR NETWORKS ……..... | 5 |
| 2.1 Basic Components in Wireless Sensor Nodes …… | 5 |
| 2.2 Wireless Sensor Networks in Health Monitoring …….…….. | 6 |
| 2.3 Technologies for WSN in Health Monitoring ……...…….. | 8 |
| 2.3.1 ZigBee ……..…….. | 9 |
| 2.3.2 Bluetooth ……..…….. | 10 |
| 2.3.3 Ultra Wide Band (UWB) …….. | 11 |
| 2.3.4 Wireless Fidelity (WIFI) ……... | 12 |
| 2.4 Technology Comparison ……...…….. | 12 |
| 3 LITERATURE REVIEW …….. | 16 |
| 3.1 Review of Wireless Sensor Networks in Health Monitoring …….. | 16 |
| 3.2 Research Issues …….. | 24 |
| 3.2.1 Reliability ……..... | 24 |
| 3.2.2 Power ……...……..... | 25 |
| 3.2.3 Portability ……..... | 26 |
| 3.2.4 Network Interference …… | 26 |
| 3.2.5 Real Time and Continuous Monitoring …… | 27 |
| 3.3 Limitation and Challenges in WSN ……...……..... | 27 |

**TABLE OF CONTENTS**
**(Continued)**

**Chapter** **Page**


4 PERFORMANCE ANALYSIS OF ZIGBEE-BASED SENSOR NETWORKS ….. 30

4.1 Introduction ……. 30

4.2 General IEEE 802.15.4 MAC Protocol ……... 31

4.3 Analysis of Un-slotted CSMA/CA ……..……... 37

4.3.1 Packet Transmission Time and Delay …….…….. 37

4.3.2 End-to-End Delay ……. 44

4.3.3 Packet Delivery Ratio …….. 46

4.4 Simulation Environment ……. 48

4.5 Simulation Results and Discussion …… 50

4.5.1 Effects of Numbers of Network Devices …….. 50

4.5.2 Effects of Data Payload Size ……. 52

4.6 Summary ……. 55

5 MODELING AND OPTIMIZATION OF UN-SLOTTED IEEE 802.15.4 …….. 57

5.1 Introduction ……. 57

5.2 Related Work ……...……... 59

5.3 Markov Chain Model Analysis for Un-slotted CSMA/CA …….…… 61

5.3.1 Steady State Probability Analysis of Markov Chain Model ……. 66

5.4 Performance Analysis ……. 72

5.4.1 Throughput ……...……. 75

5.4.2 Reliability ……...……... 80

5.4.3 Delay Analysis …….. 83

5.4.4 Energy Consumption ……. 89

**TABLE OF CONTENTS**
**(Continued)**

**Chapter** **Page**


5.5 Impacts of IEEE 802.15.4 MAC Parameters ……... 92

5.5.1 Impact of *macMinBE* Value on Reliability and Delay ……... 93

5.5.2 Impact of *macMaxCSMABackoffs* Value on Reliability and Delay ……... 95

5.5.3 Impact of *macMaxFrameRetries* Value on Reliability and Delay ……. 98

6 RECONFIGURATION OF UN-SLOTTED IEEE 802.15.4 MAC PARAMETERS FOR ECG MONITORING ……...……. 101

6.1 Introduction ……...…….. 101

6.2 Simulation Environment ……. 102

6.3 Simulation Results and Discussion ……..……... 104

6.3.1 Effects of Packet Transmission Interval ……... 104

6.3.2 Effect of *macMinBE* …….. 108

6.3.3 Effect of *macMaxBE* ……. 110

6.3.4 Effect of *macMaxCSMABackoffs* …….. 112

6.3.5 Effect of *macMaxFrameRetries* …… 115

6.4 Summary ……..…… 118

7 PRIORITY PACKET TRANSMISSION FOR HEALTH MONITORING SYSTEM…….…….... 119

7.1 Introduction ……. 119

7.2 Heart Beat Sound Monitoring System …… 119

7.2.1 Software Architecture ……... 125

7.2.2 Hardware Architecture …….. 127

7.3 Proposed MAC Protocol for Priority Packet Transmission ……..….. 129

7.3.1 Proposed Method for Network Devices to be Associated with PAN ….. 129

**TABLE OF CONTENTS**
**(Continued)**

**Chapter** **Page**

7.3.2 Adaptive MAC Parameter for Priority Data ……. 134

7.4 Simulation Results and Discussion ……. 135

7.5 Summary ……..…… 138

8 CONCLUSIONS AND FUTURE WORK …… 140

8.1 Conclusions …..……...…… 140

8.2 Summary of Contributions ……. 141

8.3 Recommendations for Future Research …….. 145

REFERENCES ……... 147

## LIST OF TABLES


| Table | | Page |
|---|---|---|
| 2.1 | Comparison of Bluetooth, UWB, ZigBee, and WI-FI Protocols ……... | 15 |
| 3.1 | Some Current Wireless Physiological Monitoring Systems …….. | 22 |
| 4.1 | Simulation Parameters ……... | 49 |
| 5.1 | Average Number of Back-off Attempts for Different Network Size …… | 88 |
| 5.2 | CC2430 Power Level Specifications ……. | 90 |
| 6.1 | Simulation Parameters ……... | 103 |
| 7.1 | Summary of the Test Results ……. | 125 |
| 7.2 | Overview of Hardware ……... | 128 |
| 7.3 | Reserved Fields in FCF …….. | 132 |
| 7.4 | Simulation Scenario, Setup and Parameters …….. | 137 |

## LIST OF FIGURES


| Figure | | Page |
|---|---|---|
| 2.1 | Basic components of a typical wireless sensor node ……. | 5 |
| 2.2 | A typical wireless sensor network infrastructure for healthcare applications ….. | 8 |
| 4.1 | IEEE 802.15.4 CSMA-CA protocol …….. | 32 |
| 4.2 | Duration for one data frame by LIFS with ACK ……... | 36 |
| 4.3 | Frame transmission sequence of IEEE 802.15.4 ……... | 38 |
| 4.4 | Impact of $L_{payload}$ and $N$ on the average number of back-off attempts ….....…… | 41 |
| 4.5 | Total back-off time with various payload size and $N$……. | 44 |
| 4.6 | Impact of payload size and $N$ on average end-to-end delay ……...….... | 45 |
| 4.7 | Impact of payload size and $N$ on average Packet delivery ratio ……...……. | 47 |
| 4.8 | 3D simulation scenario …….. | 48 |
| 4.9 | PDR of IEEE 802.15.4 star network topology with a different number of nodes . | 51 |
| 4.10 | Average End-To-End delay of IEEE 802.15.4 star network topology with a different number of nodes …….. | 52 |
| 4.11 | Number of data packet sent with varied data payload size in a same network area ……. | 53 |
| 4.12 | Number of data packets dropped with varied data payload size in a same network area ……... | 54 |
| 4.13 | Average End-To-End delay with varied data payload size in a same network area ……..……... | 55 |
| 5.1 | Markov chain model for un-slotted CSMA/CA algorithm for IEEE 802.15.4 ….. | 61 |
| 5.2 | Comparison of $\alpha$ and $\tau$ with nodes and different packet arrival rate ……. | 74 |
| 5.3 | Comparison of the average number of back-off attempts average, total back-off time and throughput with network size …….. | 78 |
| 5.4 | $P_{CAF}$ and $P_{CRT}$ vs. the number of nodes and different packet arrival rate…… | 81 |

## LIST OF FIGURES
## (Continued)


| Figure | | Page |
|---|---|---|
| 5.5 | Reliability vs. the number of nodes and packet arrival rate ……..…. | 82 |
| 5.6 | Delay vs. the number of nodes and packet arrival rate ……..…… | 89 |
| 5.7 | Energy consumption vs. the number of nodes and packet arrival rate …….. | 92 |
| 5.8 | Impact of *macMinBE* on reliability …… | 94 |
| 5.9 | Impact of *macMinBE* on average delay ……. | 95 |
| 5.10 | Impact of *macMaxCSMABackoffs* on reliability …… | 97 |
| 5.11 | Impact of *macMaxCSMABackoffs* on average delay ……. | 98 |
| 5.12 | Impact of *macMaxFrameRetries* on reliability …….. | 99 |
| 5.13 | Impact of *macMaxFrameRetries* on average delay ……... | 100 |
| 6.1 | 3D simulation scenario …….. | 102 |
| 6.2 | Performance with different packet periods …… | 107 |
| 6.3 | Performance with different *macMinBE* ……. | 109 |
| 6.4 | Performance with different *macMaxBE* ……. | 111 |
| 6.5 | Performance with different *macMaxCSMABackoffs* ……. | 114 |
| 6.6 | Performance with different *macMaxFrameRetries* ……... | 117 |
| 7.1 | Overall biomedical sensor system ……. | 120 |
| 7.2 | Conversion of heart beat sounds to digital bits …….. | 121 |
| 7.3 | Whole data packet for heart beat sound ……. | 122 |
| 7.4 | Captured data packets on air by Packet Sniffer ……. | 124 |
| 7.5 | Capture of heart beat from 802.15.4/ZigBee end device ……... | 125 |
| 7.6 | Double buffer management for transmitting and receiving data ……... | 127 |
| 7.7 | Modified association network flow for priority data transmission …… | 130 |

## LIST OF FIGURES
## (Continued)

**Figure** **Page**

7.8 Frame Control Field (FCF) …… 131

7.9 Proposed algorithm flow for priority packet transmission …… 133

7.10 Simulation scenario …… 135

7.11 Comparison of default and adaptive network scenario ……. 138

## LIST OF TERMS AND SYMBOLS

| | |
|---|---|
| ACK | Acknowledgement |
| ADC | Analog-to-digital converter |
| *b* | Number of back-off attempt periods |
| BE | Back-off exponents |
| $\boldsymbol{B_M}$ | *macMaxBE* (3 ~ 8) |
| $\boldsymbol{B_m}$ | *macMinBE* (0 ~ 8) |
| CCA | Clear Channel Assessment |
| CSMA/CA | Carrier Sense Multiple Access with Collision Avoidance mechanism |
| CDMA | Code Division Multiple Access |
| $\boldsymbol{C_{max}}$ | Most effective data capacity |
| $\boldsymbol{C_{PHY}}$ | IEEE 802.15.4 data capacity (*250kbps*) |
| ***CW*** | Contention Window length |
| DAC | Digital to Analogue Converter |
| DMA | Direct Memory Access |
| ECG | Electrocardiogram |
| EEG | electroencephalography |
| EMG | electromyography |
| FCF | Frame Control Field |
| FFD | Full Function Device |
| ISM | Industrial, Scientific and Medical Band |
| LIFS | A long inter-frame spacing |
| MAC | Medium Access Control |

## LIST OF TERMS AND SYMBOLS (Continued)

| | |
|---|---|
| MCU | Microcontroller unit |
| MHR | MAC header |
| MPDU | MAC protocol data unit |
| MSDU | MAC service data unit |
| ms | millisecond |
| $\boldsymbol{m}$ | *macMaxCSMABackoffs* (0 ~ 5) |
| NACK | No Acknowledgement |
| $\boldsymbol{NB}$ | The number of back-offs with initial value of zero |
| PAN | Personal area network |
| PC | Personnel Computer |
| $\boldsymbol{P_C}$ | Probability of channel being idle |
| $\boldsymbol{P_S}$ | Probability of access the channel |
| PDA | Personnel Digital Assistant |
| PDR | Packet delivery ratio |
| PER | Packet error rate |
| PHY | Physical |
| PPDU | physical layer protocol data unit |
| PPG | Photoplethysmography |
| PWM | Pulse width modulation |
| $\boldsymbol{q}$ | Probability of packet transmitting |
| $\boldsymbol{R}$ | *Average number of back-off* |
| $\boldsymbol{r}$ | *macMaxFrameRetries* (0~7) |
| $\boldsymbol{R_{Sam}}$ | Sampling rate |

## LIST OF TERMS AND SYMBOLS
## (Continued)

| | |
|---|---|
| RSSI | Radio Signal Strength Indicator |
| QoS | Quality of service |
| RAM | Random Access Memory |
| RIP | respiratory inductive plethysmograph |
| RF | Radio Frequency |
| RFD | Reduced Function Device |
| RFID | Radio Frequency Identification |
| SOC | Single on chip |
| SINR | Signal Interference Noise Ratio |
| SIFS | A short inter-frame spacing |
| SFD | Start of frame delimiter |
| TDMA | Time Division Multiple Access |
| $T_{IBP}$ | Initial back-off Periods |
| $T_{UB}$ | *aUnitBackoffPeriod* ($20 \cdot T_s$) |
| $T_{ACK}$ | The transmission time length of ACK frame plus an interframe spacing period ($12 \cdot T_s$) |
| $T_{CCA}$ | The period of clear channel assessments ($8 \cdot T_s$ ) |
| $T_{DATA}$ | The mean transmission period of data frame. |
| $T_{RX\_TX}$ | Turnaround time (*RX to TX*) ($12 \cdot T_s$) |
| $T_{TX\_RX}$ | Turnaround time (*TX to RX*) ($12 \cdot T_s$) |
| $T_s$ | Symbol time ($16\ \mu s$) |
| $T_{LIFS}$ | LIFS time ($40 \cdot T_s$) |
| $T_{SIFS}$ | SIFS time ($12 \cdot T_s$) |

## LIST OF TERMS AND SYMBOLS
## (Continued)

| | |
|---|---|
| $T_{pd}$ | Packet transmission delay |
| $T_{sampling}$ | Data sampling time |
| $T_{AB}$ | Average back-off times |
| $T_{ABj}$ | Sum of $T_{AB}$ of each periods |
| $T_{TB}$ | Total back-off period time |
| WBSNs | Wireless body sensor networks |
| WLAN | Wireless Local Area Network |
| WPANs | Wireless personal area networks |
| WSNs | Wireless sensor networks |

# CHAPTER 1

# INTRODUCTION

## 1.1 Background and Motivation

Wireless sensor networks (WSNs) have gained many different applications in such areas as health monitoring, industrial automation, military operations, building automation, agriculture, environmental monitoring, and multimedia [Akyildiz, *et al*., 2008; Khemapech, *et al*., 2005; Estrin, 2002; Willig, *et al*., 2005]. In particular, their application to healthcare areas received much attention recently. The design and development of wearable biomedical sensor systems for health monitoring has drawn a particular attention from both academia and industry.

Medical technology has been contributing to the population aging. All over the world, populations are aging fast. According to the U.S. Census Bureau [U.S. Census Bureau, 2010], the population aged 65 years or over is 13 percent of the USA's population. Also, this rate is expected to increase up to 20 percent in 2050. Fast growing population of old people will drive the increase in the expense of health care.

Developing patient-friendly medical equipment at a low price to provide the effective health care is a challenging task for medical service providers. Continuous real-time health monitoring based on body sensor networks (BSNs) has a great potential for the care of patients. Because of this benefit, patients can be treated in a timely fashion, before some deadly event happens by constantly monitoring the condition of patients and informing both the patients and medical professionals of any abnormalities.

BSNs consist of several distributed network devices containing sensor units, which collect and process data and communicate with other devices via a radio frequency channel [Ilyas and Mahgoub, 2005]. This wearable health monitoring system can monitor changes in a patient's vital signs and help patients maintain an optimal health status. Also, if patients wear wireless medical sensors for continuous monitoring, any emergency status detected by them can be sent to their doctors, hospitals, and other related medical entities when abnormal changes occur. This is helpful and can save the life when a patient has heart attack or treatment after surgery.

A wearable BSN can be a big part of healthcare applications. Due to the nature of medical applications, however, it has to pass the correct physical information without any data loss, error, and end-to-end delay. Also, sensor nodes should be small, light-weighted, and low-power consumed to keep good mobility of patients and to reduce the cost of healthcare services. All these issues must be resolved before wireless healthcare network application in real life.

## 1.2 Goal and Objective of this Dissertation

The main goal of this dissertation is to evaluate the acceptance of current wireless standard for enabling wireless sensor network for healthcare monitoring in real environment. This is possible by using the IEEE 802.15.4/ZigBee protocols combined with hardware and software platforms. The specific objectives are as follows.

***Objective 1: To present characteristics and challenges in WSNs for healthcare monitoring systems***

The wireless technologies such as IEEE 802.15.4/ZigBee, Bluetooth, UWB and WIFI are reviewed to help find the right wireless model of healthcare monitoring systems. Also, their comparison is made and the challenges for wireless sensor networks are indicated.

***Objective 2: To analyze IEEE 802.15.4 MAC protocol for healthcare monitoring systems***

This work analyzes and tests the transmission of real-time continuous heart beat sound by using a modified software architecture based on the IEEE 802.15.4/ZigBee. It finds the maximum capacity for real-time data and periodic small data transmission.

***Objective 3: To Analyze and propose an improved algorithm for BSN***

If real-time continuous data (i.e., heart beat) and periodic small data (i.e., human temperature) are transmitted in a same area network, data congestion or transmission error may occur. As the number of nodes in BSN increases, there is more and more transmission error based on CSMA/CA, interference and other network environments. Because Quality of Service (QoS) is critical for a healthcare monitoring system, developing a new algorithm that can improve it is very important.

## 1.3 Organization of this Dissertation

Chapter 1 presents an introduction, background and motivation of this work. The remainder of this dissertation is organized as follows. Chapter 2 introduces related wireless sensor networks in healthcare monitoring. In particular, wireless technologies such as ZigBee, Bluetooth, UWB and WIFI are presented and compared. Chapter 3 presents a review of WSNs in health monitoring and highlights the research issues to

achieve reliable WSNs. Chapter 4 explains general IEEE 802.15.4 MAC protocol and analyzes the performance of ZigBee-based BSNs. It focuses on un-slotted CSMA/CA. Chapter 5 proposes a new MAC protocol based on IEEE 802.15.4 for priority data transmission. Real experiments with a device module and simulation results are presented in Chapter 6. Finally, our conclusion for the dissertation along with the future work is given in Chapter 7.

# CHAPTER 2

# OVERVIEW OF WIRELESS SENSOR NETWORKS

## 2.1 Basic Components in Wireless Sensor Nodes

A WSN is defined as a network of wireless devices, called as nodes, which sense given objects or entities and communicate the sensed data through wireless links. The data is transmitted via a single hop or multi-hops, to a base station or PDA/cell phone, which can be connected to other networks, e.g., Internet.

A wireless sensor node consists of one or more sensors for sensing physical variables, main processing unit (a microcontroller or low-power consuming processor), analog-to-digital converter (ADC), flash memory, and RF transceiver. It often has limited power source.

Figure 2.1 presents basic components of a typical wireless sensor node. Most WSN nodes use an 8051 microcontroller as their main processing unit because of its low cost and low-power consumption as well as their limited size [Barth, *et al*., 2009; Chen and Wang, 2008; Choi, *et al*., 2007; Choi and Song, 2008; Zhang, *et al*., 2009].

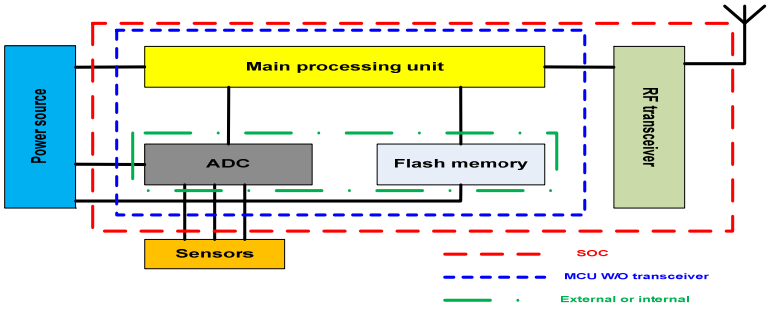


**Figure 2.1** Basic components of a typical wireless sensor node.

Some systems use the SOC (system-on-chip) such as CC2430 that includes ADC, flash memory, and RF transceiver [Chai and Yang, 2008]. Because of the small size of SOC, one can develop a small and low power-consuming sensor node. But its limitations are the low quality of ADC and small memory size. Also, some sensor nodes are developed by using a micro controller unit (MCU) such as MSP430F1611 or Atmel with external RF transceiver [Jovanov, *et al*., 2005]. Other developers [Mangharam, *et al*., 2006] use MCU with external ADC or external extra flash memory to achieve higher quality of service.

## 2.2 Wireless Sensor Network in Health Monitoring

A wireless physiological data monitoring system uses a radio channel to send real-time vital sign data from wearable biomedical sensor devices to a coordinator. Patients can wear wireless devices that sense physiological conditions and send the sensed data to their doctors in real-time.

Wireless health monitoring systems have several advantages compared to wired healthcare equipment. First, patients no longer waste waiting time to meet their doctor. Moreover, the use of wireless healthcare systems outside the hospital helps to save the healthcare cost for care providers. Also, it allows many patients to work while they are still under their doctor's care. Second, such systems can alert any medical emergency if specific vital signs change drastically, e.g., heart rate is beyond the norm.

A heart attack is the death of heart muscle from the sudden blockage of a coronary artery by a blood clot. If blood flow is not restored to the heart muscle within 20 to 40 minutes, irreversible death of the heart muscle begins to occur. Approximately one

million Americans suffer a heart attack each year. 40% of them die as a result of their heart attack [Medicinenet, 2010]. Because heart attack suddenly happens to old people or patients, their continuous and real-time monitoring of heart rates can certainly help save their lives.

Currently, most heart beat monitors, e.g., electrocardiography (ECG), are available at certain locations only, e.g., hospitals and doctor's offices. They require several wired electrodes on the skin of a patient. Medical professionals often use stethoscopes to check the heart beat sound of a patient. Unfortunately, these have critical limitation in heart beat monitoring. As mentioned before, it is highly desired to monitor heart beat continuously for unexpected heart attack. However, it is almost impossible with the existing wired medical equipment. Clearly, wireless health monitoring systems carry many advantages compared to the current wired healthcare equipment.

Figure 2.2 shows a typical wireless sensor network for healthcare applications. In this network, the data collected by the sensor nodes are transmitted using an RF channel to the base station, coordinator or PDA/cell phone, which is connected to other networks via wired or wireless connection. The whole network is controlled and monitored by a server in real-time. Depending on an application, various transmission techniques are used for wireless communication such as Wi-Fi, Bluetooth, ZigBee, UWB, and cellular networks.

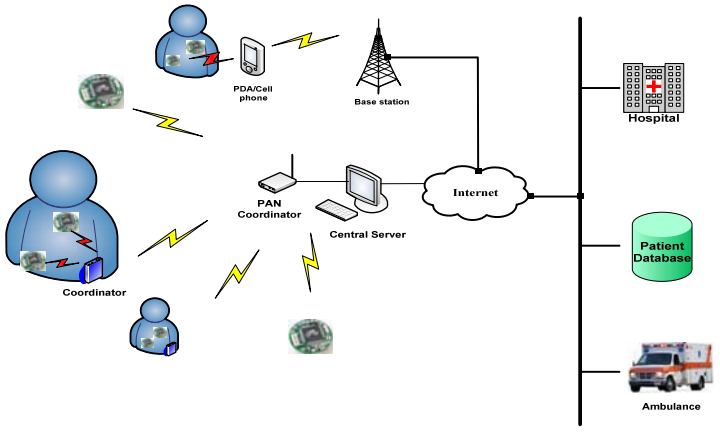


**Figure 2.2** A typical wireless sensor network infrastructure for healthcare applications.

## 2.3 Technologies for WSN in Health Monitoring

In this section three wireless standard technologies, i.e., IEEE 802.15.1 (Bluetooth), IEEE 802.15.4 (ZigBee), and IEEE 802.15.3a (UWB) for PAN, and one IEEE 802.11 a/b/g (Wi-Fi) as WLAN are briefly reviewed for their applications in wireless health monitoring systems.

WSN engage small, low-power consuming devices for collecting medical data. Their nodes sense and collect data and then communicate to a coordinator or a remote monitoring device, i.e., PDA, cell phone, or PAN coordinator directly using wireless data transfer technology.

The PAN coordinator has large-size memory and fast processors to analyze and present given data. The physical radio layer defines the operating frequency, modulation scheme, network data rate, and hardware interface among nodes and between a node and the central server. Depending on different medical objectives, such as continuous or periodic monitoring, the size of a physiological data packet, transmission range, network speed, and network size, several wireless technologies can be adopted as discussed next.

### 2.3.1 ZigBee

IEEE 802.15.4 and ZigBee are standard-based protocols that provide the network infrastructure required for WSN applications. 802.15.4 itself defines the physical and MAC layers, whereas ZigBee defines the network and application layers. They can be used to develop low data rate, low complexity, low power consumption, and low cost WSNs.

The physical layer (PHY) supports three radio bands, 2.4GHz ISM band (global) with 16 channels, 915MHz ISM band (Americas) with 10 channels, and 868MHz band (Europe) with a single channel. The data rates are 250kbps at 2.4GHz, 40kbps at 915MHz, and 20kbps at 868MHz. The MAC layer controls the access to the radio channel by using the Carrier Sense Multiple Access with Collision Avoidance (CSMA/CA) mechanism.

The IEEE 802.15.4 PHY uses direct sequence spread spectrum coding to reduce packet loss due to noise and interference. Also, it supports two PHY layer modulation options. The 868/915 MHz PHY adopts binary phase shift keying modulation, whereas the 2.4 GHz PHY uses offset quadrature phase shift keying.

A ZigBee defines three types of devices: coordinator (MAC Full Function Device-FFD), Router (MAC FFD), and end device (MAC Reduced Function Device-RFD). An FFD can serve as a network coordinator or regular device. It can communicate with any other devices. An RFD is intended for applications that are simple, such as a light switch or simple sensor device. It can communicate only with FFD.

A ZigBee coordinator is a base station node that automatically initiates the composition of the network and controls the overall network process. It needs a large

memory and high processing power. A ZigBee Router is also an FFD that links groups together and supports multi-hoping for packet transmission. It can connect with other routers and end-devices. ZigBee end devices can only communicate with an FFD. It has limited functionality.

Theoretically, ZigBee can support up to 65,536 nodes. For security, it uses 128-bit Advanced Encryption Standard (AES) encryption and authentication. The transmission range is from 10m to 75m, depending on an application's power output and environmental features. Approximately, ZigBee devices are expected to have a battery life ranging from several months to years.

### 2.3.2 Bluetooth

Bluetooth, also known as IEEE 802.15.1, is a low cost, low power wireless radio frequency standard for short-distance communication. The Bluetooth protocol stack is somewhat complicated in comparison with other IEEE networking stacks. It defines many components above the PHY and MAC layers. Some are optional, thereby complicating its overall protocol [Hackmann, 2006].

Bluetooth operates in the unlicensed 2.4 GHz ISM band, occupying 79 channels. The PHY layer uses frequency hopping spread spectrum coding to reduce interference and fading. The maximum data rate is up to 3Mbps in the enhanced data rate mode. However, the actual data payload is usually reduced due to different units' address and other header information to guarantee the compatibility among all Bluetooth sensor nodes.

Bluetooth's basic connectivity technology is the piconet based on a star network topology. It consists of one master device that communicates directly with up to seven

active slave network devices. In a given piconet, all devices are synchronized using the clock and frequency hopping pattern of the master, and slave devices communicate only with their master in the one-to-one way. Bluetooth has three power saving modes. At the hold mode, devices just process reserved slots for synchronous links. After that they enter the sleep status. At the sniff mode, a device is in the sleep mode for most of the time. It wakes up periodically in a given time for communication. At the parked mode, the device just holds the parked slave broadcast (PSB) link and turns off any other links to the master device. If the latter would like to wake up parked devices, it sends beacons to them over the PSB link [Hackmann, 2006]. A slave device at the active mode can reduce the power consumption by entering the above power saving modes.

### 2.3.3 Ultra Wide Band (UWB)

UWB (IEEE 802.15.3a) is a wireless radio technology for short-range, high-bandwidth communication at very low energy levels by using a larger portion of the radio spectrum. UWB is a latent competitor to the IEEE 802.11 standards. One of its most outstanding properties is its huge bandwidth. Wireless USB currently delivers a bandwidth of up to 480 Mbps at 3 meters and 110Mbps at 10 meters. It can support multimedia applications such as audio and video transmission in home networks. It can also be used as a wireless cable replacement of high speed serial bus such as USB 2.0 and IEEE 1394 [Lee, *et al*., 2007]. However, IEEE 802.11 is more intended for data networking such as WLAN and to replace Ethernet cables. Currently, Bluetooth is popular for small PAN-covering area applications, such as wireless mouse and cell phone set. But UWB supports much higher bandwidth than Bluetooth. It uses very low-powered, short-pulse radio signals to transfer data over a wide spectrum of frequencies.

### 2.3.4 Wireless Fidelity (WIFI)

Wi-Fi (*wireless fidelity*) is the general term for any type of IEEE 802.11 network. Examples of 802.11 networks are the 802.11a (up to 54 Mbps), 802.11b (up to 11 Mbps), and 802.11g (up to 54 Mbps). These networks are used as WLANs. Three 802.11 standards differ in their offered bandwidth, coverage, security support and, therefore, applications. 802.11a is better suited for multimedia voice, video and large-image applications in densely populated user environments. However, it provides relatively shorter range than 802.11b does, which consequently requires fewer access points for the coverage of large areas. The 802.11g standard is compatible with and may replace 802.11b, partly due to its higher bandwidth and improved security.

## 2.4 Technology Comparison

Table 2.1 [Lee, *et al*., 2007] provides a summary of the most popular wireless technologies for wireless health monitoring systems. From a general perspective, the main difference among the wireless technologies comes from the fact that they are optimized for different target applications.

Bluetooth is designed for voice application and aims to replace short distance cabling. It is good for hands free audio or multimedia file transfer with a cell phone, PDA, and any other devices. This kind of applications require just tens of meters network range with a few (1~2) Mbps network speeds.

ZigBee intends to meet the needs of sensors and control devices for short message applications. Typically, ZigBee is designed for small data packet transmission with a lightweight and simple protocol stack in network devices. Because of their small data

transmission and multi network devices, ZigBee does not need high network speed. Currently, it provides only 250 kbps data rate.

UWB provides high network speeds together with a robust communication using a broad spectrum of frequencies. It best suits for very short range networks, e.g., a few meters. It provides high network speed up to 480 Mbps.

Wi-Fi is very popular as WLAN. It is developed to replace wired Ethernet cable used in a home or office. They provide maximum data rate up to 54 Mbps in an around 50 meter range.

Clearly Bluetooth and ZigBee are suitable for low data rate applications with limited power source such as battery-operated sensor nodes or mobile devices. Low power consumption helps prolong a node's life time and reduce its size.

On the other hand, UWB and Wi-Fi would be better selections for high data rate applications such as audio/video multimedia appliance.

ZigBee is widely developed as a low-rate PAN, and its similar technology is Bluetooth. But they exhibit their different characteristics because of their originally different optimized designs. ZigBee is focused on control and automation, while Bluetooth on the replacement of wired cables among laptops, PDA’s, cell phone, and so on.

As for power consumption, a ZigBee node can operate at low power for a time period ranging from several months to 2 years from two AA batteries. But a Bluetooth node running on the same batteries would last just one week.

ZigBee networks can support a larger number of devices and a longer range between devices than Bluetooth ones. ZigBee supports the configuration of static and

dynamic star networks, a peer to peer network, and mesh network that can provide up to 65000 nodes in a network. Bluetooth allows only eights nodes in a master-slave piconet figure, i.e., it supports star networks only.

**Table 2.1** Comparison of Bluetooth, UWB, ZigBee, and WI-FI Protocols

| Standard | Bluetooth | UWB | ZigBee | Wi-Fi |
|---|---|---|---|---|
| IEEE spec. | 802.15.1 | 802.15.3a | 802.15.4 | 802.1 1a/b/g |
| Frequency band | 2.4 GHz & 2.5 GHz (Ver. 1.2) | 3.1-10.6 GHz | 868/915 MHz, 2.4 GHz | 2.4 GHz (b/g) & 5 GHz(a) |
| Max signal rate | 1 Mbps (Ver. 1.0)<br>3 Mbps (Ver. 1.2)<br>12 Mbps (Ver. 2.0) | 50-100 Mbps (480 Mbps within short range expected | 250 Kbps | 54 Mbps (802.11a)<br>11 Mbps (802.11b)<br>54 Mbps (802.11g) |
| Max data payload (bytes) | 339 (DH5) | 2044 | 102 | 2312 |
| Max overhead (bytes) | 158/8 | 42 | 31 | 58 |
| Nominal range | 10m | 20m (effective 10 m) | 10 - 100 m (effective 20 m) | 100 m (effective 50 m) |
| Nominal TX power | 0 - 10 dBm | -41.3 dBm/MHz | (-25) - 0 dBm | 15 - 20 dBm |
| Number of RF channels | 79 | (1-15) | 1/10; 16 | 14 (2.4 GHz) |
| Channel bandwidth | 1 MHz | 500 MHz - 7.5 GHz | 0.3/0.6 MHz; 2 MHz | 22 MHz |
| Modulation type | GFSK | BPSK, QPSK | BPSK (+ ASK), O-QPSK | BPSK, QPSK COFDM, CCK, M-QAM |
| Spreading | FHSS | DS-UWB, MB-OFDM | DSSS | OFDM or DSSS with CCK |
| Coexistence mechanism | Adaptive freq. hopping | Adaptive freq. hopping | Dynamic freq. selection | Dynamic freq.selection, transmit power control (802.1 1 h) |
| Basic cell | Piconet | Piconet | Star | BSS |
| Extension of the basic cell | Scatternet | Peer-to-peer | Cluster tree, Mesh (ZigBee) | ESS |
| Max number of cell nodes | 8 | 8 | > 65000 | 2007 |
| Encryption | EQ stream cipher | AES block cipher (CTR, counter mode) | AES block cipher (CTR, counter mode) | RC4 stream cipher (WEP), AES block cipher |
| Authentication | Shared secret | CBC-MAC (CCM) | CBC-MAC (ext. of CCM) | WPA2 (802.11i) |
| Data protection | 16-bit CRC | 32-bit CRC | 16-bit CRC | 32-bit CRC |
| Main applications | ·Voice applications,<br>·Replacement of short distance cable | ·Multimedia app.<br>·Healthcare app. | ·Sensors/control<br>·Remote control<br>·Large scale automation | ·Office/home networks<br>·WLAN<br>·Replace Ethernet cables |
| Pros | ·Easy synchronization of mobile devices<br>·Frequency hopping tolerant to harsh environment<br>·Dominating PAN tech. | ·High bandwidth<br>·Broad spectrum of bandwidth | ·Static network<br>·Low duty cycle<br>·Low power<br>·Network size extension<br>·Control/sensor | ·Dominating WLAN tech. |
| Cons | ·Interface with Wi-Fi<br>·Consuming medium power | ·Short range<br>·Interference | ·Low bandwidth | ·Consume high power |

*Acronyms: GFSK -Gaussian frequency SK, BPSK/QPSK-binary/quardrature phase SK, ASK-amplitude shift keying, O-QPSK-offset-QPSK, COFDM-coded OFDM, OFDM-orthogonal frequency division multiplexing, MB-OFDM- multiband OFDM, M-QAM-M-ary quadrature amplitude modulation, CCK-complementary code keying, FHSS/DSSS-frequency hopping/direct sequence spread spectrum, BSS/ESS-basic/extended service set, AES-advanced encryption standard, WEP-wired equivalent privacy, WPA-Wi-Fi protected access, CBC-MAC-cipher block chaining message authentication code, CCM-CTR with CBC-MAC, CRC-cyclic redundancy check

# CHAPTER 3

# LITERATURE REVIEW

## 3.1 Review of Wireless Sensor Networks in Health Monitoring

In this section some specific applications that have been developed or being researched for the health monitoring purpose are discussed.

In MobiCare [Rajiv, 2006], a wireless physiological measurement system (WPMS) as a MobiCare client and health care servers employs short-range Bluetooth between BSN and a BSN manager, and GPRS/UMTS cellular networks between the BSN manager and health care providers. Bluetooth is applied in this system, allowing data rate up to 1Mbps. However, it consumes high power and has limited network size (up to 7 slave nodes). Thus, it does not suit for LR-WPAN (Low-rate WPAN) as required in many healthcare applications.

Firefly is a sensor network-based rescue device used in coal mine as developed at Carnegie Mellon University [Mangharam, *et al*., 2006]. Voice streaming over WSN is implemented in this system. A TDMA based network scheduling is investigated to meet audio timing requirements. The developed hardware has a dual radio architecture for data communication and hardware based global time synchronization. This system is designed for the rescue in coal mine and has a small network size. It uses the codec chip and SD card for additional memory for sound transmission. It has high power consumption, high cost of a sensor node, and bulky size.

The CodeBlue [Malan, *et al*., 2004] projected from Harvard University explores WSN for a range of medical applications. It employs WSN in emergency medical care, hospitals and disaster area as an emergency message delivery system. With MICA motes, CodeBlue uses pulse oximetry and electrocardiogram (ECG) sensors to monitor and record blood oxygen and cardiac information from a large number of patients.

Lee *et al*. [2006] introduced a vital sign monitoring system with life emergency event detection using WSN. Vital signs such as ECG and body temperature of patients are transmitted wirelessly to the base station connected to a server or PDA.

Dagtas *et al*. [2007] presented a framework for a wireless health monitoring system within a smart home environment using ZigBee. They designed some basic processing platform that allows the heart rate and fatal failure detection. They are currently building a prototype of the proposed system using in-home ECG probes and ZigBee radio modules.

In a wireless physiological sensor system, Jovanov *et al*. [2005] intended to develop wireless sensor technology for ambulatory and implantable human psycho-physiological applications. They have developed the devices for monitoring the heart, prosthetic joints for a long period of time and other organs.

Juyng and Lee [2008] described a device access control mechanism. They proposed the reliable data transmission of physiological health data in a ZigBee based health monitoring system. They developed a wrist, chest belt, shoulder, and necklace type physiological signal devices. They use a CC2430 microcontroller as the central unit and two PDMS (Polydimethylsiloxane) electrodes for ECG, a ribbon type temperature sensor, and $SpO_2$ sensor for sensing the physiological signals. Their wrist type physiological

signal device's (W-PSD) size is of 60×65×15 mm and total system weight is 160g including one Lithium-polymer battery. A reliable data transmission mechanism is also provided by using a retransmission. They recognize the power problem for a network device. It needs small battery as its power source. It can work for 6 hours without replacement or recharging. It is small, light weight, and easy to bring, but its life time from small battery should be improved.

Chien and Tai [2006] proposed a prototype portable system to measure phonocardiography (PCG), ECG, and body temperature. They insert a capacitor-type microphone into the stethoscope's tube for PCG and develop a 3-wired lead ECG. Bluetooth transceiver and receiver modules are used with a microcontroller and PDA for wireless link between a sensing module and PDA. This system has some weak points as a health monitoring system. First, users should initiate the PDA whenever they want to measure health conditions. Thus this system is not operated automatically or in an event-driven or schedulable way. Second, this system has many sizable external circuits, wired leads for ECG, and memory unit. It is not suitable as a wearable device and thus difficult to carry, because of its heavy weight and bulky size. Third, because of their complicated and many external devices, power consumption is high. Hence, it has limitation from the viewpoints of wireless health monitoring.

Microsoft announced the HealthGear, a wearable real-time health monitoring system [Oliver and Msngas, 2006]. It consists of several physiological sensors for monitoring and analyzing the blood oxygen level ($SpO_2$), heart rate, and plethysmographic signal.

Gyselinckx, *et al*. [2007] developed a cardiac monitoring system, Human++, for ambulatory health monitoring of multi-parameters such as ECG, electroencephalography (EEG), and electromyography (EMG). This system consists of three sensor nodes in body area networks and a base station. They sample the bio-signal at 1024 Hz with a 12-bit ADC in an MSP430F149 microcontroller. The base station collects the data from each sensor node and transfers to PC or PDA through a USB interface. This system is designed to run autonomously for 3 months on two AA batteries. This system is improved in [Brown, *et al*., 2009]. A small, lightweight and low-power WPMS platform is developed for ambulatory and continuous monitoring for autonomic responses in real life applications. The Human++ UniNode uses an MSP 430 MCU, Nordic nRF24L01 2.4 GHz radio, 50 Ohm antenna, and a 165 mAh lithium-ion battery. The size of a node including battery is 20×29×9 $mm^3$. Their network topology is a star network using a static TDMA protocol. Their wearable medical sensors are developed into the chest-belt and wrist-band types. The ECG and respiration sensors (20×22×4 $mm^3$) are connected to one Human++ UniNode and integrated into a chest belt, while the skin conductance and skin temperature sensors (20×25×5 $mm^3$) are connected to a second Human++ UniNode and integrated into a wrist band. The chest node consumes 2.6 mA in full active operation, while the wrist node consumes 4 mA, resulting in a roughly battery lifetime of 63 hours and 41 hours, respectively.

Fensli, *et al*. [2005] presented a wearable ECG device for continuous monitoring. The hand-held device, which is a common PDA, collects the amplified ECG signal from a wearable device. The sensor senses ECG signals with 500 Hz sampling frequency, and this signal is digitized with 10 bit resolution. After digitizing the signal, it continuously

transmits to a hand-held device by using a modulated RF link at 869.700 MHz. This system has focused its application on the emergency situation.

Monton *et al*. [2008] presented WPMS-based patient monitoring. This BSN follows a star network technology, and is composed of two types of modules. A small device ($34\times48mm^2$), called sensor communication module (SCM) is connected to one or several sensors for sensing the health signals. SCMs transmit signals to a central processing unit ($73\times110\times25mm^3$), called personal data processing unit (PDPU) via ZigBee. PDPU is designed to connect to local external systems through: 1) UWB to connect individual devices such as PCs or PDA, 2) Wi-Fi to connect with LAN, or 3) GPRS for WAN.

The development of a belt-type wearable wireless body area network is described in [Wang, *et al*., 2009]. A photoplethysmograph (PPG) sensor and a respiratory inductive plethysmograph (RIP) sensor for pulse rate and oxygen saturation measurements are used for dynamic respiration monitoring. A WPMS node includes an MSP430F149 microcontroller as its main control unit, nRF905 as RF transceiver (915MHz), and 64 Megabit AT25DF641 as external memory. They follow a simple communication protocol. Its overall process is very simple, i.e., one sensor to one base station at a time.

Milankovic *et al*. [2006] proposed a single-hop WSN topology. Each sensor for health monitoring is directly connected to an individual PDA, which provides the connectivity to a central server. They mainly focus on the synchronization and energy efficiency issues on the single-hop communication network between network devices and PDA.

A wireless mobile healthcare application is developed to operate together with IEEE 802.15.4 enabled devices and adopted the CDMA cellular network for hospital and home environments [Yan and Chung, 2007]. Table 3.1 summarizes the major systems, their advantages, and limitations. Next, the research issues faced by the researchers of wireless sensor networks for health care monitoring as well as some existing work to address them are discussed.

**Table 3.1** Some Current Wireless Physiological Monitoring Systems

| Reference | Bio-parameter | Hardware/data rate/distance | Wireless option | Network topology | Relia-bility | Power (Lifetime) | Portability | Interference /Collision | QOS | Network size |
|---|---|---|---|---|---|---|---|---|---|---|
| Rajiv'06 | Pulse rate, ECG, temp | Algorithmic P4032 board with R5 MIPS, the RM5231 from QED, 133MHz | Bluetooth (BSN) with GPRS/UMTS Cellular network | Max 7 slave nodes to one PDA, BSN to cellular network | Un-known | Fair | Not fully developed. | Un-known | Not real time, selective data TX by user. | Small |
| Mangharam '06 | Rescue in coalmine/ Voice | CC2420/Voice codec chip/SD card for memory | TDMA | Star | Fair | Poor | Poor (bulky size) | Poor | Continu-ous real time | Extremely small (one-to-one) |
| Malan'04 | Pulse Oximeter, ECG | Berkeley MICA mote(CC1000) with PDA/ 76.8Kbps/ 20-30m | 433/ 916MHz | Ad-Hoc | Fair | Fair 2AA batteries/ Active(20mA):5~6 days Sleep(10μA): 20 years | Fair 5.7×3.2×2.2cm | Fair | Un-known | Big |
| Dagtas'07 | ECG | M16C MCU/250Kbps (802.15.4) | 802.15.4/ ZigBee | Star/Peer to Peer | Un-known | Unknown | Unknown | Un-known | Un-known | Small |
| Chien'06 | ECG , PCG, Temp | 78E516B/Bluetooth transceiver, receiver/PDA/ memory/Microphone | Bluetooth | Max 7 slave nodes to one PDA | Poor | Poor | Poor (bulky size) | Fair | Poor (Single data TX) | Small |
| Oliver'06 | ECG,$SpO_2$ | DSP/ Bluetooth transceiver, receiver/Cell phone | Bluetooth | Max 7 slave nodes to one PDA | Fair | Poor Two AAA batteries- 12 hours | Poor | | Real time | Small |
| Gyselinckx '07 | ECG, EEG, EMG | MSP430/nRF2401 | 2.4 GHz, TDMA | Star BSN to PDA | Fair | Fair 2 AA batteries 3 months | Fair | Fair | | Med |
| Brown'09 | ECG, EEG, EMG | MSP430/nRF2401 | 2.4 GHz static TDMA | Star | Fair | Fair UniNode (W/O sensor)- 7.5mW at 3V Chest node-7.7mA at 3V Wrist node-12mA at 3V | Good UniNode W battery 20×29×9 mm ECG and resp. sensor 20×22×4 mm Skin cond. Temp. 20×25×5 mm | Fair | Contin-uous real time | Small |

**Table 3.1** Some Current Wireless Physiological Monitoring Systems (Continued)

| Reference | Bio-parameter | Hardware/data rate/distance | Wireless option | Network topology | Relia-bility | Power (Lifetime) | Portability | Interference /Collision | QOS | Network size |
|---|---|---|---|---|---|---|---|---|---|---|
| Fensli'05 | ECG | ECG sensor with hand-held device | 879/700 MHz GPRS/GMS | One sensor to hand-held dev. | Fair | Unknown | Poor | Un-known | Real time | Extremely small (one-to-one) |
| Monton'08 | ECG EMG EEG | Sensor dev.- MSP430F427 ,CC2420, FRAM Central unit- AT91RM9200, GPRS modem, SD card.. | ZigBee/ UWB or Wi-Fi or GPRS | Star (BAN) | Good | Fair Li-ion battery | Good 34*48mm 73*110*25mm | Expected with Zigbee and WiFi | Un-known | Small |
| Wang'09 | PPG, RIP | MSP430F149/Ext. memory/ 3D accelerometer/Ext. ADC | 915MHz | Star | Fair | Active mode- 7.8mW Sleep mode- 860μW | Good | Un-known | Un-known | Small |
| Milenkovic '06 | ECG EMG,EEG | MSP430 with CC2420 ADXL202 | ZigBee | Star, BAN with PDA | Good | Two AA batteries | Fair | Un-known | Real time | Med |
| Yan'07 | ECG | MSP430F1611/ CC2420 4*4*0.2cm | IEEE802.15 .4/ CDMA/WL AN | Star/ CDMA(cell phone) | Good | 330μA at 1MHz(active mode) 1.1 μA (Standby mode) 0.2 μA(off mode) | Fair 4×4×0.2 cm | IEEE 802.15.4 with WLAN | Real time | Small |
| Juyng'08 | PPG, ECG, Temp. | CC2430 (sensor dev.) BIP-5000 (mobile) | ZigBee/ CDMA | Star (BAN)/ CDMA or WLAN | Good (retran smissi on) | Unknown | Good | IEEE 802.15.4 with WLAN | Delayed real time | Small |

## 3.2 Research Issues

A number of aspects should be considered when developing a miniature wireless sensor device and network for a real life health monitoring system.

### 3.2.1 Reliability

Reliability in a wireless health monitoring system is the most critical issue. Wireless health monitoring systems have to accurately transmit measured data in a timely manner to a medical doctor or other people for monitoring and analyzing the data from patients.

The reliability issue can be considered in three main stages: 1) reliable data measurement, 2) reliable data communications, and 3) reliable data analysis [Hyun, *et al*., 2008]. Stages 1 and 3 are mainly about hardware and software for sensing and analyzing the data without errors. Stage 2 needs more consideration than the other stages because it is about communication between a sensor node and coordinator or central monitoring server.

For reliable communication, Varshney [2007] proposed combined wireless networks that include WSN, ad-hoc wireless networks, cellular networks, WLAN, and satellite networks. Juyng and Lee [2008] made a reliable data transmission by using a retransmission protocol. A sensor device sends the data with ACK (Acknowledgement) request. If the sensor node doesn't receive an ACK from a mobile device or coordinator within *AckWaitDuration*, it transmits the same data frame again till it receives the ACK from the mobile device. This repeating process is limited by predefined *MaxFrame-Retries* [IEEE Std. 802.15.4-2003].

### 3.2.2 Power

The power issue is researched for all kinds of WSN applications. Since most WSN devices are battery-operated, one of the major challenges for their design is to optimize their power usage.

Some WSN applications such as passive RFID [RFID Handbook, 2003], do not require battery. Instead they use power from their reader, i.e., backscattering. However, they have limited communication range and can carry very small size data only. Other applications adopt energy harvest systems for WSNs such as solar cell [Hande, *et al*., 2007], vibration using piezoelectric devices [Roundy and Wright, 2004], temperature difference [Stark, 2006], and shoes insert [Paradiso and Starner, 2005]. But these energy harvest systems have some problems for real WSN applications, e.g., their power earning depends on their environment and they tend to be over-sized.

Van Dam and Langendoen [2003], Zheng, *et al*. [2005], Ramakrishnan, *et al*. [2004] and Miller and Vaidya [2005] presented energy efficient protocols for WSN by designing energy-efficient MAC protocols.

Omeni *et al*. [2007] proposed to control standby or sleep mode periods of sensor nodes to reduce energy consumption. They propose MAC protocol operations based on three main communication processes. A link establishment process is to associate a process to a network. A wakeup service process is to wake up a slave and master after an assigned sleep time interval. An alarm process operates only when a slave node urgently wants to send data to the master. These processes can be initiated by the master node only.

### 3.2.3 Portability

Integration of sensing components into a wireless sensor node should be conducted in a functional, robust, small, light-weight, and low-cost way. For this reason, most PANs use a small chip system, i.e., SOC, which includes a microcontroller and RF transceiver or single MCU with an external transceiver. Currently, there are some biomedical systems that suit the requirements of easy-to-wear or attach on the body for monitoring physiological signals [Barth, *et al*., 2009; Jung. *et al*., 2008]. Thus they exhibit good portability.

### 3.2.4 Network Interference

In general, a wireless link is more sensitive to interference than a wired one. In WSN environments, generally two or more different communication techniques are used together in a same network. Usually, WPANs and WLANs coexist using the same Industrial, Science and Medical (ISM) band. Therefore, they can lead to a network interference problem. Network interference or data collision problems cause intermittent network connectivity, packet loss and ultimately result in lower network throughput and increased energy expenditures [Razvan and Andreas, 2008].

The interference and coexistence problems between Bluetooth and WLAN have been presented in [Jo and Jayant, 2003; Sakal and Simunic, 2003; Howitt, 2001; Feng, *et al*., 2002]. Interference problems between IEEE 802.15.4/ZigBee and WLAN are described in [Razvan and Andreas, 2008; Kim, *et al*., 2005; Kang, *et al*., 2007; Yang and Yu, 2009; Hauer, *et al*., 2009]. BER (Bit Error Rate), PER (Packet Error Rate), RSSI (Radio Signal Strength Indicator), or SINR (Signal Interference Noise Ratio) for interference avoidance are measured and analyzed. Guo and Zhou [2010] proposed

interference prediction algorithms to explore the impacts of WiFi and microwave oven on ZigBee communications based on observations of the packet error rate.

### 3.2.5 Real Time and Continuous Monitoring

Some physiological data, such as heart beat sound, lung sound, ECG, and RIP, should be monitored continuously and in real time. Also, a biomedical sensor is imagined to operate for days, sometimes, weeks without a user's intervention. A good example is a heartbeat monitoring system for a patient who has heart disease. Since the heart rate is reported periodically, a heartbeat sensing device should be always on and transmit continuously with low transmit delay and latency for real time monitoring. If a sensing device could transmit periodic data discontinuously or transmit continuous data with much delay time, it is hard for doctors to monitor and prepare a patient's heart attack. Therefore, real-time and continuous monitoring is critical in handling a critical patient.

## 3.3 Limitations and Challenges in WSN

Table 3.1 presents several current researches or prototypes of their medical applications and issues mentioned. From it, most applications use MCU as a control unit to achieve low power consumption, and small device size. Also, all devices receive the power from batteries such as AAA, AA, and Li-ion. Size and weight of devices are mainly determined by those of the batteries. A battery's capacity is directly proportional to its size. Malan, *et al*. [2004], Oliver and Msngas [2006], Gyselinckx, *et al*. [2007], and Milenkovic, *et al*. [2006] use 2 AA or 2 AAA battery and [Juyng and Lee, 2008] and [Monton, *et al*., 2008] use the Li-ion or Li-P battery. A small Li-P battery's life time [Juyng and Lee, 2008] is about 6 hours, while AA or AAA battery's life time is several

days or even 3 months in a full active mode [Gyselinckx, *et al*., 2007]. Therefore, battery types need be carefully selected for portability and power consumption of different healthcare applications.

Some applications implement several wireless infrastructures for health monitoring systems. Rajiv [2006], Chien and Tai [2006], and Oliver and Msngas [2006] apply Bluetooth to WSN with PDA, Cell phone, or WLAN. Milenkovic, et al. [2006], Yan and Chung [2007], and Juyng and Lee [2008] apply ZigBee to BAN with PDA, or WLAN for extended network size. When several wireless infrastructures are deployed in the same network area, interference and data collision can occur in their overlapped channels. Different network topology, such as star, peer-to-peer, and mesh, should be considered for different health data applications.

Table 3.1 summarizes the platforms for physiological data sensing and monitoring with several wireless options. Each project addresses some above-mentioned issues, such as reliability, power, portability, network interference, and QoS, for real life. But none satisfies all of them. For example, some applications [Jung, *et al*., 2008; Milenkovic, et al., 2006] have good reliability, portability, and QoS, but their power consumption is not suitable for real life applications. Some applications [Mangharam, *et al*., 2006; Chien and Tai, 2006; Oliver, *et al*., 2006] have good performance, but their devices are too big and heavy to carry or attach on the body in real life applications. FireFly project [Mangharam *et al*., 2006] can send the continuous voice data in real time, but they have high power consumption, bulky size device and small network size.

Clearly, current health monitoring still has many challenges and issues that must be addressed such as reliability, portability, low-power consumption, and real-time

communication as discussed. Most reviewed systems focus on single hop topologies, and have very limited real-time monitoring capability. Also, some systems are hard to attach or carry because of their size and weight.

Even if they can monitor the health conditions, they cannot be readily available for real life applications. They use different wireless technologies for their different health parameters, situation, and areas. For example, some small data such as body temperature and patient ID are communicated by IEEE 802.15.4/ZigBee, even if this standard has low data rate. Also, these kinds of data are not much affected by time synchronization in real time. But some physiological data such as ECG, EEG, and EMG, need continuous and real-time transmission. Also, they require high data rate for reliable transmission.

As such, each application on a health monitoring system has to consider or improve their weak points for real-life use.

# CHAPTER 4

# PERFORMANCE ANALYSIS OF ZIGBEE-BASED SENSOR NETWORKS

## 4.1 Introduction

Continuous real time health monitoring based on body sensor networks (BSNs) has a great potential for the care of patients. They consist of several distributed network devices containing sensor units applied to collect and process data and communicate with other devices using a radio frequency channel [Ilyas and Mahgoub, 2005]. IEEE 802.15.4/ZigBee is a standard for low-rate, and low power wireless personal area networks in which the contention based and schedule based MAC schemes are applied as their MAC standard [IEEE, 2006]. It is based on carrier sense multiple access with collision avoidance (CSMA/CA). A ZigBee node competes with all other nodes in its network range for access to the channel for transmission. Thus the network performance depends on their data packet rate and the number of nodes in a network. The channel utilization is significantly affected by back-off time and packet collision. Successful channel access probability is an important indicator for reliable data transmission and efficient packet latency. If a node cannot access the channel after several back-off attempts, it wastes transmission time and loses its data packet.

This work analyzes the effects of back-off parameters and different network components (the number of network devices and size of data payload) on the performance of un-slotted CSMA/CA operation of a ZigBee MAC protocol. IEEE 802.15.4 and ZigBee are alternatively used in this dissertation. Section 4.2 provides an overview of a ZigBee MAC protocol. Section 4.3 performs the analysis of un-slotted

CSMA/CA operations. Analytic results for total back-off time and probability of accessing the channel are described. Also, based on these, end-to-end delay and packet delivery ratio are discussed under various parameter settings. Section 4.4 provides simulation results for end-to-end delay and PDR. Especially, they are simulated in the same network place with different data payloads. Section 4.5 summarizes this chapter.

## 4.2 General IEEE 802.15.4 MAC Protocol

In the CSMA/CA algorithm in Figure 4.1, a random back-off period easily causes an unnecessary waste of bandwidth and increases power consumption. Therefore, ZigBee suggests that the initial *BE* value is set to 3. However, if the network load is heavy, this approach leads to high collision rate, high power consumption and low network throughput. Non-beacon enabled ZigBee network systems use an un-slotted CSMA-CA channel access mechanism. The proposed system uses it for sound transmission of human heart beat monitoring. In CSMA-CA, each time a device needs to transmit data, it waits for a random number of unit back-off periods in the range $\{0, 2^{BE} - 1\}$ before performing a CCA (Clear Channel Assessment) step, where *BE* can have a value between $B_m$=*macMinBE* and $B_M$=*macMaxBE*. By default, they are 3 and 5, respectively.

Initially, the back-off exponent (*BE*) is set to 0~3. One symbol period is equal to 16 $\mu s$ with 2.4 GHz IEEE 802.15.4/ZigBee standard. The CCA time period ($T_{CCA}$) is defined as 8 symbol periods and *aUnitBackoffPeriod* ($T_{UBO}$) is defined as 20 symbol periods.

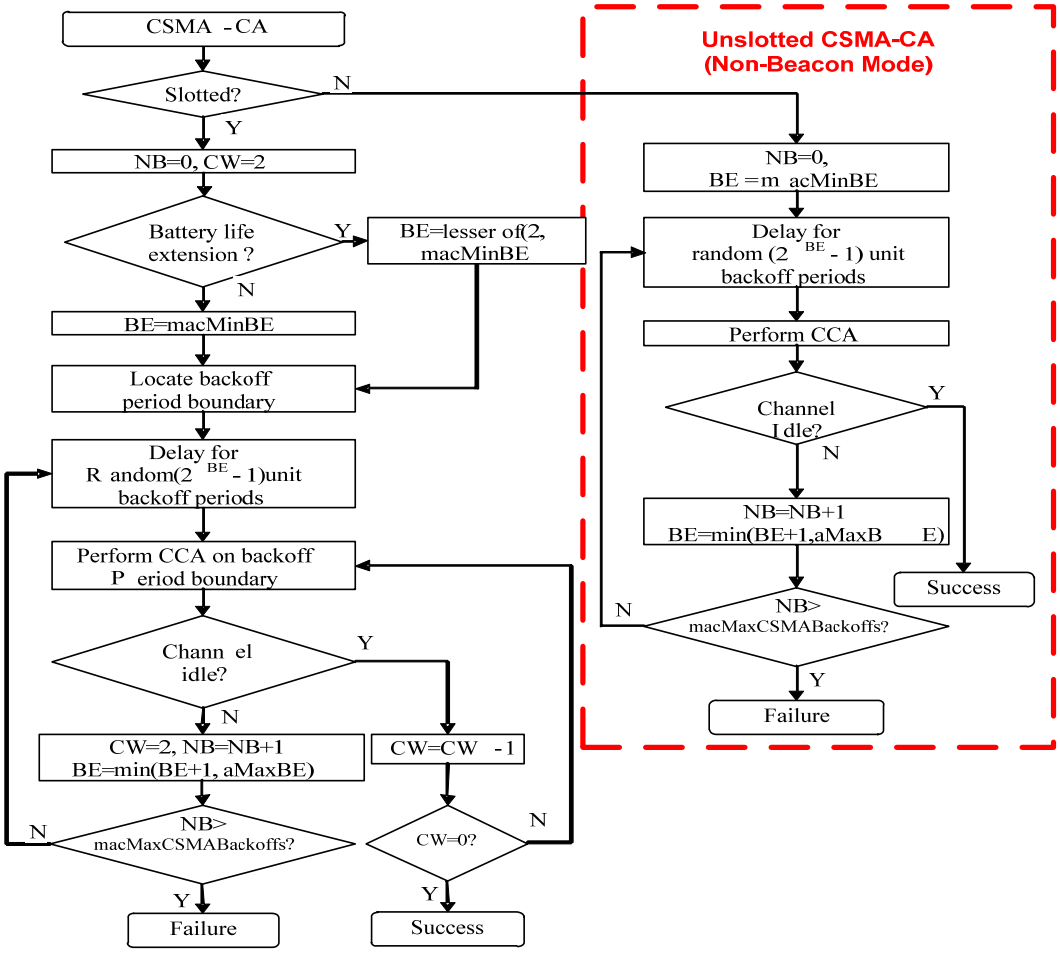


**Figure 4.1** IEEE 802.15.4 CSMA-CA protocol flow.

Note that a back-off period is the time required to transmit 20 *symbols*, where a symbol is equivalent to 4 bits, on a 250 kbps channel. Using the default value and assuming that the channel is found to be idle by the first channel access attempt, an idle channel access time can be calculated as:

$$T_{CA} = InitialbackoffPeriods + T_{CCA} = 7\times 20\ symbols + 8\ symbols \tag{4.1}$$

$$= 7\times 320\mu s + 128\ \mu s = 2.368\ ms$$

Note that *IntialbackoffPeriods* is defined by the product of a random number from [0, $(2^{BE} - 1)$] and $T_{UBO}$. In Equation (4.1), the random number is selected as 7 to derive the maximum time delay.

After the CSMA wait is over, the node determines if the channel is *idle*. This CCA is performed over the time duration of 8 *symbols*. If the channel is busy (*CCA fails*), the node increments *BE* up to a pre-defined maximum one, i.e., $B_M$, and repeats the CSMA procedure and CCA to transmit data packets. If the available channel cannot be found (*CCA fails*) even after predefined *macMaxCSMABackoffs* reattempts, a CAF (*channel access failure*) is declared and further attempt is not processed to transmit data packets. ZigBee provides a variable "*macMaxCSMABackoffs (0~5)"* that regulates the number of transmission trials. The default value of *macMaxCSMABackoffs* is 4, i.e., a transmitter is allowed to access the channel 4 consecutive times at most, each of which may have different back-off periods, before it declares access failure and drops the packet. If CCA succeeds, the node changes the mode from *transmit* to *receive* (*TX-to-RX turnaround*) to obtain the ACK packet from a coordinator. After the latter receives the data packet from a node, it changes the mode from *receive* to *transmit* (*RX-to-TX turnaround*) to send the ACK packet to the former.

Typically, ZigBee uses the *half-duplex* system. In other words, it cannot perform both *transmit* (*TX*) and *receive* (*RX*) operations at the same time. The *RX-to-TX* and *TX-to-RX turnaround time* is defined as 12 symbols.

In the CSMA-CA algorithm, each node shall maintain three parameters for each transmission attempt, i.e., *NB*, *CW*, and *BE*. *NB* is the Number of Back-offs. The algorithm is required to back-off before attempting the current transmission. *NB* should

be initialized to "0" before each new transmission attempt. *CW* is the contention window length, defining the number of back-off slots that needs to be clear of channel activity before the transmission can commence. This value is initialized to 2 before each transmission attempt and reset to 2 when the channel is assessed to be busy. *BE* is the Back-off Exponent, which is a variable that determines the number of back-off slots a device shall wait before attempting to assess a channel's status. It is chosen randomly in the range of 0 to $(2^{BE} - 1)$. For a non-beacon mode, un-slotted CSMA-CA is used. Thus MAC sub-layer initializes *NB* and *BE* without *CW*.

The next step is to decide random waiting delay for collision avoidance. It is the product of the back-off period and a random number from $[0, 2^{BE} - 1]$. If *BE* set to 0, the collision avoidance procedure is disabled at the first iteration, and the node performs the CCA directly without waiting. *BE* is increased each attempt for the channel that is sensed busy. If more nodes join the same network area, the traffic becomes heavier. Then *BE* must increase to reduce data collision in CSMA-CA operations. It cannot exceed a predetermined $B_M$ value, which can be reached by the competing nodes at most after 5 ($B_M = 5$, default value) transmissions of other nodes. If $B_M$ is set as 5 by default, the back-off period is a random number in [0, 31] multiplied by *aUnitBackoffPeriod* in all remaining nodes waiting to access the channel.

In this process, $B_M$ is more critical than $B_m$ for the back-off delay distribution. Its impact can change with different network environments as characterized by traffic, interference, size, and data payloads. If a channel is available in un-slotted CSMA-CA, MAC sub-layer begins transmitting a packet frame. If $B_M$ is set as a smaller value, e.g., 4,

the average back-off delay decreases and so does MAC processing time. Consequently, power consumption can be reduced.

The maximum effective data capacity, denoted as $C_{max}$, is defined as the maximum achievable data rate for a user application in the absence of any kind of cross traffic or interference by other systems with different communication standards and those using the same frequency range (2.4GHz). The effective data capacity, denoted as $C$, under several conditions can be calculated and tested. Short addresses are used to reduce the size of a packet. Optional acknowledge frames (*ACK*) are enabled and the back-off exponent *BE* is set to "0". At the 2.4GHz PHY layer, the transmission duration of 1 *byte* = 2 *symbols* = 32 $\mu s$.

$C_{max}$ can be calculated for a single hop connection between two devices, under the ideal conditions. For the MAC layer to process the data received from the PHY layer, each data packet is followed by an inter-frame spacing (*IFS*). Depending on the size of the *MPDU* (MAC protocol data unit), *LIFS* (a long *IFS*) and *SIFS* (a short *IFS*) can be used for frame spacing. If it is larger than 20 bytes, *LIFS* is used. Otherwise, *SIFS* is selected. An LIFS takes 640 $\mu s$ (40 *symbols*) and an SIFS 192 $\mu s$ (12 *symbols*). From Fig. 4.2, the space between a data frame and its corresponding acknowledgement (*ACK*) is same as the Rx-to-Tx turnaround time ($T_{TA}$) calculated before, i.e., 192 $\mu s$.

Packet maximum size is 133 bytes long and includes 6 byte overhead. Its packet transmission takes the channel time of 340 symbols (266 symbols packet transmission + 12 symbols for turnaround time (Rx-Tx) + 22 symbols for ACK transmission + 40 symbols for $T_{LIFS}$). Hence it can take at most 183.8 (62500/340) packets per second with a 2.4 GHz channel of 250 kbps (62500 symbols/sec) capacity. To calculate $C$ for a single-

hop connection network, the size of an *MPDU* is set to 127 bytes (its maximum size). We can set an *MPDU*'s size as 113 bytes (*MSDU* = 100 bytes) for heartbeat sound. The *ACK* frame size is 11 bytes. For this scenario, there is no back-off delay and *BE*=0.

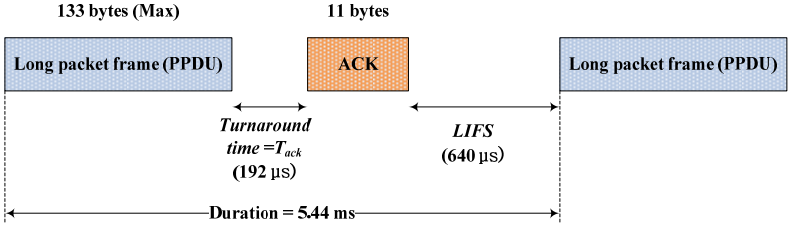


**Figure 4.2** Duration for one data frame by LIFS with ACK.

As shown in Figure 4.2, the total time between two long packet frames $T_{total}$ is given by

$$T_{total} = T_{longframe} + \delta + T_{TA} + \delta + T_{ack} + T_{LIFS} = 5.824\ ms \tag{4.2}$$

where $T_{longframe} = 133 \times 32\mu s = 4.256\ ms$ , $\delta = 222 \times 10^{-6}\ ms$, $T_{ack} = 11 \times 32\ \mu s = 0.352 ms$ and $T_{LIFS} = 0.64\ ms$

According to [Sun, *et al*., 2006]

$$C_{max} = \frac{T_{applicationdata}}{T_{total}} \times C_{PHY} = 174.45\ kbps \tag{4.3}$$

where $T_{applicationdata} = 127 \times 32\mu s = 4064\ \mu s$, the time it takes to send the application data via the *PHY* layer, and $C_{PHY} = 250$ kbps.

The theoretical maximum heart beat sound data throughput for single-hop transmission is given by

$$C_{HB} = \frac{T_{HB}}{T_{total}} \times C_{PHY} = 182.48\ kbps \tag{4.4}$$

where $T_{HB}$= 100 × 32$\mu s$ = 3200 $\mu s$.

Therefore, the maximum effective data capacity available for a user is only 69% of the PHY data rate (250 kbps) via theoretical analysis. For heart beat sound data, it is only 72% of the PHY data rate. In our real test using CC2430 sensor modules for continuous sound data (100 byte payload), the packet period time is 12 *ms* for reliable transmission of sound data. This is because the modules have a low-performance processing unit, i.e., 8051 MCU. Therefore, the achievable maximum throughput for continuous sound data is only 79 kbps or 84 packet/sec i.e., 31.6% of the PHY data rate.

## 4.3 Analysis of Un-slotted CSMA/CA

### 4.3.1 Packet Transmission Time and Delay

For the uplink process between a node and coordinator, we consider its packet transmission delay ($T_{pd}$). It includes the back-off period, packet transmission time, coordinator's turnaround time switching from transmitting to receiving, ACK transmission time, and IFS time with *SIFS* = 12 and *LIFS* = 40 *symbols*. The average back-off time of each transmission attempt consists of several back-off periods. The number of back-off attempts is limited up to the predefined *macMaxCSMABackoffs*, and

depends on the network traffic. CCA time $T_{CCA}$ = 8 *symbols* transmission time. $T_{TA}$ is the transceiver's transmitting to receiving turnaround time (12 *symbols*).

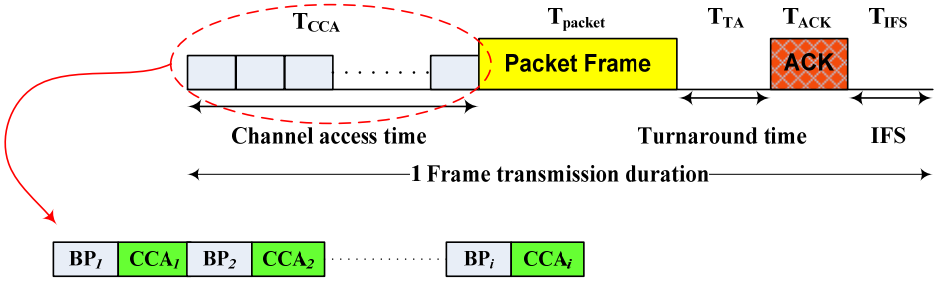


**Figure 4.3** Frame transmission sequence of IEEE 802.15.4.

As shown in Figure 4.3, the average packet transmission delay can be calculated.

$$T_{pd} = T_{packet} + T_{ACK} + R \cdot T_{CCA} + f\left(R, T_{BO(a)}\right) + T_{TA} + T_{IFS} \tag{4.5}$$

$T_{packet}$ is the transmission time for a data packet.

$$T_{packet} = \frac{L_{SHR} + L_{PHR} + L_{MHR} + L_{payload} + L_{MFR}}{R_{data}} \tag{4.6}$$

where $L_{SHR}$, $L_{PHR}$, $L_{MHR}$, $L_{payload}$, and $L_{MFR}$ are the number of bytes in a SHR header, PHY header, MAC header, MAC footer, respectively, and $R_{data}$ is the raw data transmission rate. $T_{ACK}$ is transmission time for an ACK frame.

$$T_{ACK} = \frac{L_{SHR} + L_{PHR} + L_{MHR} + L_{MFR}}{R_{data}} \tag{4.7}$$

An acknowledgement frame consists of 11 bytes. Given a fundamental data rate into the modem of 250 kbps it takes 0.352 *ms* to transmit. The following discussion in this section will not consider the use of ACK.

*R* indicates the average number of back-off intervals. It is calculated as follows [Wang and Li, 2009],

$$R = (1 - P_S) \cdot b + \sum_{a=1}^{a=b} a \cdot P_C \cdot (1 - P_C)^{(a-1)} \tag{4.8}$$

The probability $P_S$ means the one that a node can successfully access the channel. In Equation (4.9), $b$ is the number of back-off attempt periods.

$$P_S = \sum_{a=1}^{a=b} P_C \cdot (1 - P_C)^{(a-1)} \tag{4.9}$$

The probability of channel being idle ($P_C$) in a clear CCA period can be calculated as

$$P_C = (1 - q)^{n-1} \tag{4.10}$$

The transmitting probability ($q$) is

$$q = \frac{T_{packet}}{T_{packet} + T_{sampling}} \tag{4.11}$$

where $T_{sampling}$ is data sampling time, i.e.,

$$T_{sampling} = \frac{L_{payload} \times 8}{Sampling\ rate} \tag{4.12}$$

$T_{ABj}$ is the sum of the average back-off times. It may consist of several back-off periods and depends on both parameters of a node and traffic load. Because each back-off attempt delay period is calculated from a random number between *0* and ($2^{BE} - 1$) multiplied by *unitbackoffperiods*, we use the average back-off time in each range as

$$T_{AB} = \left[ \sum_{i=0}^{2^{BE}-1} 2^{-BE} \cdot i \right] \times unitbackoffperiods \tag{4.13}$$

Also, the *jth* back-off time for the number of channel access attempts can be calculated as

$$T_{ABj} = \left[ \sum_{i=0}^{2^{(BE+j-1)}-1} 2^{-(BE+j-1)} \cdot i \right] \times unitbackoffperiods \tag{4.14}$$

Based on the above analysis, we can obtain the average back-off attempts depending on the different payload size, denoted by $L_{payload}$, and the number of network devices, denoted by *N*, as shown in Figure 4.4.

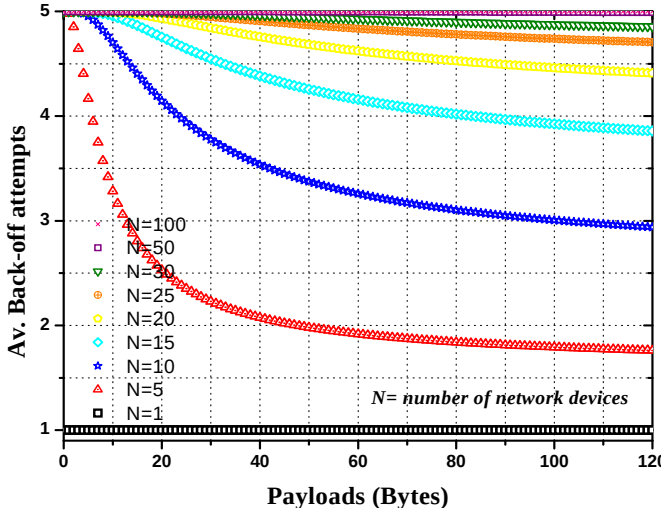


**Figure 4.4** Impact of $L_{payload}$ and $N$ on the average number of back-off attempts.

Figure 4.4 shows that the average number of back-off attempts is smaller for a longer payload frame than a shorter one. The number of average back-off attempts increases with $N$. The advantage of small average back-off attempts is to reduce the transmission delay by transmitting a long data frame instead of separated small data frames.

If just one node is communicating with the coordinator, it does not need to compete for the channel access and is not affected by its payload size. Thus the average number of back-off attempts is 1. As $N$ increases, they have to compete for the channel access with each other. For this reason, the average number of back-off attempts approaches *macMaxCSMABackoffs*. Because a long data frame occupies the periods on the channel longer than a small one during its transmission, other devices waiting for channel access have more back-off attempts often than the case with the transmission of a short data frame. By increasing back-off attempts, back-off exponent increases for each

such attempt. This leads to longer back-off delays. From Figure 4.4, it is shown that the payload size once over 40 bytes affects the average back-off attempts only slightly. A large *N* leads to the maximum back-off attempts regardless of payload.

The back-off exponent *BE* is a critical parameter in the back-off algorithm of CSMA-CA. It is used as an estimate of the random back-off delay before trying to access the channel. As described before, in MAC operations, the CSMA channel access wait time depends on *BE*. For every transmission attempt, *BE* is initialized to be $B_m$ and each CCA failure increases *BE* by 1 until it reaches $B_M$. Therefore, the channel access wait duration depends on how many CCA failures have already been processed prior to the current attempt. It is related to the number of back-off period times and $T_{CCA}$.

The back-off delay time is determined by a random number from 0 ~ ($2^{BE}$ -1). Thus, the mean value of back-off delay (13, 14) is used for $T_{TB}$ in the following discussions. Total back-off period time is

$$T_{TB} = \left[\sum_{j=1}^{j=u} T_{ABj}\right] + v \cdot T_{AB(u+1)} \tag{4.15}$$

$$= \sum_{j=1}^{j=u}\left[\left(\sum_{i=0}^{2^{(BE+j-1)}-1} 2^{-(BE+j-1)} \times i\right) \times 0.32ms\right] + v$$

$$\times \left[\left(\sum_{i=0}^{2^{(BE+(u+1)-1)}-1} 2^{-(BE+(u+1)-1)} \times i\right) \times 0.32ms\right]$$

where average *R*'s integer part = *u* and fraction part = *v* For example, If *R* = 3.5, then *u* = 3 and *v* = 0.5.

Total back-off time for channel access and data transmission is sum of all back-off attempt times. Thus, $T_{TB}$ is affected by $R$ and $BE$. To simplify our calculation, we set *macMaxCSMABackoffs* as 5. Table 2 shows $BE$ for each back-off attempt as different $B_m$ (0~8) and $B_M$ (3~8). If average back-off time in each range is applied and $R$ is 5, the shortest $T_{TB}$ is achieved as (0, 1, 2, 3 and 3) in Table 2 for each back-off attempt $BE$ when $B_m$ = 0 and $B_M$ = 3. $T_{TB}$ increases with $B_m$ and $B_M$. After $BE$ reaches $B_M$, each back-off attempt keeps the same $B_M$. The reason is that CSMA-CA compares $B_m$ and $B_M$ for each back-off attempt. If they are equal, after several CCA failures, $B_m$ has to keep the same value as $B_M$ for any remaining back-off attempt.

Figure 4.5 shows the total back-off time periods for different payloads and $N$. It shows the impact of increasing $N$ on total back-off time. Note that $B_m$=3, $B_M$=5, and $m$=4 as default values of IEEE 802.15.4. $T_{TB}$ increases as $N$. It can be explained as follows. If just one device joins a coordinator, it does not need to compete for channel access. Hence, it takes only one back-off attempt to access the channel and transmits the data packet. However, as $N$ increases, the number of devices competing for channel access at certain time interval could be large and leads to multiple back-off attempts as a result of channel access failure. Increasing payload size can reduce $T_{TB}$. However, after certain size (20~50 bytes) is reached, reducing $T_{TB}$ with increasing payload size becomes less significant.

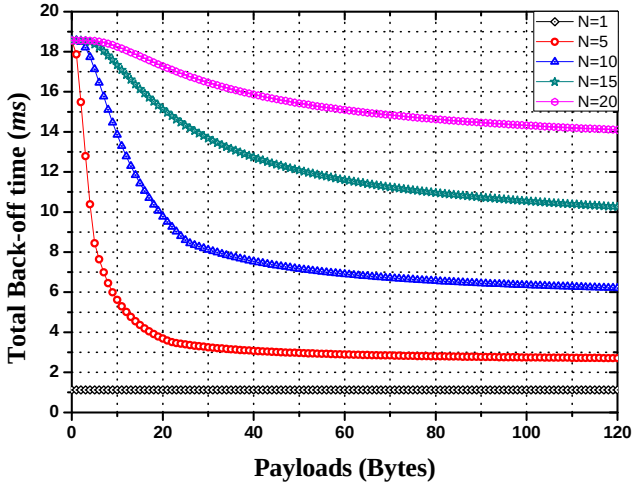


**Figure 4.5** Total back-off time with various payload size and *N*.

### 4.3.2 End to End Delay

The end-to-end delay ($T_{ETE}$) is an important parameter for healthcare monitoring applications. $T_{ETE}$ is the total time between a packet's generation time at the network device and the time which the packet is received by the coordinator.

Normally, the total time for one packet to be successfully transmitted includes its generating time, queuing delay, total back-off time period, channel sensing time for channel access, data packet and ACK transmission time and ACK waiting time. In this study, the processing delay and queuing delay are not considered, because these are related with a hardware part, such as MCU, sensor and memory. The propagation delay in $T_{ETE}$ is considered for more realistic transmission.

$$T_{pd} = R \cdot T_{CCA} + T_{TB} + T_{packet} + \delta + T_{TA} + \delta + T_{ack} + T_{LIFS} \tag{4.16}$$

$$T_{ETE} = T_{sampling} + T_{pd} \tag{4.17}$$

Figure 4.6 shows the average end-to-end delay with various payload size and network size. These results show that $T_{ETE}$ increases as the number of nodes, $N$. $T_{ETE}$ increases with $N$ since packet contention and collision are increased. Also, $T_{ETE}$ increases as the size of payloads. Actually, delay is influenced by different back-off stages due to network traffic by the number of nodes and size of payloads. The average back-off attempts and total back-off time with various numbers of nodes and payloads are analyzed in Figures 4.4 and 4.5. From these results, it can be found that average back-off attempts and total back-off time increase as $N$. But they decrease as the payload. From these results, $T_{ETE}$ should decrease as the payload increases, but actually it increases. The reason for this is that the data sampling time is much longer than packet transmission time. For example, the sampling time of 10 bytes payload and 100 bytes payload are 10*ms* and 100*ms* respectively.

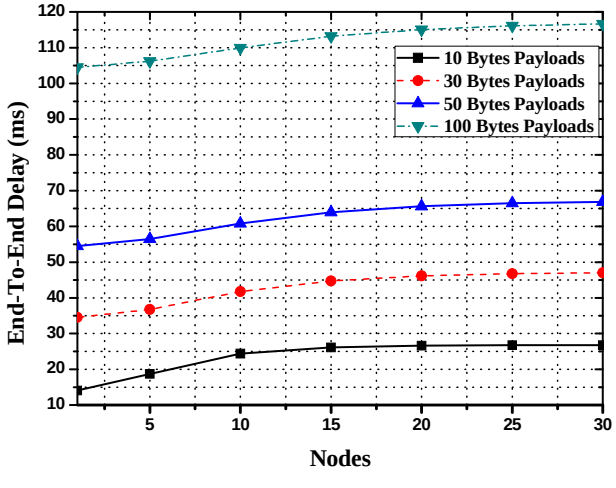


**Figure 4.6** Impact of payload size and $N$ on average end-to-end delay.

### 4.3.3 Packet Delivery Ratio

Normally, under the IEEE 802.15.4 CSMA/CA channel conditions, packets are discarded for two reasons: (1) channel access failure that refers to the situation that network traffic becomes heavy when many nodes try to transmit packets in a certain period of time. It is assumed that all *N* devices have at least one packet frame to transmit all the time. Actually, channel access failure occurs when a packet fails to obtain an idle channel in CCA within ***m***+*1* back-off stages; and (2) packet loss, which refers to packet collision. Packet collision can happen when more than one node tries to transmit their packet at the same time after finishing CCA at the same time. This analysis does not consider discarded packets due to retransmission limits.

Actually, back-off time is selected from [0, $2^{BE}$ -1] randomly. This study assumes that the same back-off time for each node occurs for each packet collision, because a node transmits its packet right after CCA. Therefore, define this probability simply as

$$P_{BC} = \frac{1}{2^{BE}} \tag{4.18}$$

With the number of *N -1* contending network devices, define packet delivery rate as [Liang and Balasingham, 2006]

$$PDR = \sum_{a=1}^{b} P_C \cdot (1 - P_C)^{(a-1)} \cdot (1 - P_{BC})^{(N-1)q} \tag{4.19}$$

Figure 4.7 shows the packet delivery rate (PDR) with the number of network devices and payload size. In Figure 4.7(a), PDR decreases as *N* increases with the same payload size (50 bytes). PDR decreases from 1 to 0.62 as *N* increases from 1 to 32. The reason for this is that more nodes compete to access the channel and thus more channel access failure and packet collisions occur.

In Figure 4.7(b), PDR increases as the payload size grows from 5 to 100 bytes with *N*=16. Especially, increasing rate is significant, i.e., from 0.4 to 0.85 between 5 and 30 bytes. The reason is that as the payload size increase, nodes transmit packets for longer time periods. Therefore, the probability of successful channel access is increasing. Also, nodes which try to transmit bigger packets have a higher chance to obtain the channel for transmitting than other nodes which try to transmit small packets in the same network area. It is because of the channel efficiency. Because a bigger packet uses the channel for longer time, other nodes having small packets are hard to access the channel for transmission. This effect of the size of payloads for successful channel access will be further discussed in the next section via simulation.

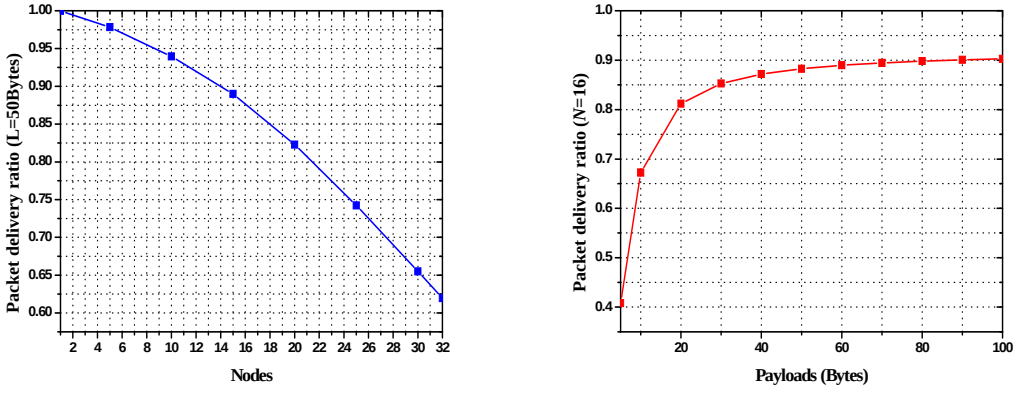


(a) (b)

**Figure 4.7** Impact of payload size and *N* on average packet delivery ratio.

## 4.4 Simulation Environment

In this section, various network scenarios are designed and evaluated by simulations. primary objective is to measure and analyze the performance of different network scenarios and parameters on IEEE 802.15.4 star network topology. The network performance simulation has been developed by using the Qualnet version 5.0 developer platform produced by the scalable network technology [Scalable-networks, 2011]. The simulation environment is specified to suit the real network.

Figure 4.8 shows the simulation model of a 3D space. In this model, a star network topology with one PAN coordinator and 1 to 32 network devices are located at same distance as 20 meters in an area of 50m×50m×5m. For this model, the coordinator's location is set as (25, 25, 5).

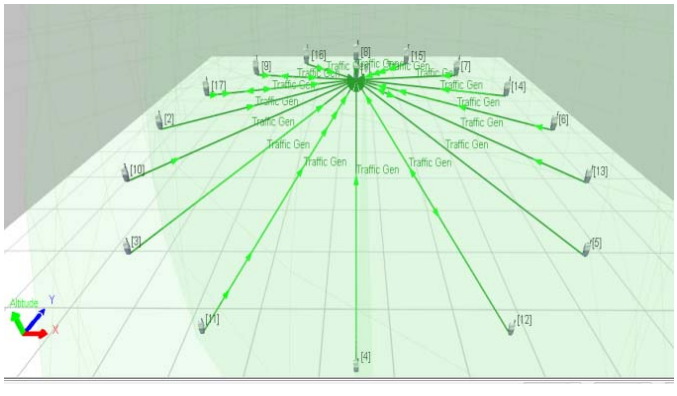


**Figure 4.8** 3D simulation scenario.

In other words, it is placed at the center of the given area and is located 5 meters from the floor. Also, other network devices are placed 1 meter from the floor, i.e., (*x, y,* 1). This is assumed that people carry the network device. Because of different height of the coordinator and network devices, 20 meters is the diagonal distance between them. In

this simulation, only uplink traffic is considered, because it is usually applied to the BSN applications like healthcare monitoring systems. Some network devices transmit to the PAN coordinator to allow one to collect the data from sensor nodes.

The simulation parameters are given in Table 4.1. In our simulation model, BO and SO are set to 15, i.e., non-beacon mode. To analyze the simulations closer to the real system, we choose the "Traffic Generator" as a type of traffic from the Qualnet simulator. This model simulates random distribution based network traffic.

**Table 4.1** Simulation Parameters

| **Parameters** | **Value** |
|---|---|
| Size of area | 50m × 50m × 5m (*x,y,z*) |
| Num. of nodes | 1 ~ 32 |
| Channel freq. and data rate | 2.4 GHz and 250kbps |
| Transmission range | 35 meter |
| Modulation type | O-QPSK |
| TX power | 0 dBm |
| PHY and MAC model | IEEE 802.15.4 |
| Path loss model | Two Ray Model |
| Simulation time | 1 hour, 1000sec |
| Traffic Type | Traffic Generator |
| Energy Model | MICAZ Mote |
| Battery Model | Simple linear, 1200mAhr |
| BO, SO | *15/15 |
| *MinBE* | 3 |
| *MaxBE* | 6 |
| *aMaxFrameRetries* | 3 |
| Size of data payload | 5 ~ 100 bytes |
| *Non-beacon mode | |

As described earlier, in theory, to make sure that their mathematical result is actually applied to a real network system, we have used the following performance parameters:

- **PDR** is defined as the ratio of successfully received packets to a destination node, relative to the total number of data packets transmitted by source nodes.
- **Average End-to-End delay** represents the average length of time taken for a packet to travel from the source to destination. In other words, it shows the average data packet delay in applied network communication during the data packet transmission.
- **Number of packets sent and dropped at MAC with varying MSDU** indicates that different size of data payload can affect channel access competition and data transmission.

## 4.5 Simulation Results and Discussion

This section describes the simulation results of various performance parameters for evaluation of PDR (packet delivery ratio), number of packet sent for channel competition, and average end-to-end delay on IEEE 802.15.4 star topology using varying traffic loads. The simulation parameters are applied to simulate WSN scenarios.

### 4.5.1 Effects of Numbers of Network Devices

In this simulation, the data payload size is fixed to 50 bytes. Figure 4.9 shows the packet delivery ratio (PDR) of IEEE 802.15.4 star network topology between the coordinator and nodes whose count *N* varies from 1 to 32. The results show that as *N* increases, PDR

decreases because of the presence of packet collision and random back-off process from heavy channel competition.

Figure 4.10 represents the performance of average End-to-End delay as *N* varies from 1 to 32. Actually, the End-to-End delay of a packet transmission considers all delay of data queuing, channel access process time, packet transmission delays and route discovery latency. The results show that as *N* increases, the overall average End-to-End delay increases since the effect of more channel access processes, possibility to collide with other packets and transmission delay due to the heavy traffic load.

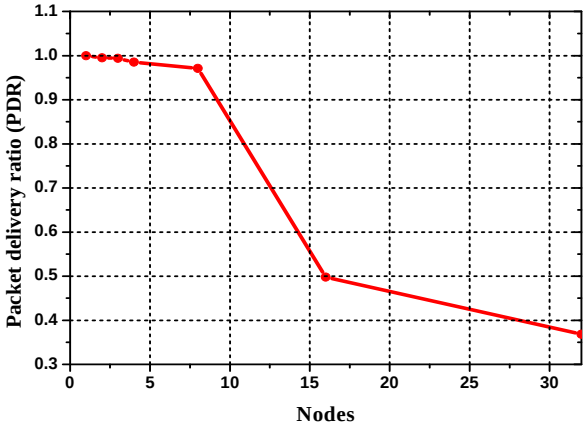


**Figure 4.9** PDR of IEEE 802.15.4 star network topology with *N* nodes.

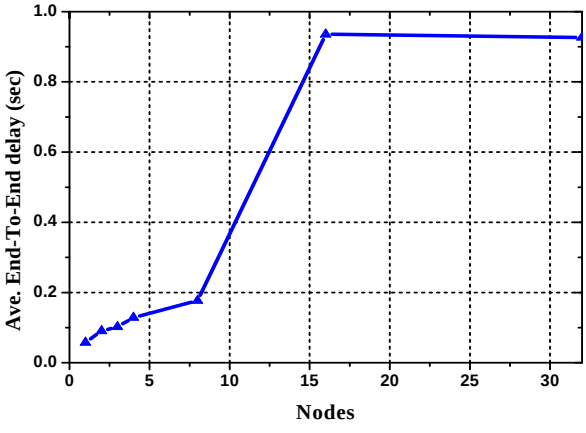


**Figure 4.10** Average End-To-End delay of IEEE 802.15.4 star network topology with *N* nodes.

### 4.5.2 Effects of Data Payload Size

In IEEE 802.15.4, data are transferred in packets. They have a maximum size of 133 bytes (PPDU), allowing for a maximum payload of 102 bytes (MSDU). We can set the size of data from a sensor up to 102 bytes. This depends on the different applications.

In this section, channel access competition and data transmission with different size of data payload are analyzed by using Qualnet 5.0 and *N* is fixed to 16. The number of data packets sent and number of data packets dropped at MAC layer in a given time need to be considered in order to analyze them. If some node has more chances for channel access competing with other nodes, it can transmit more packets in a same given time. Also, if one node loses the chance of the channel access more than other nodes, it drops more packets after retrying back-off attempts up to *macMaxCSMABackoffs*.

In Figures 4.4 and 4.5, the average number of back-off attempts and total back-off time as data payload size varies are theoretically analyzed. From Figure 4.4, the number of average back-off attempts decreases as payload size increases. As mentioned before, a

large MSDU packet charges the periods on the channel longer than a small MSDU packet during its transmission time. Thus small MSDU packets should wait more for channel access and more back-off attempts open. Also, because of their more back-off attempts, total back-off time increases. If one node has few back-off attempts and short total back-off time, it could transmit more packets and reduce the packet's drop rate. In this simulation scenario, the MSDU size varies from 5 bytes, 30 bytes, and 60 bytes to 100 bytes.

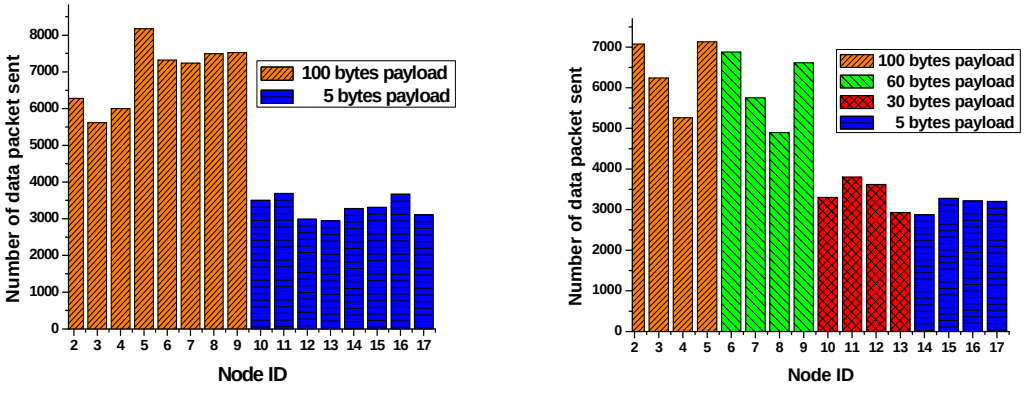


(a) (b)

**Figure 4.11** Number of data packets sent with varied data payload size in a same network area.

Figure 4.11 shows the number of data packets sent from 16 nodes to the coordinator with varying data payload (MSDU) size. In Figure 4.11(a), 100 bytes MSDU to 8 nodes (namely nodes 2~9) and 5 bytes MSDU to other 8 nodes (namely nodes 10~17) are applied. In Figure 4.11(b), 100 bytes, 60 bytes, 30 bytes and 5 bytes MSDU are applied to each 4 nodes for more specific results.

From Figure 4.11(a), 8 nodes generating 100 byte MSDU send 70% of expected packets (average 10000 data packets) in a given time. But other 8 nodes generating 5

byte MSDU send only 33% of expected packets. For more detailed results, we simulate by dividing payload into four categories as 100, 60, 30, and 5 bytes payloads in Figure 4.11(b). The result shows that 4 nodes sending 100 bytes and 4 nodes sending 60 bytes send 65% and 60% each, while other 8 nodes sending 30 and 5 bytes MSDU just send 34% and 31%. This is because as the size of MSDU increases, a large packet can get fewer back-off attempts and access the channel more easily than other small size packets.

Also, Figure 4.12 represents that small MSDU packet transmission drops packets more than large MSDU packet transmission at a MAC layer.

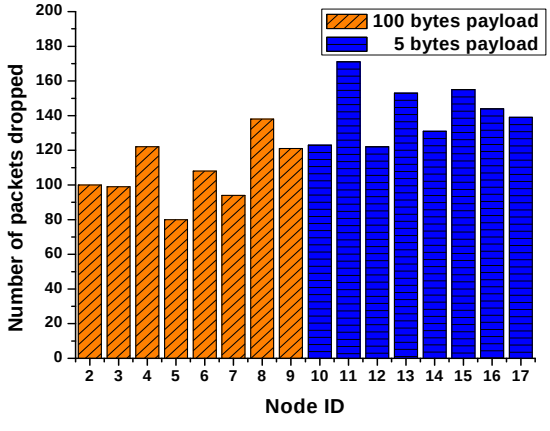


**Figure 4.12** Number of data packets dropped with varied data payload size in a same network area.

From Figure 4.13, average end-to-end delay with various sizes of payload is analyzed. It shows that the end-to-end delay increases as the payload size. The network has 16 nodes with different data payloads as 100, 60, 30 and 5 bytes. Average end-to-end delay of nodes (100 bytes) is almost more than twice than nodes (5 bytes). The reason for

this is that their sampling time and packet transmission delay are much longer than those of a short packet.

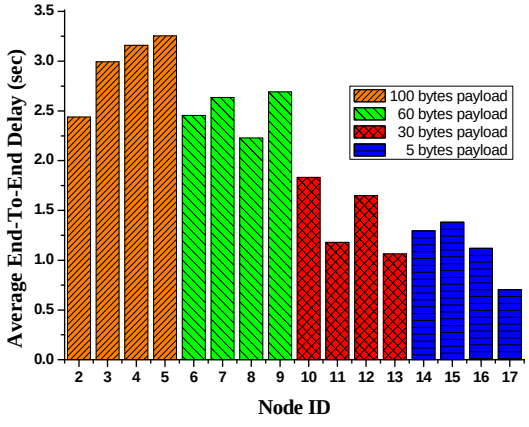


**Figure 4.13** Average end-to-end delay with varied data payload size in a same network area.

## 4.6 Summary

IEEE 802.15.4/ZigBee devices are used for many sensor network applications because of ZigBee's advantages, i.e., low-power consumption, multiple accesses, low-cost and easy expansion of a network. However, for the wireless healthcare monitoring application, it suffers from low data rate. Small size data like temperature and humidity are not a problem in a real-time and reliable monitoring system. But large and continuous data streams like sound data need more communication capacity. When ZigBee medical sensors are applied to some patients, real-time transmission and data reliability are critically important. For example, emergency data have to be transmitted reliably without delay in any kind of situations including heavy network traffic. This poses a significant challenge to researchers and engineers. This chapter presents the theoretical and

simulation-based performance analysis of QoS for BSNs based on an IEEE 802.15.4 star network. The simulation results validate the theoretical analysis results well.

# CHAPTER 5

# MODELING AND OPTIMIZATION OF UN-SLOTTED IEEE 802.15.4

## 5.1 Introduction

Wireless sensor networks (WSNs) in such applications as factories, health monitoring, home and building automation are expected to have effects on our life. Since the successful release of the IEEE 802.15.4 standard, WSNs have been developed for many applications in recent years. The IEEE 802.15.4 standard is composed of the physical (PHY) layer and the medium access control (MAC) layer for low-rate, low-power and low-cost wireless networking. IEEE 802.15.4 MAC protocol can support two operational modes, non-beacon and beacon. In the former, nodes in a personal area network (PAN) communicate with each other according to an un-slotted CSMA/CA protocol. Both the PAN coordinator and devices can operate without time synchronization, and packet frame can be reduced by using un-slotted CSMA/CA. In the beacon mode, the PAN coordinator generates beacon frames periodically to synchronize in time with its network devices.

In this section, an IEEE 802.15.4 based one-hop star network is considered. The network performance depends on the number of nodes competing for channel access and their packet generation rates. Also, the configuration of IEEE 802.15.4 MAC parameters should be considered. IEEE 802.15.4 standard recommends default values for different MAC parameters, such as *macMinBE*, *macMaxBE*, *macMaxCSMABackoffs* and *macMaxFrameRetries*. WSNs based on the IEEE 802.15.4 can be applied to different

environments with their different applications. In structural monitoring system [Wijetunge *et al*., 2010, Zixue Qiu *et al*., 2011, Xu *et al*., 2004, Pakzad *et al*., 2008], small packets can be transmitted periodically with long packet interval or just transmitted upon a base station's request. In home automation, on/off or dimmable light, dimmer or on/off switch and room temperature sensor do not require continuous or high data rate communication. However, much medical information such as ECG, heart beat sound, and lung sound require high packet generation rate, high data and low latency communication. The health monitoring applications are more sensitive to QoS compared to the other applications.

Reliable, energy efficient, timely packet transmission can be affected by the medium access control parameters, i.e., *macMinBE*, *macMaxCSMABackoffs*, and *macMaxFrameRetries* in the IEEE 802.15.4 MAC protocol. However, tuning these MAC parameters for WSNs is not a simple task. Also, accurate and simple models of the influence of these parameters on the probability of successful packet transmission, energy consumption and packet delay are not available and clear, because all applications of WSNs have different network environment and requirements. In fact, it seems extremely difficult to determine a single IEEE 802.15.4 MAC configuration that results in optimal network performance in all network environments.

This chapter provides an analytical Markov model that predicts the performance of the IEEE 802.15.4 un-slotted CSMA/CA. In contrast to the previous work, the presence of limited number of packet retransmissions, acknowledgements, unsaturated traffic and packet generation is considered. Reliability, average end-to-end delay and energy consumption of the network by varying network parameters including payload

size, packet arrival rate, *macMinBE*, *macMaxCSMABackoffs* and *macMaxFrameRetries* are analyzed.

The rest of the chapter is organized as follows. Section 5.2 summarizes the existing work of analytical modeling of a CSMA/CA mechanism. In Section 5.3, a generalized Markov chain model of CSMA/CA with unsaturated traffic and retransmission limits is proposed. In Section 5.4, the network performance based on the proposed Markov chain is analyzed. In Section 5.5, impact of CSMA/CA MAC parameters is explored on the performance of IEEE 802.15.4 MAC layer under different traffic loads.

## 5.2 Related Work

Many researchers have aimed at analyzing and evaluating standards and protocols. Especially, IEEE 802.15.4 is being considered as a critical wireless standard for WSNs, and a great deal of research has been carried out to study the CSMA/CA MAC protocol. Most analytical studies use the Markov chain model initially proposed by Bianchi [2000]. The IEEE 802.11 MAC is modeled by a Markov chain under saturated traffic and ideal channel conditions. In [Zhai et al, 2006 and Daneshgaran et al, 2008], the Bianchi approach is extended deal with the cases under more realistic assumptions.

Inspired by Bianchi's work, some researchers analyze and propose the Markov chain models for IEEE 802.11 and IEEE 802.15.4. Pollin et al. [2008] provided an analytical Markov chain model that predicts the performance and detailed behavior of the IEEE 802.15.4 slotted CSMA/CA mechanism. In their work, unacknowledged packet transmission is considered. They upgrade their model to consider the ACK packet. The

main difference that results from ACK process in slotted IEEE 802.15.4 operation is the fact that the transmission channel could be idle for one slot between the transmissions of the packet and its ACK.

Jung *et al*. [2009] proposed a discrete Markov chain model for slotted IEEE 802.15.4 operation under unsaturated traffic conditions. They assume that another attempt to transmit the packet can be decided even though the previous attempt ends in a channel access failure. They do not model the length of data and ACK packets, which is crucial to analyze the performance metrics for IEEE 802.15.4 networks.

Misic *et al*. [2006] presented a Markov chain model for CSMA/CA behavior in slotted IEEE 802.15.4 operation. They use this model as a building block in a Markov chain to model the operation of a node, where a node can transmit packets to its base station via direct transmission or receive packets from the base station via indirect transmissions.

Bae *et al*. [2010], proposed an enhanced contention access mechanism to compensate for the problems caused by a large population of devices based on the discrete Markov chain model for slotted IEEE 802.15.4 operation.

Kim *et al*. [2008] presented a model for un-slotted IEEE 802.15.4 MAC operation. They identify two collision windows in un-slotted IEEE 802.15.4 operation and the need for CCA duration to exceed the turnaround time in order to avoid collisions involving ACKs. They model an IEEE 802.15.4 node as an M/G/1 queue with the packet latency as the service time of the queue. They assume that the CCA duration is set to be more than the turnaround time and hence no ACK collisions are possible. The main

weakness of this model is that they just consider for light traffic loads. They ignore the collisions in packet transmission under the assumption that such collisions are infrequent.

## 5.3 Markov Chain Model Analysis for Un-slotted CSMA/CA

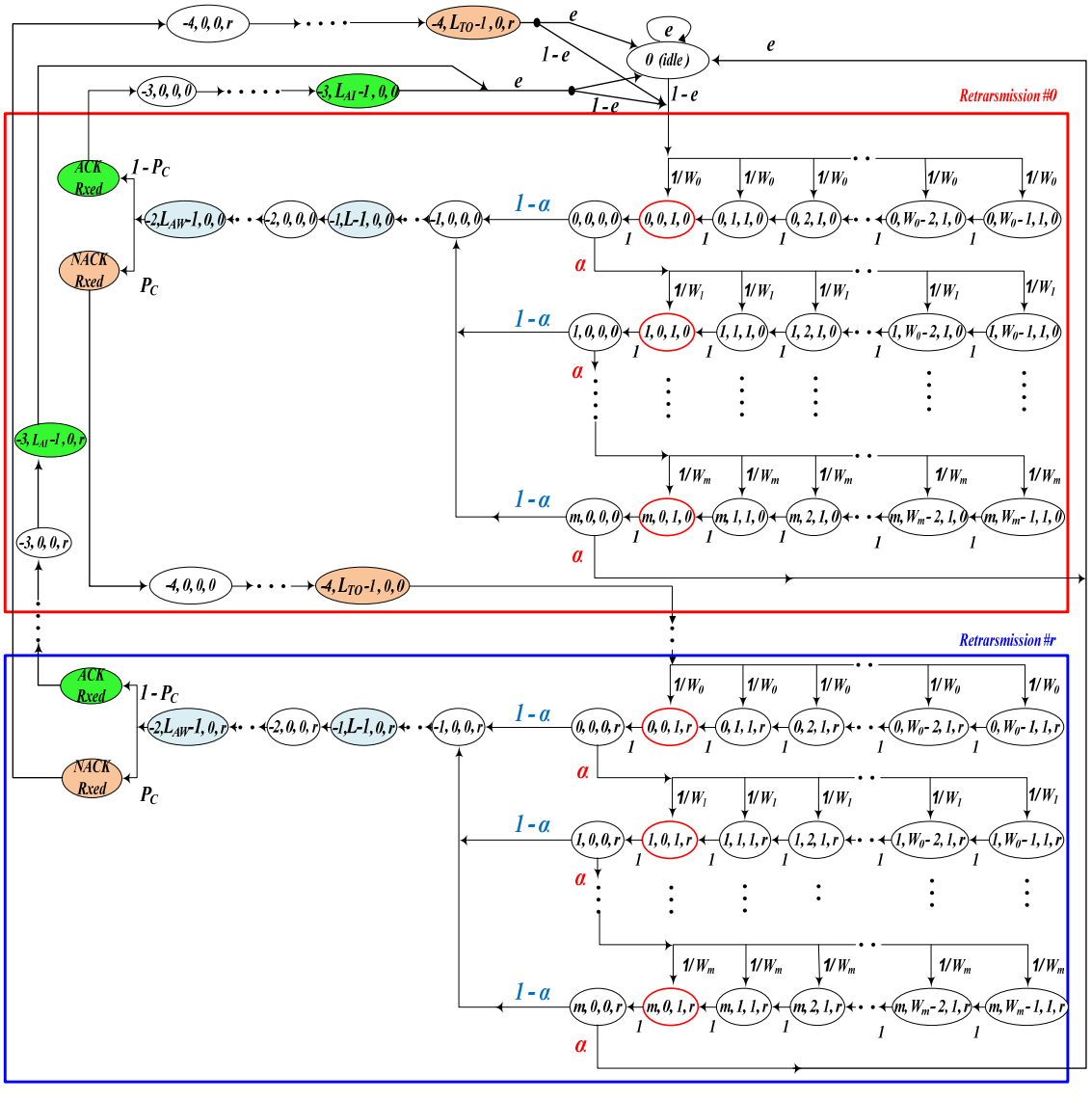


**Figure 5.1** Markov chain model for un-slotted CSMA/CA algorithm for IEEE 802.15.4.

For the performance analysis purpose, this work models the operation of the CSMA/CA algorithm in a non-beacon mode by using a discrete time Markov chain, and applies the key factors of the IEEE 802.15.4 MAC protocol such as back-off stages, acknowledgements, and retransmission schemes. The model considers uplink traffic only and the impact of different parameters such as the packet arrival rate, packet size, number of nodes, back-off components, and buffer size at each node.

This study considers a star network with a WPAN coordinator, and $N$ nodes with un-slotted CSMA/CA and ACK under the assumption of ideal channel conditions with no hidden nodes and capture. It is assumed that all nodes contend to send sensing data to the PAN coordinator. Also, packet arrivals to each device follow the Poisson process with the mean arrival rate of $\lambda$ and each node accepts new packets through a buffer until the buffer is full. Once it is full, the device does not allow new packets coming from its sensors. Note, most prior studies deal with the slotted CSMA/CA for their application and analyze the IEEE 802.15.4. For example, Park *et al*. [2009], Pollin *et al*. [2008], and Misic *et al*. [2006] proposed analytical Markov chain models for the slotted CSMA/CA of IEEE 802.15.4 MAC protocol.

From the standard, the nodes must use a CSMA/CA to access the channel to transmit packets. For our model, we apply un-slotted CSMA, i.e., non-beacon mode, protocol, because it has better throughput and higher probability of successful transmission than slotted CSMA, i.e., beacon mode.

As shown in Figure 5.1, state "0" indicates the idle state. In this state, the packet queue is empty and the node is waiting for a newly generated packet. A back-off state is described by ($i$, $W_m$ -1, 1, $l$) to ($i$, $W_0$ -1, 1, $l$). The back-off counter value of each back-off

state is in the set {0,…, $W_i$ -*1*}. Zero of this value indicates that there is no back-off time and it senses the channel for packet transmission immediately. State (*i*, *0*, *0*, *l*) represents the CCA stage. In the Markov chain model analysis, CCA is processed once for the un-slotted mode. Let $\alpha$ and 1 - $\alpha$ be the probabilities that the channel is busy and idle, respectively. Next, when entering the transmission state, packet transmission duration should be considered. State (*-1*, *j*, *0*, *l*) represents the transmission state after accessing the channel by CCA. A node transmits the packet frame when the given back-off counter reaches 0 and one CCA is successfully processed. When the node is in this state, {*0*,…, *L-1*} value of *b*(*t*) represents the state of packet transmission where *L* is the total length of a packet including overhead (PHY and MAC headers) and data payload.

Normally, after transmitting a packet, a node needs to wait for ACK packet from the receiver to confirm the successful packet transmitting and receiving. State (*-2*, *j*, *0*, *l*) represents the ACK waiting state, [*0*, $L_{AW}$ *-1*]. When the node is at this state, it switches the mode from TX to RX. Note that the waiting time to receive an ACK packet is in the range from *aTurnaroundTime* (12 *symbols*) to *aTurnaroundTime* + *aUnitBackoffPeriod* (32 *symbols*).

After ACK waiting time, if the node receives the ACK from the receiver, state (*-3*, *j*, *0*, *l*) is following a successful transmission (1 – $P_C$) mode. The reception of ACK means successful packet transmission. However, if the node fails to receive ACK, state (*-4*, *j*, *0*, *l*) is following packet collision ($P_C$) mode with probability of packet collision. When the node is at state (*-3*, *j*, *0*, *l*), time duration of an ACK frame and IFS should be considered before the next idle state. The time at state [*0*, $L_{AI}$ *-1*] represents this time duration, where $L_{AI}$ is the length of ACK frame ($L_{ACK}$) plus *IFS*. The *IFS* time depends on

the length of the transmitted data frame. When the node is at state (*-4*, *j*, *0*, *l*), [*0*, $L_{TO}$ *-1*] should be counted, where $L_{TO}$ is the timeout of ACK. After the timeout of ACK, the node moves to the next retransmission state, (*0*, *0*, *1*, *r*), to retry to transmit the failed data packet. *r* is increased by one up to *macMaxFrameRetries*.

Normally, network devices try to access the channel for transmitting their data packet during one of four states: back-off, sensing (CCA state), transmitting, and idle. In the un-slotted CSMA/CA of IEEE 802.15.4, the process {*n*(*t*), *b*(*t*), *c*(*t*), *r*(*t*)} defines the state of the device at back-off stages. *n*(*t*) represents the value of $NB \in [0,m]$, at time t, where *m* = *macMaxCSMABackoffs*. *b*(*t*) represents the value of the back-off time counter which, at the beginning of the back-off countdown, obtains a random value in the range [0, $2^{BE}$-1]. *c*(*t*) represents the remaining number of CCAs to be done for transmission at time *t*. $r(t) \in [0, r]$ represents the value of the retransmission at time *t*, where *r* = *aMaxFrameRetries.*

For convenience, probability $P\{n(t+1) = i, b(t+1) = j, c(t)=k, r(t)=l \mid n(t) = i, b(t) = j, c(t)=k, r(t)=l \}$ is written as $P\{i, j, k-1, l \mid 0, j, k, l\}$. The maximum number of retransmission attempts *macMaxFrameRetries* is denoted with *r*, and the *macMax-CSMABackoffs* (same as the maximum value of the variable *NB*) denoted with *m*. The value of *r* is defined by *macMaxFrameRetries-1,* and *m* represents the maximum value of *NB*, *macMaxCSMABackoffs-1*.

The parameter $\alpha$ in Figure 5.1 is the probability of the channel being busy during CCA. The state transmission probabilities in Figure 5.1 can be described with the following equations:

$$P\{i, j+1, 1, l \mid i, j, 1, l\} = 1, \forall\, i \in [0, m], j \in [0, 2^{BE}\text{-}1], l \in [0, r], \quad (5.1)$$

$$P\{i+1, j, 1, l \mid i, 0, 1, l\} = \frac{\alpha}{W_{i+1}}, \forall\, i \leq m, \quad (5.2)$$

$$P\{0, j, k-1, l \mid i, 0, k, l-1\} = \frac{(1-\alpha)\cdot P_C}{W_0}, \forall\, l \leq r, \quad (5.3)$$

$$P\{i, 0, 0, l \mid i, 0, 1, l\} = 1-\alpha, \forall\, i \in [0, m], l \in [0, r], \quad (5.4)$$

$$P\{0, j, 1, 0 \mid i, 0, 0, 0\} = \frac{(1-P_C)\times(1-e)}{W_0}, \forall\, i \in [0, m], j \in [0, 2^{BE}\text{-}1] \quad (5.5)$$

$$P\{0, j, 1, 0 \mid idle\} = \frac{1-e}{W_0}, \forall\, i \in [0, m], j \in [0, 2^{BE}\text{-}1], \quad (5.6)$$

$$P\{idle \mid m, 0, 0, l\} = \alpha \times e, \forall\, l < r, \quad (5.7)$$

$$P\{idle \mid i, 0, 0, r\} = (1-\alpha) \times e, \forall\, i < m, \quad (5.8)$$

$$P\{idle \mid m, 0, 0, r\} = e, \quad (5.9)$$

$$P\{idle \mid i, 0, 0, l\} = (1-P_C) \times e, \forall\, i \in [0, m], l \in [0, r], \quad (5.10)$$

Equation (5.1) shows the probability that the back-off period is decremented after each *aUnitBackoffPeriod*. This probability happens with probability 1. Equation (5.2)

represents the probability that the device sensing the busy channel chooses another random back-off in the range [*0*, $W_{i+1}$ *-1*]. Equation (5.3) represents the unsuccessful transmission probability after sensing an idle channel in a CCA process, and the device goes to the next retransmission stage. Equation (5.4) determines the probability *1-α* that the channel is sensed to be idle at the first CCA process. Note that the Slotted CSMA, process checks the CCA twice after it finishes the back-off periods, while the un-slotted CSMA, process checks the CCA only once [IEEE 802.15.4 spec., 2006]. The transition probability in equation (5.5) represents the probability of choosing a random duration of the back-off period after a channel access. "*1-e*" represents the probability for a node to stay at the transmission state. In other words, Equation (5.5) models the probability of going back to the first back-off stage from back-off stage. Equation (5.6) corresponds to the probability of moving from the idle stage to one back-off stage. Equations (5.7) and (5.8) describe the probabilities of going back to the idle stage due to the channel access failure and retransmission limits. Equation (5.9) is the probability of going back to the idle stage at back-off counter *m* and retransmission stage *r*, by considering the offered traffic load. The last equation (5.10) represents the probability when the node buffer has no more arrived data packet, i.e., buffer being empty, after the channel access and the node goes to the idle stage.

### 5.3.1 Steady State Probability Analysis of Markov Chain Model

Denote the Markov chain's steady state probabilities by $b_{i,j,k,l} = P\{(n(t), b(t), c(t), r(t)) = (i, j, k, l)\}, \forall\ i \in \{-2, m\},\ j \in \{0, \max(W_i - 1,\ L - 1, L_{AW} - 1,\ L_{AI} - 1, L_{TO} - 1)\},\ k \in \{0, 1\}$ and $l \in \{0, r\}$.

$$b_{i,j,k,l} = \frac{W_i - j}{W_i} \cdot b_{i,0,k,l} \tag{5.11}$$

where

$$W_i = \begin{cases} 2^i \times W_0\,, & (i \le B_M - B_m) \\ 2^{BM-Bm} \times W_0\,, & (B_M - B_m < i \le NB) \end{cases} \tag{5.12}$$

For simplification, let $W_0$ stand for $2^{Bm}$, and let $i$ represent the current value of $NB$ during the execution of the algorithm. The maximum value of the random back-off waiting time can be represented as $W_i = 2^{min(i,\ BM-Bm)} \cdot W_0 = 2^{min(i+Bm\ ,\ BM)}$.

From equations (5.2) and (5.4), for $i \le m$

$$b_{i-1,0,0,l} = \alpha \cdot b_{i,0,0,l}\,, \quad 0 < i \le m \tag{5.13}$$

which leads to

$$b_{i,0,0,l} = \alpha^i \cdot b_{0,0,0,l}\,, \quad 0 < i \le m \tag{5.14}$$

For sum of all back-off stage before a CCA procedure is

$$\sum_{i=0}^{m} b_{i,0,0,l} = \frac{1-\alpha^{m+1}}{1-\alpha} \times b_{0,0,0,l} \tag{5.15}$$

$$b_{-1,0,0,l} = (1-\alpha^{m+1}) \cdot b_{0,0,0,l} \tag{5.16}$$

$$b_{000l} = P_c \cdot b_{-1,0,0,l-1} = P_c \cdot (1-\alpha) \cdot \sum_{i=0}^{m} b_{i,0,0,l-1} = \left(P_c \cdot (1-\alpha^{m+1})\right)^l \cdot b_{0000} \tag{5.17}$$

$$b_{-1,0,0,l} = (1-\alpha^{m+1})^{l+1} \cdot (P_C)^l \cdot b_{0,0,0,0} \qquad (5.18)$$
$$= (1-\alpha^{m+1}) \cdot ((1-\alpha^{m+1}) \cdot P_C)^l \cdot b_{0,0,0,0}$$

The sum of all probabilities must be 1. Therefore,

$$\sum_{i=0}^{m}\sum_{j=0}^{W_i-1}\sum_{k=0}^{1}\sum_{l=0}^{r} b_{i,j,k,l} + \sum_{l=0}^{r}\left(\sum_{j=0}^{L-1} b_{-1,j,0,l} + \sum_{j=0}^{L_{AW}-1} b_{-2,j,0,l} + \sum_{j=0}^{L_{AI}-1} b_{-3,j,0,l} + \sum_{j=0}^{L_{TO}-1} b_{-4,j,0,l}\right) \qquad (5.19)$$
$$+ b_{idle} = 1$$

Equation (5.19) describes the normalized condition of all steady state probabilities in the Markov chain model. The Markov chain can be treated to have five different steady state probabilities only. First is the probability of a distributed back-off process, the second part is the probability of CCA processing, the third part is that of successful packet transmission, the fourth part is that of unsuccessful transmission and the last one is that of the idle state.

$$\sum_{i=0}^{m}\sum_{j=0}^{W_i-1}\sum_{l=0}^{r} b_{i,j,k,l} = \sum_{i=0}^{m}\sum_{l=0}^{r}\frac{W_i+1}{2}\cdot b_{i00l} = \sum_{i=0}^{m}\sum_{l=0}^{r}\frac{W_i+1}{2}\cdot \alpha^i \cdot b_{000l}$$

$$= \begin{cases} \dfrac{b_{0000}}{2}\left(\dfrac{1-(2\alpha)^{m+1}}{1-2\alpha}\cdot W_0 + \dfrac{1-\alpha^{m+1}}{1-\alpha}\right)\dfrac{1-(A)^{r+1}}{1-A}, \\ \qquad m \le B_M - B_m \\ \dfrac{b_{0000}}{2}\left(\dfrac{1-(2\alpha)^{B_M-B_m+1}}{1-2\alpha}W_0 + \dfrac{1-\alpha^{B_M-B_m+1}}{1-\alpha} + \alpha^{B_M-B_m+1}(2^{B_M}+1)\dfrac{1-\alpha^{m-B_M+B_m}}{1-\alpha}\right)\dfrac{1-(A)^{r+1}}{1-A}, \\ \qquad B_M - B_m < m \le NB \end{cases}$$

(5.20)

where $L_{AT} = L + L_{AW}$ and $A = P_c \cdot (1 - \alpha^{m+1})$

Equation (5.20) shows the probability of the back-off process. When $m \leq B_M - B_m$ and $B_M - B_m < m \leq NB$, $W_i$ is subtracted as $2^i W_0$ and $2^{B_M - B_m} \cdot W_0$ from Equation (5.12).

$$\sum_{l=0}^{r}\left(\sum_{j=0}^{L-1} b_{-1,j,0,l} + \sum_{j=0}^{L_{AW}-1} b_{-2,j,0,l}\right) \tag{5.21}$$

$$= \sum_{l=0}^{r}\left(\sum_{j=0}^{L_{AT}-1} b_{-1,j,0,l}\right) = \sum_{l=0}^{r}\left(L_{AT}(1-\alpha^{m+1}) b_{0,0,0,l}\right)$$

$$= L_{AT}(1-\alpha^{m+1}) \sum_{l=0}^{r} A^l \; b_{0,0,0,0} = L_{AT}(1-\alpha^{m+1}) \frac{1-A^{r+1}}{1-A} \; b_{0,0,0,0}$$

Equation (5.21) represents the probability of transmission state ($b_{-1,0,0,l}$) and sum of the packet transmission period ($L$) and ACK waiting time ($L_{AW}$).

$$\sum_{l=0}^{r}\left(\sum_{j=0}^{L_{AI}-1} b_{-3,j,0,l}\right) = \sum_{l=0}^{r}\left(L_{AI}(1-P_C)(1-\alpha^{m+1}) b_{0,0,0,l}\right) \tag{5.22}$$

$$= L_{AI}(1-P_C)(1-\alpha^{m+1}) \sum_{l=0}^{r} A^l \, b_{0,0,0,0}$$

$$= L_{AI}(1-P_C)(1-\alpha^{m+1}) \frac{1-A^{r+1}}{1-A} b_{0,0,0,0}$$

Equation (5.22) represents the sum of probabilities of successful packet transmission with received ACK and time period of $T_{ACK}$ and *IFS*. After this time period,

back-off processing for transmitting another packet or idle state for waiting for newly generated packets is as follows.

$$\sum_{l=0}^{r}\left(\sum_{j=0}^{L_{TO}-1} b_{-4,j,0,l}\right) = L_{TO}(P_C)(1-\alpha^{m+1})\sum_{l=0}^{r} A^l\, b_{0,0,0,0} \tag{5.23}$$

$$= L_{TO}(P_C)(1-\alpha^{m+1})\frac{1-A^{r+1}}{1-A} b_{0,0,0,0}$$

Equation (5.23) represents the sum of probabilities of unsuccessful packet transmission without receiving ACK and time period of $L_{TO}$. After this time period, back-off processing of the next retransmission state due to failed packet transmission for retransmitting a packet or idle state for waiting for newly generated packet due to the limit of *macMaxFrameRetries* is as follows.

$$idle(0) = e \cdot idle(0) + e \times \left[\sum_{l=0}^{r} \alpha \cdot b_{m,0,0,l} + P_C \cdot b_{-1,0,0,r} + \sum_{l=0}^{r}(1-P_C)\cdot b_{-1,0,0,l}\right] \tag{5.24}$$

$$= \frac{e}{1-e}\cdot\left[\alpha^{m+1}\cdot\frac{1-A^{r+1}}{1-A} + A^{r+1} + (1-P_C)(1-\alpha^{m+1})\cdot\frac{1-A^{r+1}}{1-A}\right]\cdot b_{0000}$$

Equation (5.24) shows the idle probability. It contains the probability for repeating the idle state for waiting for newly generated packets, channel access failed ($\alpha$) due to a busy channel, probability for packet collision after the maximum retransmission limit is reached and probability of successful transmission.

Equations (5.20) ~ (5.24) represent all the possible state values $b_{i,j,k,l}$ in terms of $b_{0,0,0,0}$. Equation (5.19) shows the sum of all possible state values $b_{i,j,k,l}$ to 1. Therefore, the expression for $b_{0,0,0,0}$ can be obtained by replacing Equation (5.19) with

Equations (5.20) ~ (5.24). Also, $b_{0,0,0,0}$ is used for figuring out the probabilities of τ and $\alpha$.

When $m \leq B_M - B_m$, we can obtain $b_{0,0,0,0}$ as follows:

(5.25-1)

$$b_{0000} = \left[\frac{B}{2}\left(\frac{1-(2\alpha)^{m+1}}{1-2\alpha}W_0 + \frac{C}{1-\alpha}\right) + L_{AT}\cdot B\cdot C + L_{AI}(1-P_C)B\cdot C + L_{TO} \cdot P_C \cdot B \cdot C + \frac{e}{1-e}(\alpha^{m+1}B + A^{r+1} + (1-P_C)B\cdot C)\right]^{-1}$$

When $B_M - B_m < m \leq NB$, we can obtain $b_{0,0,0,0}$ as:

(5.25-2)

$$b_{0000} = \left[\frac{B}{2}\left(\frac{1-(2\alpha)^{B_M-B_m+1}}{1-2\alpha}W_0 + \frac{1-\alpha^{B_M-B_m+1}}{1-\alpha} + \alpha^{B_M-B_m+1}(2^{BM}+1)\frac{1-\alpha^{m-B_M+B_m}}{1-\alpha}\right) + L_{AT}\cdot B\cdot C + L_{AI}(1-P_C)B\cdot C + L_{TO}\cdot P_C\cdot B\cdot C + \frac{e}{1-e}(\alpha^{m+1}B + A^{r+1} + (1-P_C)B\cdot C)\right]^{-1}$$

where $\frac{1-A^{r+1}}{1-A} = B$ and $(1-\alpha^{m+1}) = C$.

The packet collision probability $P_C$ is that at least one of the remaining nodes ($N$-$1$) transmits in the same time period.

$$P_C = 1 - (1-\tau)^{N-1} \tag{5.26}$$

where $N$ is the total number of nodes.

## 5.4 Performance Analysis

In Section 5.3, the steady state probabilities of the Markov chain of a CSMA/CA mechanism used in un-slotted IEEE 802.15.4 are analyzed. The start of packet transmitting operation in IEEE 802.15.4 is performed according to carrier sensing probability and channel access probability. If a node tries to transmit a packet, first it needs to wait in a back-off stage by a pre-given back-off exponent (*BE*) parameter. After back-off counter reaches 0, it attempts to sense the channel's status in a randomly chosen time slot. From Equations (5.15) and (5.17), the first carrier sensing probability (τ) that a node attempts a CCA can be derived as follows

$$\tau = \sum_{i=0}^{m}\sum_{l=0}^{r} b_{i,0,0,l} = \sum_{l=0}^{r}\left(\frac{1-\alpha^{m+1}}{1-\alpha}\right)\cdot b_{0,0,0,l} = \left(\frac{1-\alpha^{m+1}}{1-\alpha}\right)\cdot\left(\frac{1-(A)^{r+1}}{1-A}\right)\cdot b_{0,0,0,0} \tag{5.27}$$

After the channel is sensed to be idle once for CCA, it can start the packet transmission in un-slotted IEEE 802.15.4. If the channel is sensed to be busy after CCA due to any data transmission from other nodes, it goes to the next back-off stage for another channel sensing. In other words, at least one of *N*-1 remaining nodes transmits in the same time slot as the current transmitting node intends to do so. *N* is the total number of nodes in the same network area.

The parameter $\alpha$ is the probability of the channel being busy during CCA. Note that CCA proceeds twice in slotted CSMA/CA while only once in un-slotted CSMA/CA. In the same network area, the probability of channel being idle, 1- $\alpha$, at CCA of a certain device is same with the probability that all other *N*-1 devices, are in other states except

the packet transmission state. The busy channel probability $\alpha$ at CCA of a certain device can be found as

$$\alpha = 1 - \left(1 - \sum_{k=1}^{r} b_{-1,0,0,l}\right)^{N-1} \tag{5.28}$$

where $b_{-1,0,0,l}$ is the steady state probability of packet transmission in the Markov chain as shown in Figure 5.1.

Following [Park, *et al.*, 2009 and S. Pollin, *et al.*, 2008], the probability of a busy channel as $\alpha$ in a non-beacon mode with an ACK option can be defined. Then

$$\alpha = \alpha_1 + \alpha_2 \tag{5.29}$$

where $\alpha_1$ is the probability of finding the channel being busy during CCA due to data transmission by another node and $\alpha_2$ is the probability of finding the channel being busy during CCA due to *ACK* transmission (from the coordinator to another node). They can be derived as

$$\alpha_1 = L_{Packet} \times (1 - (1 - \tau)^{N-1}) \times (1 - \alpha) \tag{5.30}$$

$$\alpha_2 = L_{ACK} \times \frac{N \times \tau \times (1 - \tau)^{N-1}}{1 - (1 - \tau)^N} \times (1 - (1 - \tau)^{N-1}) \times (1 - \alpha) \tag{5.31}$$

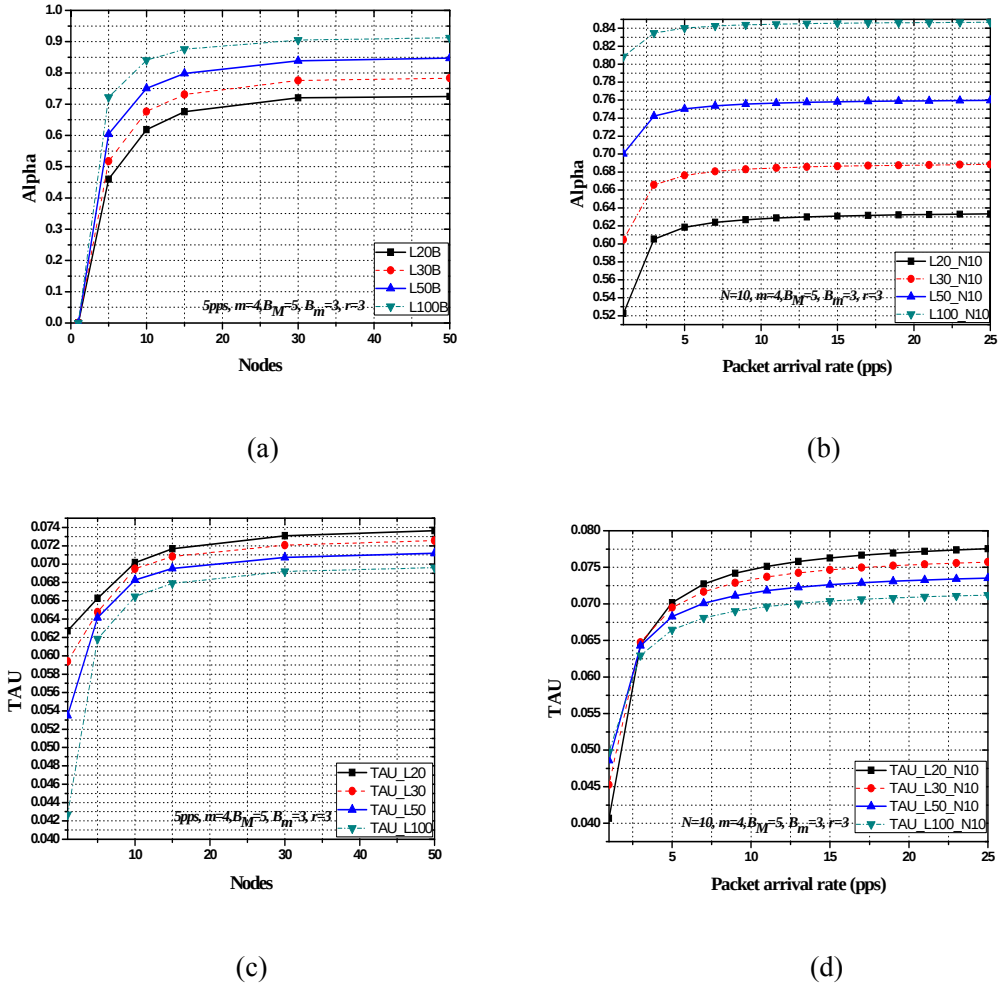


**Figure 5.2** Comparison of $\alpha$ and $\tau$ with nodes and different packet arrival rate.

The beginning of the network transmission is determined by the probability, $\tau$, that a node attempts a first carrier sensing and the probability, $\alpha$, that channel is busy. These are derived from Equations (5.27) ~ (5.31) based on the Markov chain analysis. Figure 5.2 shows the characteristics of parameters $\tau$ and $\alpha$ with a different number of nodes, packet arrival rate and different size of payload. In this figure, CSMA/CA MAC parameters are set as default values, i.e., $B_M$=5, $B_m$=3, $m$=4, and $r$=3. Figures 5.2(a) and (c) show $\alpha$ and $\tau$ with a fixed packet arrival rate at 5pps and from 1 to 50 nodes. Figures

5.2(b) and (d) show $\alpha$ and $\tau$ with a fixed number of nodes at 10 and packet arrival rate from 1pps to 25pps.

From Figure 5.2, it is found that these two parameters increase with the number of nodes and packet arrival rate. According to Equations (5.30) and (5.31), $\alpha$ increases with the number of nodes and size of data packet or ACK. As the network reaches the size of 10 nodes, $\alpha$ and $\tau$ increase to their relatively high value while their growth rate slows down thereafter. The probability of the channel being busy is large with a large number of nodes due to much contention for the channel. As for the different size of a packet, $\alpha$ and $\tau$ show a different pattern. From Figure 5.2(a), $\alpha$ increases with the size of data payload. As the packet size grows, other nodes are hard to sense the idle channel for their packet transmission. It is because a large-size packet takes a longer time to stay in the channel than a small size packet. The probability that a node attempts to sense the channel decreases with an increasing size of data payload in Figure 5.2(c). This is because a smaller data packet has more chances to access the channel than a larger data packet because a smaller data packet has shorter time for packet transmission than a larger one. In this analysis, it is assumed that each node transmits the data continuously based on different packet arrival rate.

### 5.4.1 Throughput

In this section the Markov chain model to analyze the network throughput behavior of IEEE 802.15.4 in a non-beacon mode is used. A WPAN consisting of one PAN coordinator and *N* devices in uplink traffic network is considered. In addition, it is assumed that all *N* devices have at least one packet frame to transmit all the time. The normalized system throughput *S* is defined as the fraction of successfully transmitting

payload bits to total processing time. Total processing time consists of the mean idle duration that the channel is idle, and means duration of time for a packet's successful transmission and collision. To analyze the throughput, the successful transmission probability based on the Markov chain model should be derived. $P_s$ as the successful data transmission probability occurs at the channel for exactly one node transmitting its packet. It can be found as

$$P_S = \frac{N \times \tau \times (1-\tau)^{N-1} \times (1-\alpha)}{P_{tr}} = \frac{N \times \tau \times (1-\tau)^{N-1}}{1-(1-\tau)^N} \tag{5.32}$$

where $P_{tr}$ is the probability when there is at least one packet transmission in the same network area. $P_{tr}$ is calculated as $(1-(1-\tau)^N) \cdot (1-\alpha)$. Then the channel throughput can be represented as

$$S = \frac{E[Successful\ transmitted\ payload\ bits]}{BusyTime + IdleTime} \tag{5.33}$$

$$= \frac{P_{tr} \cdot P_S \cdot E[L_{Packet}]}{(1-P_{tr})\sigma + P_S \cdot P_{tr} \cdot T_S + (1-P_S) \cdot P_{tr} \cdot T_C}$$

where *BusyTime* is the mean duration that some device transmits a packet in the same network area and *IdleTime* is the mean idle duration that the channel is idle. $T_S$ is the average time required for the successful packet transmission and $T_C$ is that for packet collision. $T_S$ and $T_C$ are represented as follows

$$T_S = T_{Packet} + \delta + T_{W\_ACK} + T_{ACK} + \delta + T_{IFS} \tag{5.34}$$

$$T_C = T_{Packet} + \delta + T_{Ack\_Time\_Out} \tag{5.35}$$

$P_{tr} \cdot P_S \cdot E[L_{Packet}]$ is the average payload size in slots for successful packet transmission. $E[L_{Packet}]$ is average packet payload size in number of slots. If there is at least one packet transmission in a network window in the channel, successful and failed packet transmission probabilities are represented as $P_S \cdot P_{tr}$ and (1-$P_S$) $\cdot$ $P_{tr}$, respectively. Also, besides the processing for transmission, the remaining time is configured as an idle period and this is represented as $(1 - P_{tr})\sigma$. Idle period, $\sigma$, contains contention window period time. It includes total back-off period time and total channel accessing time ($T_{CCA}$) until successful packet transmission is performed. Contention window period is represented by $T_{TB} + \lceil R \rceil \times T_{CCA}$ in slots. $R$ is the average number of back-off attempts and $T_{TB}$ [Choi and Zhou, 2010] is the sum of the average back-off times in slots of each period. Note that this analysis, considers no retransmission.

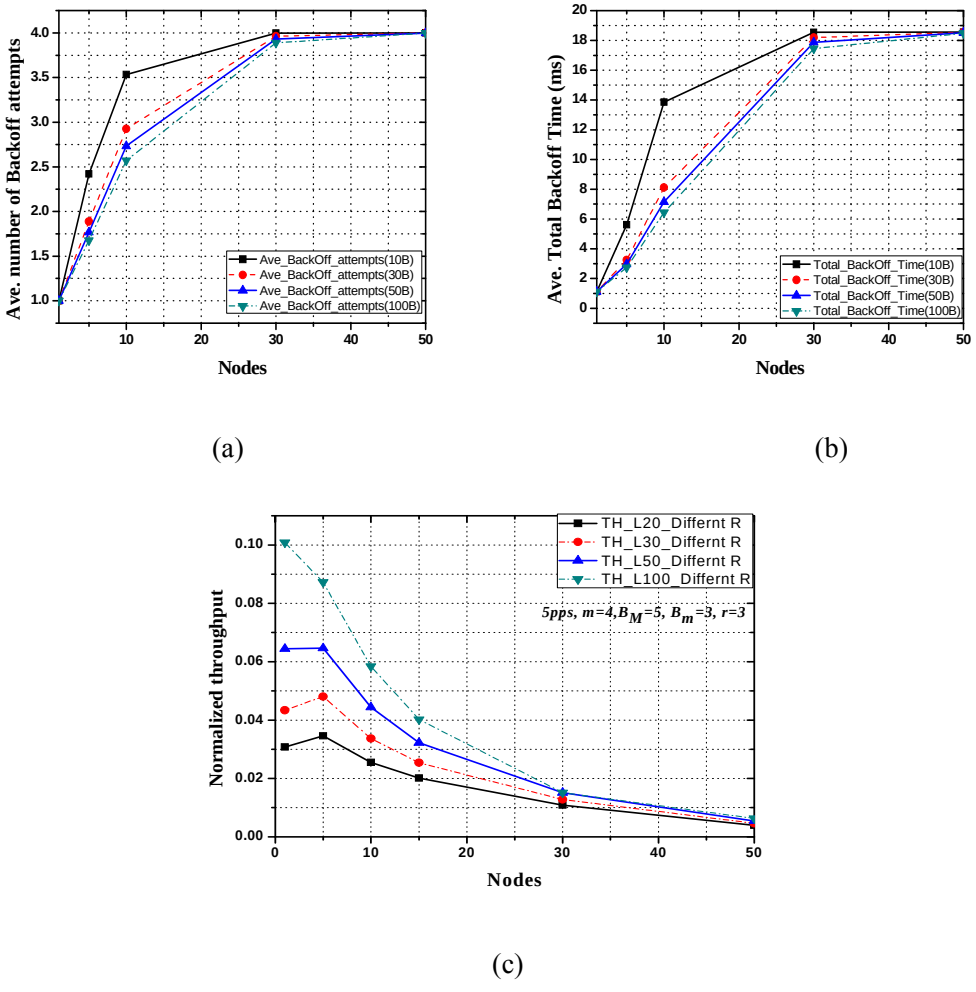


**Figure 5.3** Comparison of the average number of back-off attempts, total back-off time and throughput with the number of nodes and payload size.

From Equation (5.33), throughput is affected by packet length, idle time and busy time based on the probabilities of successful and failed packet transmission. In this analysis, packet length varies from 20 to 100 byte payloads. The number of back-off attempts based on the channel status is a critical factor in throughput. If it increases due to the busy channel, throughput decreases because a node can transmit more packets in few back-off attempts (short back-off period time). In other words, throughput decreases

since packets need to wait for longer back-off period time before sensing the channel. Actually, each different back-off period depends on the value of *BE*. As mentioned in Chapter 4, back-off period is randomly determined by *k*unitbackoffperiods* where $k \in \{0, 1, \cdots 2^{BE}\text{-}1\}$. So it is hard to measure the exact back-off period time for different status. In this study, we use the average back-off time for each back-off interval as analyzed in Chapter 4.

In general, increasing network traffic due to an increasing number of nodes increases the number of back-off attempts for packet transmission. This is due to the busier channel caused by the heavier traffic. As the network size increases, nodes are easier to have collision with others when they transmit their packet in the same time slot right after accessing the idle channel. This is because each node cannot recognize other nodes that are also sensing the channel and trying to transmit their packets in the same period of time.

Figure 5.3 shows the average number of back-off attempts, average total back-off time and throughput versus the number of nodes and payload size. Average number of back-off attempts and total back-off time increase with the number of nodes and payload size. Also, they increase as payload size decreases. When the number of nodes exceeds 30, as shown in Figures 5.3(a) and (b), there is no big difference in the average number of back-off attempts and total back-off time. This is because that the possible number of back-off attempts is limited to the given *macMaxCSMABackoffs* as 4. When the number of nodes is from 1 to 10, however, back-off attempts and total back-off time change to 3.5 times and 14 times higher, respectively.

Figure 5.3(c) represents the normalized throughput with the number of nodes and size of payload. Normalized throughput decreases as the number of nodes increases due to more contention. Because of more contention for the channel due to the heavy traffic, they are hard to get an idle channel for packet transmission. Hence, they need to try more back-off attempts and more time for back-off periods. A large number of nodes thus lowers throughput. Also, normalized throughput increases for larger payload, because larger payload has longer transmission time than a small one.

### 5.4.2 Reliability

Normally, packets are resumed or dropped due to the channel access failure or retry limits for an uplink data packet. To transmit the data packet successfully for an uplink traffic mode, each node has to compete for the access to the channel first. If a node could not obtain the idle channel status in one CCA within $m$+1 back-offs at un-slotted CSMA/CA, channel access failure is declared. If a node accesses the idle channel, it transmits its packet. After transmitting the data to the coordinator, a node waits for ACK from the coordinator. If it does not receive the ACK from the coordinator due to packet collision or loss, it tries to retransmit the data up to the number of $r$ =*macMax-FrameRetries*. Finally, if the transmission fails for repeating packet collisions after $r$+1 attempt, a packet is dropped.

Discarded packet probability due to channel access failure is

$$P_{CAF} = \sum_{l=0}^{r} \alpha \cdot b_{m,0,0,l} = \alpha^{m+1} \times \frac{1 - \left(P_c(1-\alpha^{m+1})\right)^{r+1}}{1 - P_c(1-\alpha^{m+1})} \tag{5.36}$$

Packet drop probability due to the retransmission limit is

$$P_{CRT} = \sum_{i=0}^{m} P_C \cdot b_{Tx} = \sum_{i=0}^{m} P_C \cdot (1-\alpha) \cdot b_{i,0,0,r} = \left(P_c(1-\alpha^{m+1})\right)^{r+1} \tag{5.37}$$

where $b_{Tx} = b_{i,-1,0,r} = (1-\alpha) \cdot b_{i,0,0,r}$

From Equations (5.36) and (5.37), the reliability of the network is

$$P_{Re} = (1 - P_{CAF}) \times (1 - P_{CRT}) \cong 1 - (P_{CAF} + P_{CRT}) \tag{5.38}$$

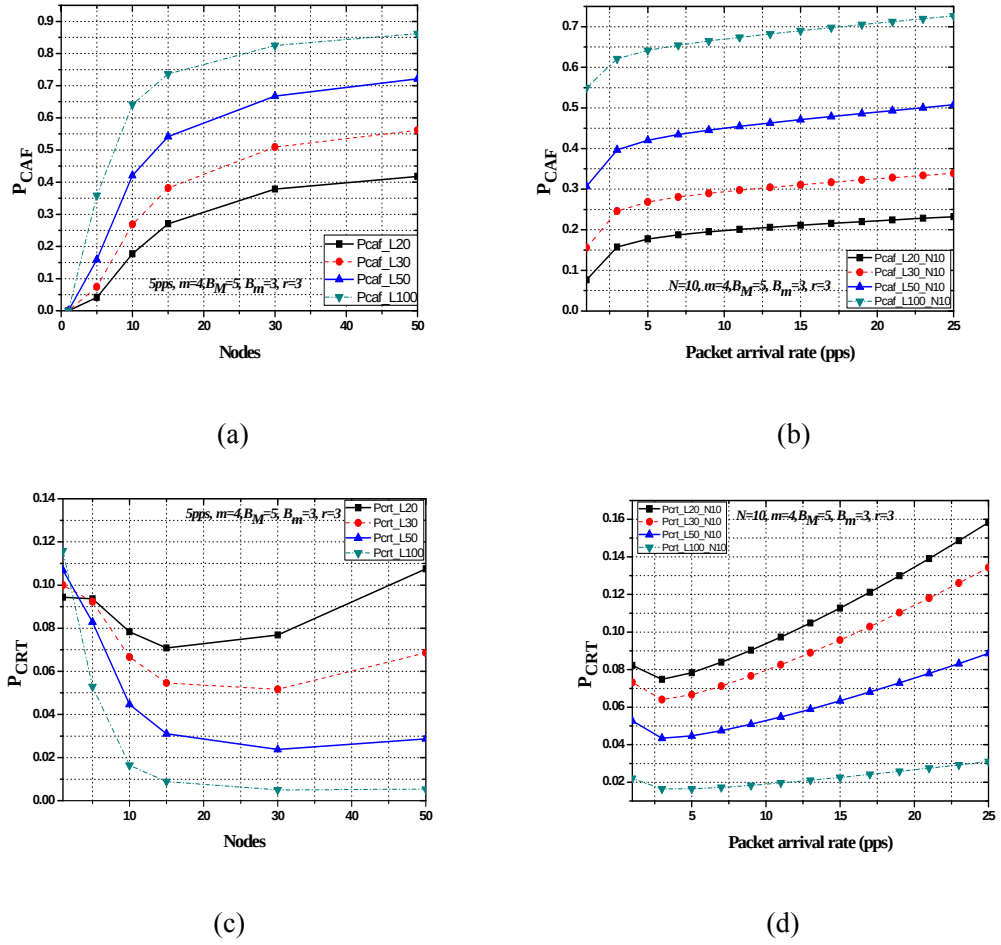


**Figure 5.4** $P_{CAF}$ and $P_{CRT}$ vs. the number of nodes and different packet arrival rate.

$P_{CAF}$ and $P_{CRT}$ influenced by the number of nodes and packet arrival rate are illustrated in Figure 5.4. In Figures 5.4(a) and (c), network parameters, such as 5*pps*, $m$=4, $B_M$=5, $B_m$=3 and $r$=3, are used for analyzing $P_{CAF}$ and $P_{CRT}$. $N$=10, $m$=4, $B_M$=5, $B_m$=3 and $r$=3, are used in Figures 5.4 (b) and (d).

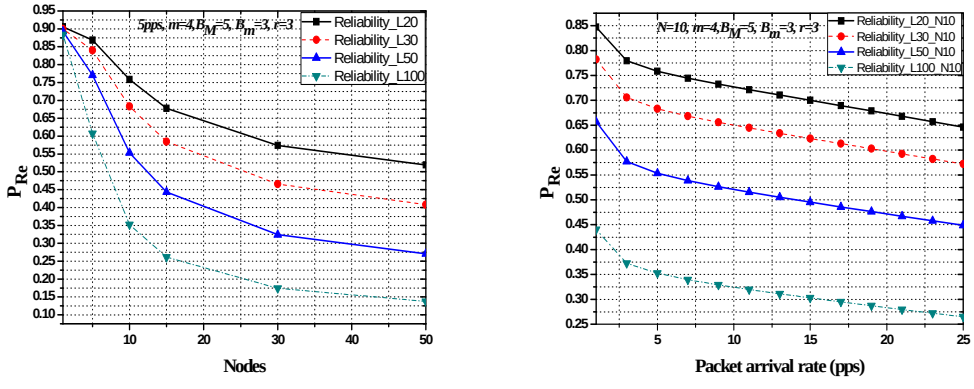


(a) (b)

**Figure 5.5** Reliability vs. the number of nodes and packet arrival rate.

Figure 5.5 (a) shows the reliability that decreases with the size of payload and number of nodes for the same packet arrival rates. Reliability decreases for cases from 1 to 60 nodes. As nodes increase at the same packet arrival rate, more and more packet transmissions should happen at a certain time. It would lead to decreased reliability. Also, it can be shown that smaller size payload result in higher reliability than larger one at the same number of nodes and packet arrival rate in Figures 5.5(a) and (b). This reason is that large size of payload charges more channel and transmission time for each packet at the same network size and data rate.

### 5.4.3 Delay Analysis

In low-rate wireless network applications, access delay is also an important metric. Generally, total delay in a communication network includes processing delay, queuing delay, access delay, and propagation delay [Misic, *et al*., 2005].

In this section, it is derived that the delay for a successfully transmitted and received packet as the time from when the generated packet is ready to be transmitted from the MAC buffer of each network device, to when an ACK is received from the coordinator for successful transmission. Also, if an ACK option is not considered for data transmission, delay is reduced. Since the turnaround time and ACK receiving time no longer exist. ACK option, however, has been adopted in this analysis.

The total successful packet transmission time as $T_S$ and the packet collision time as $T_C$ with ACK are assigned. $T_S$ is computed when there is no retransmission attempt due to the data collision or packet lost. It does not include back-off time period and channel sensing time. Also, successful packet transmission time without ACK is described as $T_{NACK}$.

$$T_S = T_{Packet} + \delta + T_{W\_ACK} + T_{ACK} + \delta + T_{IFS} \tag{5.39}$$

$$T_C = T_{Packet} + \delta + T_{Ack\_Time\_Out} \tag{5.40}$$

$$T_{NACK} = T_{Packet} + \delta + T_{IFS} \tag{5.41}$$

where $T_{Packet}$ is the total time of packet length including packet overhead and data payload, $\delta$ is the propagation delay, $T_{W\_ACK}$ is the waiting time to receive the ACK frame from the receiver, $T_{ACK}$ is the length of the ACK frame time, $T_{IFS}$ is the IFS time, and $T_{ACK\_Time\_Out}$ is the timeout of the ACK. The IFS time depends on the length of the data frames and $T_{W\_ACK}$ is in the range between $T_{TA}$ and $T_{TA} + T_{UB}$.

Normally, total time for a packet's successful transmission includes its generating time, queuing delay, total back-off time period due to *aMaxCSMABackoffs* and *macMaxFrameRetries*, channel sensing time for channel access, time for transmission failure until successful transmission and successful packet transmission time in the end.

This study does not consider the processing delay and queuing delay because these are related with the hardware part, such as MCU, sensor and memory. Note that, other models [Jung *et al*., 2009 and Pollin *et al*., 2008] do not consider the packet transmission time, ACK waiting time and ACK packet receiving time before declared packet collision or packet failure. Especially, most of them [Pollin *et al*., 2008, Park *et al*., 2009, Sahoo and Sheu, 2008, Jung *et al*., 2009, Bae *et al*., 2010, Lee *et al*., 2010, Kim *et al*., 2011 and Wang *et al*., 2011] declare successful packet transmission or packet collision just after channel access sensing without any time period. CSMA/CA protocol can transmit a packet and wait for the ACK from the coordinator to confirm the successful packet transmission right after channel access sensing (1 - $\alpha$). If a node receives ACK from the coordinator within the waiting time, it declares successful packet transmission ($1 - P_C$) and goes to the idle stage or back-off stage for transmitting the next packet. If it does not receive the ACK within the ACK waiting time, however, it declares packet collision with probability $P_C$ or packet failure and goes to the next retransmission

stage depending upon if *macMaxFrameRetries* is reached. But most of the Markov models [Jung *et al*., 2009, Pollin *et al*., 2008, Sahoo and Sheu, 2008] do not consider this time period in the computation of total delay time. As mentioned in Section 5.4.2, a packet is discarded if there is in channel access failures. If a packet is successfully transmitted at the $i^{th}$ back-off stages of the $r^{th}$ retransmission, the maximum back-off stages of packet transmission is $(m+1) \times r + (i+1)$, i.e., the maximum back-off stages of unsuccessful channel access is $(m+1) \times r + i$. Because the value of back-off is drawn according to a discrete uniform distribution in [0, $W_i$ - 1], the mean number of slots spent in a back-off stage can be obtained as $(W_i - 1)/2$. It is assumed that total delay for one packet transmission is a normalized sum of total back-off period time until successful packet transmission, channel access time after each back-off period, time period for transmission failure and last time period for successful transmission at the $i^{th}$ stage of the $r^{th}$ retry.

First, delay for average back-off time and channel accessing unsuccessfully at the $(i-1)^{th}$ and $r^{th}$ retry can be described as

$$D1 = T_{BF} + E[CCA] \times P_{CCA} \tag{5.42}$$

$$= \sum_{l=0}^{r-1} \sum_{i=0}^{m} \left( \frac{W_i - 1}{2} \cdot b_{i01l} \right) + \sum_{i=0}^{i-1} \left( \frac{W_i - 1}{2} \cdot b_{i01l} \right) + (T_{ta} + T_{CCA})$$

$$\times \left( \sum_{l=0}^{r-1} \sum_{i=0}^{m} \alpha \cdot b_{i00l} + \sum_{i=0}^{i-1} \alpha \cdot b_{i00l} \right)$$

From Equation (5.12), D1 can be represented as two different equations, depending on the different back-off stages, i.e., *m*

When $i \le B_M - B_m$ , $W_i = 2^i \times W_0$

$$D1 = \frac{1-A^r}{1-A} \cdot \frac{b_{0000}}{2} \cdot \left( \frac{1-(2\alpha)^{m+1}}{1-2\alpha} \cdot W_0 - \frac{1-\alpha^{m+1}}{1-\alpha} \right) + \frac{b_{0000}}{2} \cdot A^l \cdot \left( \frac{1-(2\alpha)^i}{1-2\alpha} \cdot W_0 - \frac{1-\alpha^i}{1-\alpha} \right) + (T_{ta} + T_{CCA}) \cdot \left( \frac{1-A^r}{1-A} \cdot \frac{\alpha \cdot (1-\alpha^{m+1})}{1-\alpha} \cdot b_{0000} + A^l \cdot \frac{\alpha \cdot \left(1-\alpha^i\right)}{1-\alpha} \cdot b_{0000} \right) \quad (5.43)$$

When $B_M - B_m < i \le NB$, $W_i = 2^{B_M - B_m} \times W_0$

$$D1 = \frac{W_0 \cdot 2^{B_M - B_m} - 1}{2} \times \frac{b_{0000}}{1-\alpha} \times \left( \frac{1-A^r}{1-A} \times (1-\alpha^{m+1}) + A^l \times \left(1-\alpha^i\right) \right) + (T_{ta} + T_{CCA}) \cdot \left( \frac{1-A^r}{1-A} \cdot \frac{\alpha \cdot (1-\alpha^{m+1})}{1-\alpha} \cdot b_{0000} + A^l \cdot \frac{\alpha \cdot \left(1-\alpha^i\right)}{1-\alpha} \cdot b_{0000} \right) \quad (5.44)$$

where *r* and *i* are the $i^{th}$ stage of the $r^{th}$ retry for one packet's successful transmission, and *l* is the value of *macMaxFrameRetries*.

Second, delay for transmission failures until successful transmission for a packet can be described as:

$$D2 = T_{BF} + E[time\ for\ trasmission\ failure] \times P_C \tag{5.45}$$

$$= \ D1 + \ P_C \times \left( \sum_{j=0}^{L_{AT}-1} b_{-1j0l} \right)$$

$$= D1 + P_C \times L_{AT} \times \ (1 - \alpha^{m+1}) \times \frac{1 - A^r}{1 - A} \times b_{0000}$$

Finally, total delay for one packet transmission is normalized as:

$$D_{Total} = D2 + E[time\ for\ successful\ trasmission\ in\ last\ state] \times P_S \tag{5.46}$$

$$= D2 + \frac{W_i - 1}{2} \times b_{i00r} + (T_{ta} + T_{CCA}) \times b_{i00r} + L_{AT}$$

$$\times (1 - P_C) \times (1 - \alpha) \times b_{i00r}$$

$$= D2 + b_{i00r}$$

$$\times \left( \frac{W_i - 1}{2} + (T_{ta} + T_{CCA}) + L_{AT} \times (1 - P_C) \times (1 - \alpha) \right)$$

$$= D2 + \ \alpha^i \cdot \left( P_C \cdot (1 - \alpha^{m+1}) \right)^r \cdot b_{0000}$$

$$\times \left( \frac{W_i - 1}{2} + (T_{ta} + T_{CCA}) + L_{AT} \cdot (1 - P_C) \cdot (1 - \alpha) \right)$$

In Equations (5.42) ~ (5.46), total delay for transmitting one packet is analyzed. Parameters of $B_M$, $B_m$, $m$, size of payload and $r$ affect the delay. This analysis assumes that a packet is transmitted at the $i^{th}$ back-off stage and the $r^{th}$ retransmission state. To obtain the total delay time, parameters of the $i^{th}$ back-off stage and the $r^{th}$ retransmission state should be determined. The average number of back-off attempts (the $i^{th}$ back-off

stage) from Equation (4.9) can be obtained. Table 5.1 shows the average number of back-off attempts for a different number of nodes and different size of payloads. This average number of back-off attempts is analyzed from Equation (4.8) in Chapter 4.

**Table 5.1** Average Number of Back-off Attempts for Different Network Size

| L10B # Nodes | $\bar{r}$ | L30B # Nodes | $\bar{r}$ | L50B # Nodes | $\bar{r}$ | L100B # Nodes | $\bar{r}$ |
|---|---|---|---|---|---|---|---|
| 1 | 1 | 1 | 1 | 1 | 1 | 1 | 1 |
| 5 | 2.4219 | 5 | 1.8879 | 5 | 1.7682 | 5 | 1.6768 |
| 10 | 3.5333 | 10 | 2.9258 | 10 | 2.7333 | 10 | 2.5698 |
| 30 | 3.9981 | 30 | 3.9633 | 30 | 3.9314 | 30 | 3.8895 |
| 50 | 4 | 50 | 3.9989 | 50 | 3.9968 | 50 | 3.9928 |
| • L10B = 10 byte payloads, $\bar{r}$ = Average number of back-off attempts | | | | | | | |

Figure 5.6 shows the average total delay for transmitting one packet successfully in different network status. The result shows that delay increases as the number of nodes and payload size. More transmitters and larger size of payload increase the probability of packet collision. For this reason, a node needs to have more CSMA wait time and back-off stages for channel access. Also, due to the channel access failure, more retransmission is needed for packet transmission. Therefore, the delay grows as the number of nodes and size of payload as shown in Figure 5.6.

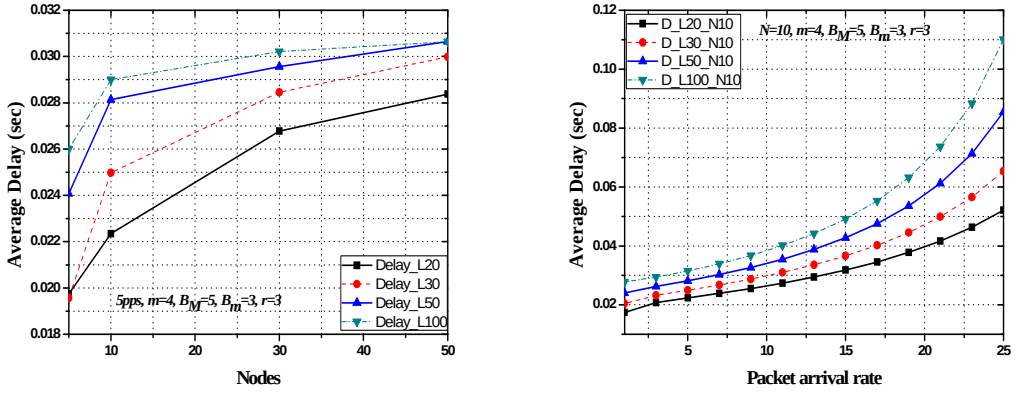


(a) (b)

**Figure 5.6** Delay vs. the number of nodes and packet arrival rate.

### 5.4.4 Energy Consumption

Energy consumption is a critical factor in low-rate wireless applications. In this section, the total energy consumption based on the Markov chain model is developed. For every successful packet transmission or packet transmission failure due to the limit of *macMaxCSMABackoffs* and *macMaxFrameRetries*, the nodes have different states of a network procedure such as packet transmitting, receiving, sleeping and idling. For these states, different power level can be used depending on an 802.15.4 compliant RF transceiver. To analyze total energy consumption, we use different power level parameter values specified for 2.4 GHz IEEE 802.15.4/ZigBee RF module CC2430 [TI CC2430]. The CC2430 supports four different power modes from PM0 to PM3. PM0_TX is supply to packet transmission and PM0_RX is used in packet receiving modes. Also, PM2 is used in the idle state mode. Table 5.2 shows the current consumptions of CC2430 power modes and supply voltage.

**Table 5.2** CC2430 Power Level Specifications

| Power Mode | Current (*I*) | Power |
|---|---|---|
| PM0_TX | 26.9 mA | 80.7 mW |
| PM0_RX | 26.7 mA | 80.1 mW |
| PM2 | 0.5 μA | 1.5 μW |
| $V_{DD}$ = 3V | | |

$$E_{total} = (I_{OFF} \cdot T_{OFF} + I_{TX} \cdot T_{TX} + I_{RX} \cdot T_{RX}) \times V \tag{5.47}$$

$E_{total}$ is the total energy consumption, $I_{TX}$ and $I_{RX}$ are current draw by the transceiver during transmitting and receiving, $T_{TX}$ and $T_{RX}$ are the time taken for packet transmitting and receiving, $I_{OFF}$ and $T_{OFF}$ are the currents when the transceiver is powered off and the duration for the node is powered off, and $V$ is the supply voltage. For our analysis purpose, we assume that 1) nodes transmit the packet continuously without sleeping (power off period) status, and 2) back-off stage periods are considered as an idle state mode.

By considering the Markov chain model shown in Figure 5.1, the total energy consumption for a packet's successful transmission is given:

$$\begin{aligned} E_{total} = {} & P_I \sum_{i=0}^{m} \sum_{k=1}^{W_i-1} \sum_{l=0}^{r} b_{i,1,k,l} + P_{CS} \sum_{i=0}^{m} \sum_{l=0}^{r} b_{i,0,0,l} + P_{TX} \sum_{l=0}^{r} \sum_{j=0}^{L-1} b_{-1,j,0,l} \\ & + P_{RX} \sum_{l=0}^{r} \sum_{j=0}^{L_{AW}-1} b_{-2,j,0,l} \\ & + P_{RX} \sum_{l=0}^{r} \sum_{j=0}^{L_{AI}-1} b_{-3,j,0,l} + P_{RX} \sum_{l=0}^{r} \sum_{j=0}^{L_{TO}-1} b_{-4,j,0,l} + P_I \cdot idle(0) \end{aligned} \tag{5.48}$$

where $P_I$ , $P_{CS}$ , $P_{TX}$ and $P_{RX}$ are the energy consumption in an idle stage, channel sensing, packet transmitting and receiving, respectively. It is assumed that the RF power level is applied as idle state in the back-off stages and RX power mode is set during channel sensing periods. Also, it is receiving mode when the node is waiting for or receiving an ACK packet and it is in transmission mode when the node is transmitting a packet. In Equation (5.48), the first part describes the idle power consumption in back-off stages and second part is the power consumption of channel access periods. Energy consumption of a packet transmission stage is described in the third part with packet size being $L$. The fourth, fifth and sixth parts represent the receiving energy consumption of ACK waiting period, receiving the ACK packet with IFS time and ACK timeout periods for packet transmission failure. The last part is the energy consumption of the idle stage between the packet transmission procedure and being ready to transmit newly generated packets.

Figure 5.7(a) shows the energy consumption depending on the number of node and size of payload. Note that the packet arrival rate is fixed at 5pps. Energy consumption decreases with increasing nodes. As the number of nodes increases, there is more competition for channel access and packet collision. The CSMA wait time and back-off stages as the idle state are considered. From Table 5.2, the idle stage consumes very low power compared to the TX or RX state. As the probability of channel access failure and packet collision increases, nodes would have more back-off attempts for accessing the channel. For this reason, energy consumption decreases as the number of nodes increases.

Figure 5.7(b) shows the energy consumption with different packet arrival rate and size of payload. In this figure, the number of nodes is fixed at 10. From this result, it is found that energy consumption grows at certain traffic load and then decreases. The reason is that a node transmits its packets successfully until their bottleneck of traffic load, so energy consumption increases. However, after that threshold, there is more collision due to the high traffic load. Therefore, a node has more back-off periods and needs to discard packets. It leads to low energy consumption.

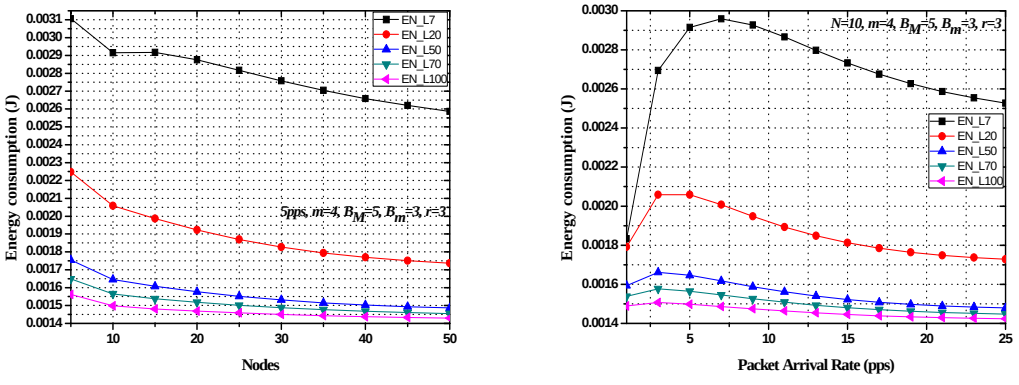


(a) (b)

**Figure 5.7** Energy consumption vs. the number of nodes and packet arrival rate.

## 5.5 Impacts of IEEE 802.15.4 MAC Parameters

As described in the previous section, network performance is analyzed on the non-beacon IEEE 802.15.4 based on the Markov chain model under different network environments. These results, however, are based on the fixed default value of MAC parameters recommended by IEEE 802.15.4 specification. They limit IEEE 802.15.4 MAC parameters to $B_m$ =3, $B_M$=4, $m$=5 and $r$=3. Traffic load size is critical for network performance, because CSMA/CA MAC protocol is used in IEEE 802.15.4. Impact of

various MAC parameters should be considered to suit various applications and network environments. In this section, impact of CSMA/CA MAC parameters ($B_m$, $m$ and $r$) is explored on the performance of beaconless operation of IEEE 802.15.4 MAC layer under different traffic loads.

Health monitoring applications require reliable packet transmission. Successful packet transmission and short delay are two key elements for a real time vital sensing system. For this reason, the performance is evaluated in terms of the reliability and average delay. This is based on the Markov chain model. Let us consider the network environment where no hidden nodes are present.

### 5.5.1 Impact of *macMinBE* Value on Reliability and Delay

*macMinBE* ($B_m$) is the initial value of BE at the first back-off. Its default value is 3. One may vary it from 0 to 8. Figures 5.8 and 5.9 show the impact of increasing $B_m$ on different performance metrics as the traffic load on the network increases. In this analysis, $m$ and $r$ are considered at their default values (4 and 3 respectively). Also, the number of network devices is fixed at 10 and size of payload at 10 bytes.

Figure 5.8 shows the impact of increasing $B_m$ value (0~8) on the reliability with different traffic loads (1pps~25pps). From the graph, reliability increases with decreasing traffic load at same value of $B_m$ and, overall, reliability increases with increasing value of $B_m$. Actually, the increases in $B_m$ increase the range of CSMA wait time. In other words, larger $B_m$ values imply larger back-off period, which causes the possibility of sensing an idle channel to increase.

As the traffic load decreases, the reliability with bigger $B_m$ becomes less significant. At low traffic loads (1~5pps), the reliability grows slowly as $B_m$ increases and at high traffic loads, the reliability increases significantly with $B_m$.

These results can be explained as follows. Suppose that certain nodes are competing for channel access at a certain time. At low traffic loads, they have a packet to send, for a relatively long time, because they have a low packet arrival rate (long packet interval). Moreover, as packets are successfully transmitted, there is less competition for channel access. Therefore, the probability of channel access failure goes down. For these reasons, reliability is not affected too much by increasing CSMA wait time at low traffic load network. At high traffic loads, the number of nodes that have a high packet arrival rate competing for channel access at a certain time may be huge and new packets continuously enter the channel. Therefore, short CSMA wait time leads to busy channel status. Thus, increasing the range of CSMA wait time by larger $B_m$ to spread out the packet transmissions help to increase the reliability.

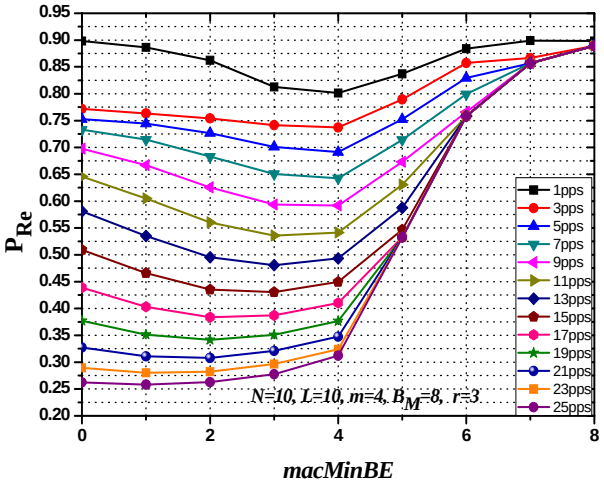


**Figure 5.8** Impact of *macMinBE* on reliability.

Figure 5.9 shows that the packet average delay is consistently higher for higher $B_m$ values. This is because as $B_m$ increases, CSMA wait time increases. As mentioned in Cheater 4, $B_m$ is the Back-off Exponent (*BE*), which is a variable that determines the number of back-off slots a device shall wait before attempting to assess a channel's status. It is chosen randomly in the range from 0 to $(2^{BE} - 1)$.

It is shown that as the packet arrival rate increases, the average delay grows significantly with $B_m$. The reason for this is that for higher packet arrival rate, the traffic load grows significantly. Also, as the competition of channel access is more, more back-off attempts and retransmissions are required.

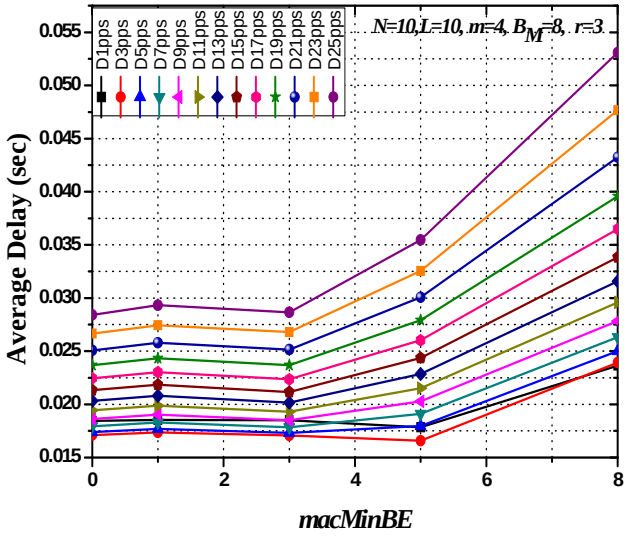


**Figure 5.9** Impact of *macMinBE* on average delay.

### 5.5.2 Impact of *macMaxCSMABackoffs* Value on Reliability and Delay

*macMaxCSMABackoffs* (*m*) is the maximum number of CSMA back-offs. Its default value is 4. One may vary it from 1 to 5. The analytical results regarding the impact of *m*

on non-beacon IEEE 802.15.4 operation with the different traffic loads are shown in Figures 5.10 and 5.11. From them, $B_m$ and $r$ are set to 3 as their same default value from IEEE 802.15.4. Also, the number of network devices and size of payload are fixed at 10 and 10 bytes, respectively.

Figure 5.10 shows the impact of $m$ (1~5) on the reliability with different traffic loads (1pps~25pps). From it, reliability increases with decreasing traffic load at same value of $m$. At low traffic load, reliability increases with $m$. If nodes with pending packets sense the channel to be busy, they would increase the back-off stage up to the limit $m$, referring to the maximum of back-off procedure. For smaller $m$, chance to sensing the channel for more time is low if channel accessing is unsuccessful. Thus, as $m$ increases, the node can obtain more back-off stages to access the channel for packet transmission. It leads to higher reliability. However, when the value of $m$ reaches a certain threshold, the situation becomes opposite at high traffic load (9~25pps). Due to the high traffic load, the collision probability is large enough to exceed the impact of low channel access failure probability. Therefore, reliability decreases for larger $m$ at high traffic load.

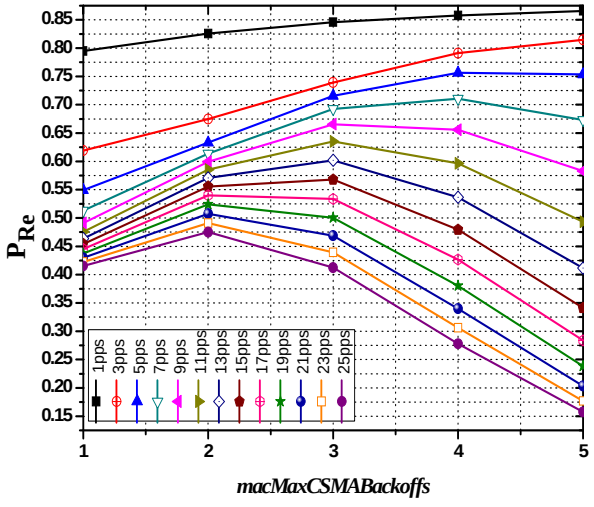


**Figure 5.10** Impact of *macMaxCSMABackoffs* on reliability.

Average delay is influenced by the number of back-off stages due to the channel access failure. The average delay increases as traffic increases due to high busy channel probability and collision probability. As shown in Figure 5.11, the delay increases as *m*. Since the back-off procedure is performed more and more. It is low and slightly increases with *m* at the condition of low traffic load but increases sharply to a high value at high traffic load.

At low traffic load, the chance to sense the channel to be idle increases. Therefore, accumulated packets would have more chances to transmit successfully, leading to less delay. When heavy traffic load is applied, delay grows significantly with *m*. The reason is that nodes that access the channel unsuccessfully need to go to the next back-off stage for reassessing the channel. This leads to high delay.

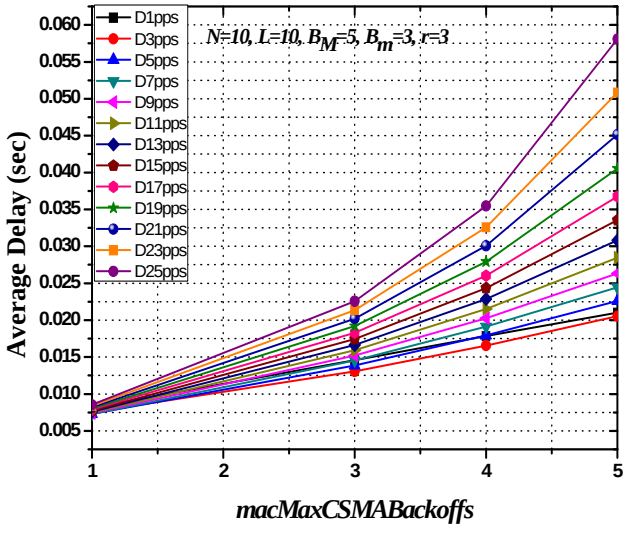


**Figure 5.11** Impact of *macMaxCSMABackoffs* on average delay.

### 5.5.3 Impact of *macMaxFrameRetries* Value on Reliability and Delay

*r* = *macMaxFrameRetries* refers to the maximum times of retransmission. As mentioned in Chapter 4, if the number of retransmission times of a packet exceeds *r*, it is discarded. Its default value is 3. One may vary it from 0 to 7. For the purpose of comparison, $B_m$ and *m* parameters are set to value 3 and 5 as the default value from IEEE 802.15.4 with different network loads. Also, the number of network devices and size of payload are fixed as 10 and 10 bytes, respectively.

At lower traffic loads, the probability of collision is not significant. Because of small packet arrival rate, the idle channel is more likely. Therefore, as *r* increases, reliability increases. In Figure 5.12, it can be shown that reliability grows significantly at certain value of *r* (3 or 4) and does not change until the maximum number of *r* is reached

at light traffic loads (1pps and 3pps). This reason is that most packets can be transmitted with 3 or 4 times retransmission, because of less packet collision due to light traffic loads.

At higher traffic loads, the probability of packet collision is significant. Therefore, it can be expected that increasing *r* should increase the number of transmissions a packet is transmitted before its successful delivery or collision failure. However, as the packet arrival rate increases, the network load becomes heavier and probability of collision increases. Many packets need to be retransmitted for more times. If attempts of retransmission due to packet collision increase with higher value of *r*, network load becomes larger and other waiting packets could be overcrowded. This leads to the fact that reliability grows at certain value (1~3) of *r* and decreases with the increase of *r*. From Figure 5.12, the reliability of a network device with 9pps~25pps packet arrival rate has lower reliability at *r*=7 compared to reliability at *r*=0.

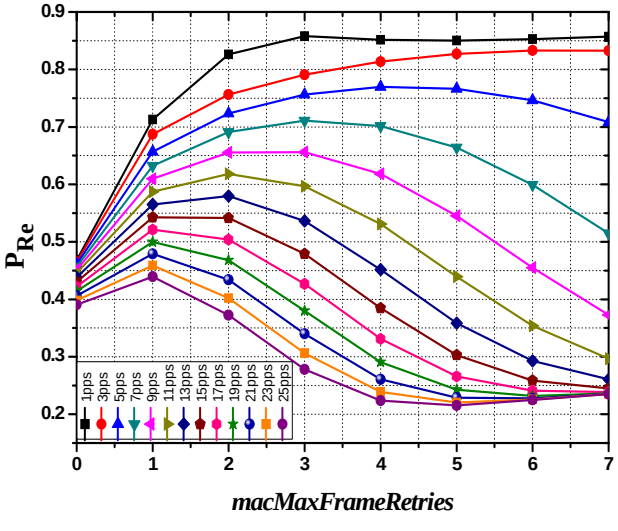


**Figure 5.12** Impact of *macMaxFrameRetries* on reliability.

Figure 5.13 shows the average delay with different packet arrival rate and *r* from 0 to 7 given the number of nodes and payloads at *N=10* and *L=10*. From Figure 5.13, it is found that the delay is influenced by different *r* values. Delay increases with *r*. Pending packets attempt several retries before successful transmission, which takes much time.

Similarly to the reliability, delay grows at certain value of *r* (3 or 4) and after this value it does not change to the maximum value of *r* at light traffic loads. This is because the probability of collision is not significant. Because of small packet arrival rate, the idle channel is more likely. Therefore, as *r* increases, reliability increases. In Figure 5.12, it can be found that reliability grows significantly at certain value of *r* (3 or 4) and does not change at light traffic loads (1pps and 3pps). The reason is that most packets can be transmitted with 3 or 4 times retransmission, because of less packet collisions due to light traffic loads.

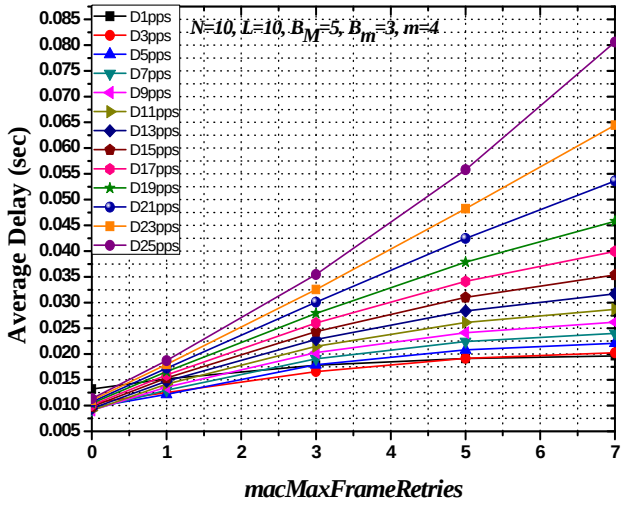


**Figure 5.13** Impact of *macMaxFrameRetries* on average delay.

# CHAPTER 6

# RECONFIGURATION OF UN-SLOTTED IEEE 802.15.4 MAC PARAMETERS FOR ECG MONITORING

## 6.1 Introduction

The channel utilization is significantly affected by back-off time and packet collision [Choi and Zhou, 2010]. Successful channel access probability is an important indicator for reliable data transmission and small packet latency. If a node cannot access the channel after several back-off attempts, it wastes transmission time and loses the data packet. The network performance is affected by IEEE 802.15.4 MAC parameters, i.e., *macMinBE*, *macMacBE*, *macMaxCSMABackoffs* and *macMaxFrame-Retries*.

This Chapter provides the performance of IEEE 802.15.4 at 2.4GHz in the un-slotted CSMA/CA mode for one-hop star networks. We analyze such QoS parameters such as effective data rate, average end to end delay and PDR under different network parameters including payloads size, the number of network devices and data rate. To better understand such kind of QoS of IEEE 802.15.4, simulations have been carried out by using Qualnet 5.0, a network software that provides scalable simulations of wireless networks.

The remainder of this Chapter is organized as follows. Section 6.2 gives the simulation scenario and setup as well as the network metrics used for this research. Section 6.3 presents the simulation results for electrocardiogram transmission regarding a suitable packet interval and payload, and also results about QoS under different MAC parameters. Finally, Section 6.4 concludes the Chapter.

## 6.2 Simulation Environment

Various network scenarios are designed to run the simulations. The primary objective is to measure and analyze the performance of different network scenarios and parameters on IEEE 802.15.4 star network topology.

The network performance simulation has been developed by using the Qualnet version 5.0 developer platform produced by Scalable Network Technology [Scalable-networks, 2011]. The simulation environment is specified to suit the real network.

Figure 6.1 shows the 3D simulation model. In this model, a star network topology with one PAN coordinator and 1 to 15 network devices are located at same distance as 20 meters in an area of 50m×50m×5m. For this model, the coordinator's location is set as (25, 25, 5). In other words, it is placed at the center of the given area and is located 5 meters from the floor. Also, other network devices are placed 1 meter from the floor, i.e., (*x, y,* 1). Note that people carry this network device. Because of different height of the coordinator and network devices, 20 meters is the diagonal distance between them. In this simulation, only uplink traffic is considered, because BSN nodes in healthcare monitoring are normally required to pass the medical information from a subject to a coordinator and/or base station.

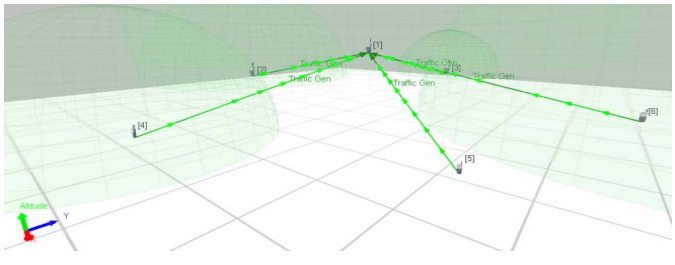

**Figure 6.1** 3D simulation scenario.

The simulation parameters are given in Table 1. In our simulation model, BO and SO are set to 15 to mean a non-beacon mode. To make the simulations close to a real system, we choose the "Traffic Generator" as a type of traffic from the Qualnet simulator. This model simulates random distribution based network traffic. The traffic generator with the following mean packet rates as 3.7 packets per second (pps), 7.7 pps, 20 pps and 37 pps with 100, 50, 20, 10 bytes MSDU for ECG data rate (3kbps) are applied.

**Table 6.1** Simulation Parameters

<table>
<tr><th>Parameters</th><th colspan="4">Value</th><th>Parameters</th><th>Value</th></tr>
<tr><td>Size of area</td><td colspan="4">50m × 50m × 5m (x,y,z)</td><td>Simulation time</td><td>10000 sec</td></tr>
<tr><td>Num. of nodes</td><td colspan="4">1 ~ 10</td><td>Traffic Type</td><td>Traffic Generator</td></tr>
<tr><td>Channel freq. and data rate</td><td colspan="4">2.4 GHz and 250kbps</td><td>macBeaconOrder (BO)</td><td>*15</td></tr>
<tr><td>Transmission range</td><td colspan="4">35 meter</td><td>macSuperframeOrder(SO)</td><td>*15</td></tr>
<tr><td>Modulation type</td><td colspan="4">O-QPSK</td><td>MinBE</td><td>3 (default), 0~8</td></tr>
<tr><td>TX power</td><td colspan="4">0 dBm</td><td>MaxBE</td><td>5 (default), 3~8</td></tr>
<tr><td>PHY and MAC model</td><td colspan="4">IEEE 802.15.4</td><td>macMaxCSMABackoffs</td><td>4 (default), 0~5</td></tr>
<tr><td>Path loss model</td><td colspan="4">Two Ray Model</td><td>aMaxFrameRetries</td><td>3 (default), 0~7</td></tr>
<tr><td>MSDU size (Byte)</td><td>10</td><td>20</td><td>50</td><td>100</td><td colspan="2" rowspan="2">*Non-beacon mode</td></tr>
<tr><td>Packet transmit interval (sec)</td><td>0.027</td><td>0.05</td><td>0.13</td><td>0.27</td></tr>
</table>

The following performance parameters have been used:

- **Effective data rate** is

$$D_{eff} = \frac{\sum P_{success} \times L_{Payloads}}{T_{tx}}$$

where $P_{success}$ is the total number of data packets that are received successfully from all nodes in the whole transmission time. $L_{Payloads}$ is the length (bits) of payload for each node. $T_{tx}$ is the total transmission time.

- **Packet Delivery Ratio (PDR)** is defined as the ratio of successfully received packets to a destination node, to the total number of data packets transmitted by source nodes.
- **Average End-to-End delay** represents the average length of time taken for a packet to travel from the source to destination. In other words, it shows the average data packet delay in applied network communication during the data packet transmission.

## 6.3 Simulation Results and Discussion

This section describes the simulation results of various performance parameters for the evaluation of effective data rate, PDR (packet delivery ratio) and average end-to-end delay on IEEE 802.15.4 star topology using varying traffic loads. The simulation parameters are applied to simulate various WSN scenarios.

### 6.3.1 Effects of Packet Transmission Interval

This section presents the impact of different payload size with packet interval up to normal ECG data rate (3kbps) on the network performance. Different MSDU with packet

interval such as 10 bytes with 0.027 sec, 20 bytes with 0.05 sec, 50 bytes with 0.13 sec and 100 bytes with 0.27 sec is simulated for the same data rate as 3kbps. With this scenario, effective data rate, end-to-end delay and PDR are analyzed with a different number of nodes for best QoS of an ECG monitoring system.

Figure 6.2(a) presents the measured effective data rate with various network devices for each different MSDU and packet interval. As the number of nodes increases, the effective data rate first grows and then decreases. The reason for this is that as the number of nodes increases, more packets are sent to the coordinator. This leads to increased effective data rate. But if traffic loads reaches to a certain threshold, effective data rate decreases due to higher possibility of packet collision.

Figure 6.2(b) shows the average end-to-end delay for each node. It can be found that as the packet interval decreases, end-to-end delay grows at the same number of nodes. Also, it increases significantly with an increasing number of nodes. The reason is that small packet interval and an increasing number of nodes produce the heavy traffic load. Heavy traffic load leads to more packet collisions and heavy channel competition among nodes. Because of these, each node needs more back-off attempts, channel sensing time and retransmission for any successful packet transmission.

Figure 6.2(c) shows the average PDR for each node. It can be found that as the number of nodes increases, PDR decreases significantly. The reason for this is that as the number of nodes increases, more packets are required to send at the same time period. This increases traffic load and dropped packets due to more data collisions.

It is observed that PDR for the case with larger packet interval (0.27 sec) with 100 bytes payload has good performance compared with the case with shorter packet interval.

From Figure 6.2(c), for a certain number of nodes, PDR decreases as the packet interval decreases even if the size of payload decreases. Also, the PDR decreases as the packet interval decreases. The reason is that larger packet intervals produces lighter traffic load and thus little packet collision happens. PDR for the case with 0.27 sec packet interval and 100 bytes payload decreases from 100% to 83%, when the number of nodes changes from 1 to 5. It decreases from 83% to 35% when the number of nodes increases from 5 to 10. Due to the nature of an ECG monitoring system that requires accurate QoS, PDR should be more than 80%.

From the above results, it can be decided the best network scenario for an ECG monitoring system is 0.27 sec packet interval with 100 bytes payload by 5 nodes. Under these conditions, various CSMA/CA MAC parameters will be simulated and decision on them most suitable values will be shown in the next section.

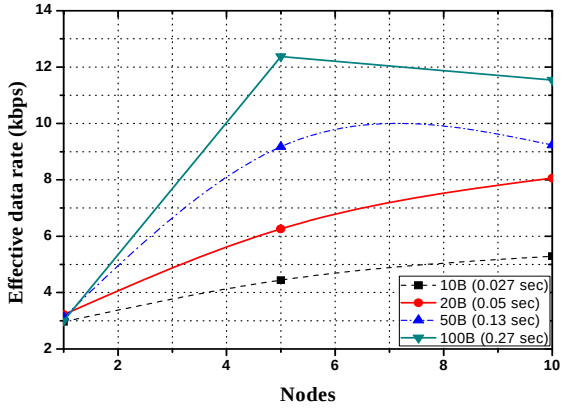


(a)

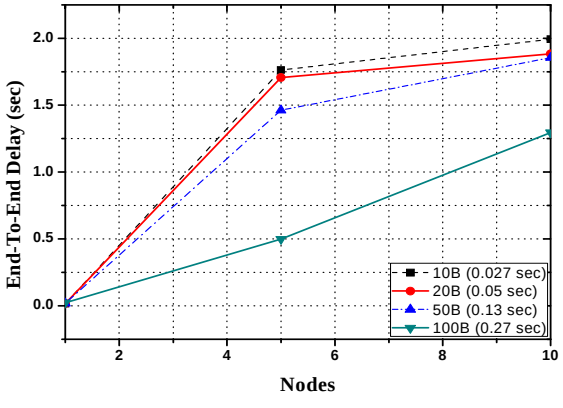


(b)

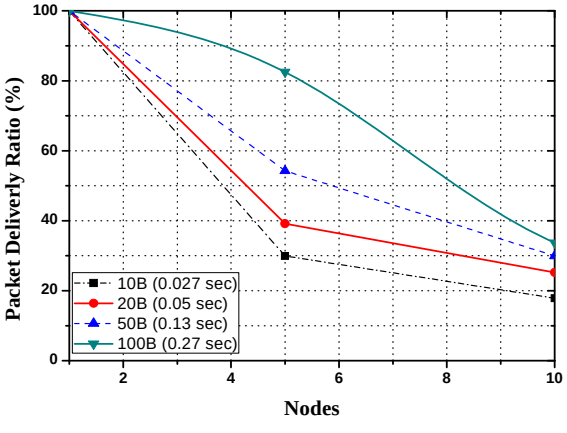


(c)

**Figure 6.2** Performance with different packet periods.

### 6.3.2 Effect of *macMinBE*

Fixed data payloads and packet interval as 100 bytes and 0.27 sec are used for an ECG monitoring system. Also, 5 network devices are applied for all network scenarios, which can achieve the best network performance results as shown in the previous section. The back-off time is chosen randomly from [0, $2^{BE}$ – 1] unit of time before sensing the channel. *macMinBE* is the value of *BE* at the first back-off. We can vary this value from 0 to 8. Its default value is 3.

Figure 6.3 shows the measured effective data rate, average end-to-end delay, and PDR with different values of *macMinBE*. It is clear that the effective data rate and PDR grow as *macMinBE*. Especially, it can be obtained that PDR is more than 95% when *macMinBE* is from 6 to 8. If it uses its default value 3, PDR is below 85 %. The reason is that a larger initial back-off period reduces the packet collision probability in the first back-off stages. Figure 6.3(b) shows the average end-to-end delay. The end-to-end delay increases with the increase of *macMinBE*. Because initial back-off period increases due to large *macMinBE*, end-to-end delay also increases.

From the results of simulation with various *macMinBE*, it can be found that default value, 3, of *macMinBE* is not the best parameter to achieve the best network performance for ECG transmission. For continuous real time monitoring of ECG, end-to-end delay should be below 1 sec. Therefore, the best value of *macMinBE* is 4 or 5 based on this study.

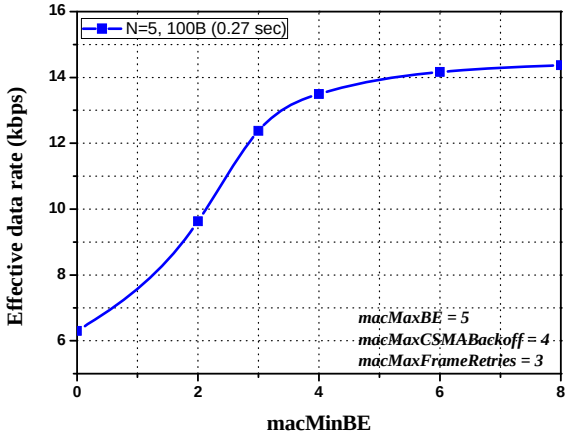


(a)

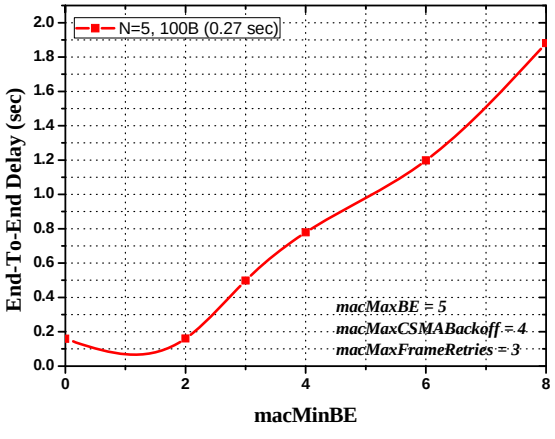


(b)

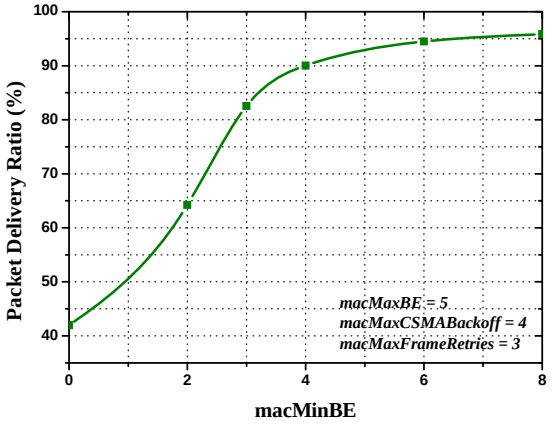


(c)

**Figure 6.3** Performance with different *macMinBE*.

### 6.3.3 Effect of *macMaxBE*

*macMaxBE* is the maximum value of back-off exponent in the CSMA/CA protocol [IEEE 802.15.4. 2006]. Figure 6.4 shows its impact on the network performance. Figures 6.4(a) and (b) give the effective data rate and PDR when *macMaxBE* changes from 3 to 8. They grow with *macMacBE*. However, after *macMaxBE* reaches 6, they do not change significantly. This is because with increased *macMaxBE*, longer back-off periods are applied in the CSMA/CA protocol. It can reduce packet collisions.

Figure 6.4(b) shows the end-to-end delay with different *macMaxBE*. From it, it increases as *macMaxBE*. This is because back-off exponent for back-off period increases before sensing the idle channel for packet transmission. As mentioned before for CSMA/CA protocol, the value of back-off exponent can be selected as min(*BE*+1, *macMaxBE*) for back-off periods after CCA failure. Therefore, it leads to longer end-to-end delay. From these results, the best value of *macMaxBE* is 6.

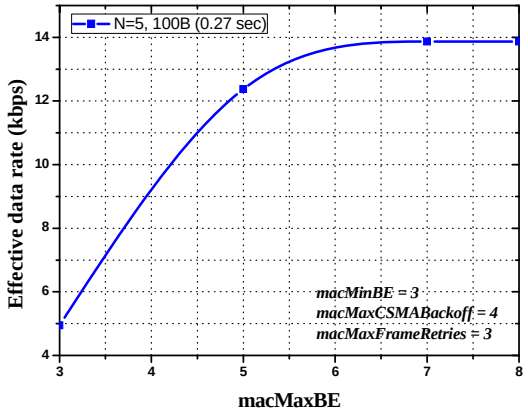


(a)

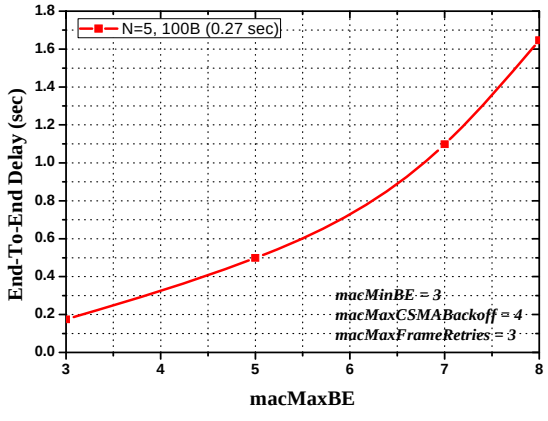


(b)

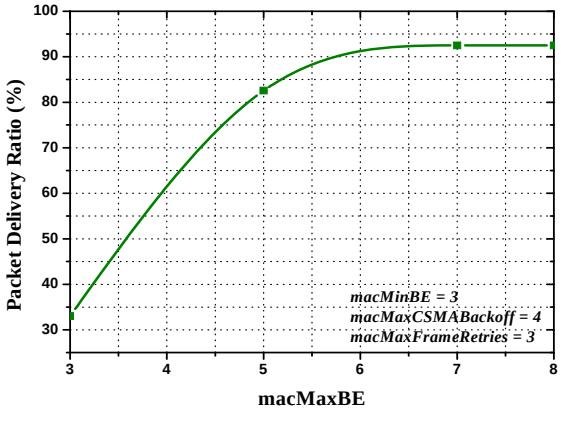


(c)

**Figure 6.4** Performance with different *macMaxBE*.

### 6.3.4 Effect of *macMaxCSMABackoffs*

The simulation results regarding the effect of *macMaxCSMABackoffs* value on non-beacon IEEE 802.15.4 operation for ECG monitoring are illustrated in Figure 6.5 *macMaxCSMABackoffs* is the maximum number of back-off stages with its default value 4. It is changed from 0 to 5. Except dropped packets by the limitation of retransmissions, almost all generated packets are dropped by the CSMA/CA MAC protocol. This is because the exceeded number of maximum back-off stages is determined by *macMaxCSMA-Backoffs*. As mentioned before, a node tries to sense the channel for packet transmission after some back-off periods. After failing to find the idle channel, it attempts back-off again for the next CCA. But this attempt is limited by *macMaxCSMABackoffs*. It is clear that increasing it reduces the channel access failure probability, because more CCA failures are allowed before channel access failure is declared. Therefore, it can be expected that a large value of *macMaxCSMABackoffs* would be helpful for reliable packet transmission.

Figures 6.5(a) and (c) show the effective data rate and PDR with various *macMaxCSMABackoffs*. They show that increasing *macMaxCSMABackoffs* produces a significant increase in effective data rate and PDR. From Figure 6.5(c), it can be found that the big difference, i.e., 15% to 90% increase in PDR from *macMaxCSMABackoffs*=0 to 5. This is an almost 6 times improvement. Based on the results in Figure 6.5, it can be expected that an increase in the maximum number of back-off stages gives a significant impact on the network QoS.

Figure 6.5(b) represents the end-to-end delay with various *macMaxCSMA-Backoffs*. It grows with *macMaxCSMABackoffs*. This is because with increased *macMax-*

*CSMABackoffs*, more back-off stages are proposed, which leads to longer end-to-end delay. Unlike the results of *macMinBE* and *macMaxBE*, the default value of *macMaxCSMA-Backoffs* is the best parameter to achieve the desired network performance.

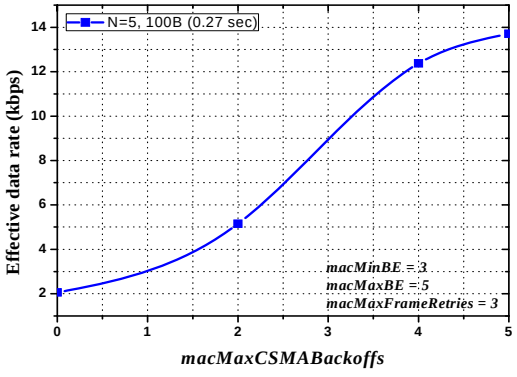


(a)

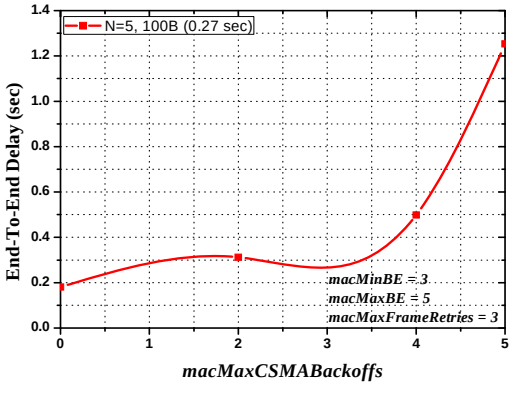


(b)

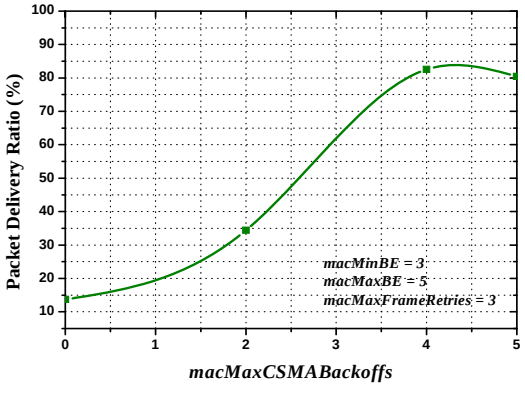


(c)

**Figure 6.5** Performance with different *macMaxCSMABackoffs*.

### 6.3.5 Effect of *macMaxFrameRetries*

*macMaxFrameRetries* is the maximum number of retransmissions. Its default value is 3. One may change it from 0 to 7. Normally, packets are resumed or dropped due to the channel access failure or retransmission limits. To transmit the data packet successfully, each node has to compete for the access to the channel first. If a node could not obtain the idle channel status in one or two CCA within *macMaxCSMABackoffs* + 1 back-offs, channel access failure is declared. If a node finds the idle channel, it transmits its packet. After transmitting the data to the coordinator, a node waits for ACK from the coordinator. If it does not receive the ACK from the coordinator due to packet collision or loss, it tries to retransmit the data up to *macMaxFrameRetries* times. Finally, if the transmission fails for repeating packet collision after *macMaxFrameRetries* + 1 attempts, a packet is discarded.

Figure 6.6(a) shows the simulated effective data rate with various *macMaxFrame-Retries*. For given five network devices for ECG transmission, the effective data rate increases largely with *macMaxFrameRetries* until this value is 3. After *macMaxFrame-Retries* is larger than 3, effective data rate increases very slightly. The reason is that some nodes are hard to transmit the packet successfully within first or second attempts due to the busy channel and packet collision. In this scenario, the best threshold value of *macMaxFrameRetries* is 3.

Figure 6.6(c) shows the PDR with various *macMaxFrameRetries*. It has the same pattern as the effective data rate. If more transmitters or shorter packet interval with heavy traffic is applied, the critical threshold value should be more than 3. It can be found

that a higher number of retransmissions would be helpful when the traffic is heavy due to high data generation rate of nodes.

Figure 6.6(b) shows the end-to-end delay with various *macMaxFrameRetries.* If every packet frame can be transmitted successfully for the first attempt, MAC processing delay is very low. However, as the packet collision increases due to heavy traffic load, packet frames need to be retransmitted and the number of such retransmission is limited by *macMaxFrameRetries*. Because of this reason, end-to-end delay increases with *macMaxFrameRetries*. From these results, the best value of *macMaxFrameRetries* should be 4.

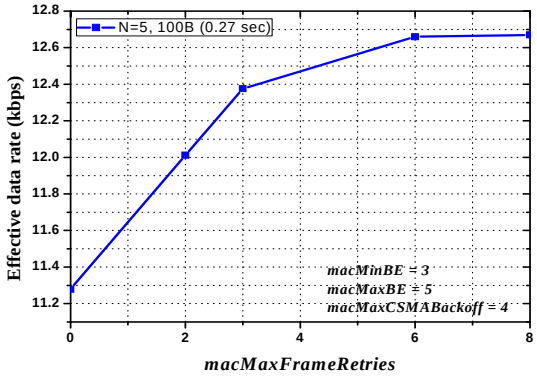


(a)

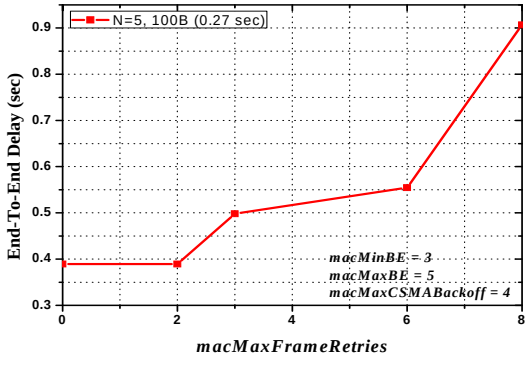


(b)

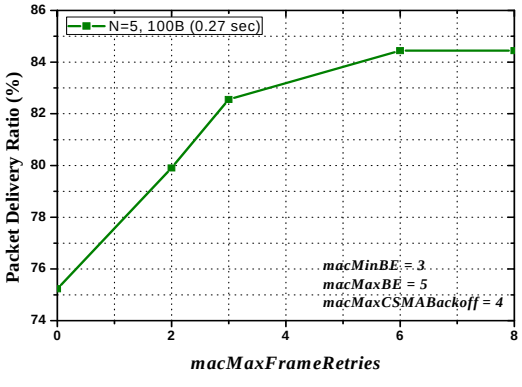


(c)

**Figure 6.6** Performance with different *macMaxFrameRetries*.

## 6.4 Summary

This chapter presents the simulation based performance analysis of QoS for a real time ECG monitoring system based on an IEEE 802.15.4 star network. The network to find effective data rate, PDR and end-to-end delay as QoS indicators of ECG transmission have been analyzed and simulated. It can be found that larger payload size and longer packet interval at same data rate can improve the network performance. Also, it can be recognized the default parameters from IEEE 802.15.4 standard are not always most suitable to achieve the best QoS. As a result, some CSMA/CA parameters should be changed according to specific network scenarios such as continuous real time monitoring, traffic load and network size.

# CHAPTER 7

# PRIORITY PACKET TRANSMISSION FOR HEALTH MONITORING SYSTEM

## 7.1 Introduction

This chapter presents a continuous heart beat sound and human temperature monitoring system using a TI CC2430 Zigbee module. Chapter 5 analyzes the QoS parameters such as reliability and average delay by different network parameters including the size of payloads, the number of network devices and data rate with different MAC parameters. In this chapter, the priority packet transmission for continuous signals, especially heart beat sound by modifying the CSMA/CA protocol based on the adaptive CSMA MAC parameters is proposed.

The remainder of this chapter is organized as follows. Section 7.2 gives the heart beat sound and temperature monitoring system with software and hardware designs. Section 7.3 presents the proposed MAC protocol for priority packet transmission. Section 7.4 gives simulation results and discussions. Finally, Section 7.5 concludes the chapter.

## 7.2 Heart Beat Sound Monitoring System

This experiment is performed by using a TI CC2430 Zigbee module for monitoring the human temperature, device battery remaining check, and heart beat sound. An 802.15.4 MAC based sound transmission network consists of a coordinator and end devices. For the 802.15.4/ZigBee biomedical sensor system, the end device is connected to the microphone to listen the heart beat sound, and the coordinator is connected to the speaker or PC for hearing or monitoring the heartbeat or temperature information. This system is

constructed by using the direct data transmission mode. Data and control are streamed from the end device to the coordinator. Also this system is executed with 802.15.4 ACK's turned on. Figure 7.1 shows this overall biomedical sensor system using low-power 8051 microcontroller (CC2430).

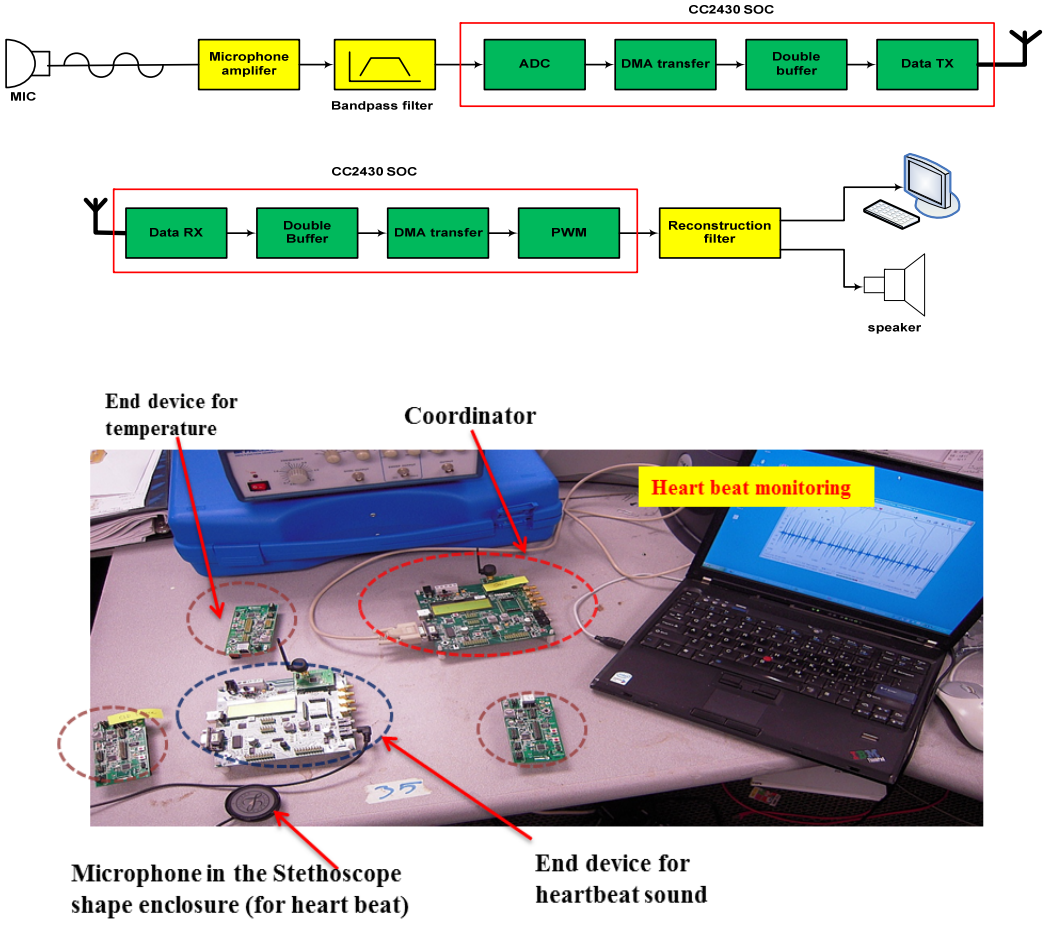


**Figure 7.1** Overall biomedical sensor system.

The sizes of human temperature data or battery check data are about 5 bytes (including no overhead, i.e., 5 bytes data payload). Their communication does not need to be continuous. But heart beat sound transmission should be continuous for real-time monitoring. If the end device transmits continuous heart beat sound data to the base station all over the time, it has high power consumption and also gives data congestion due to the CSMA-CA protocol. If periodic continuous transmission is applied to a network device, however, power consumption and data congestion could be reduced. Periodic continuous transmission means that a node sends the heart beat sound data for several minutes and sleeps for some period of time and wakes up again. Figure 7.2 shows the process to convert heart beat sounds to digital bits.

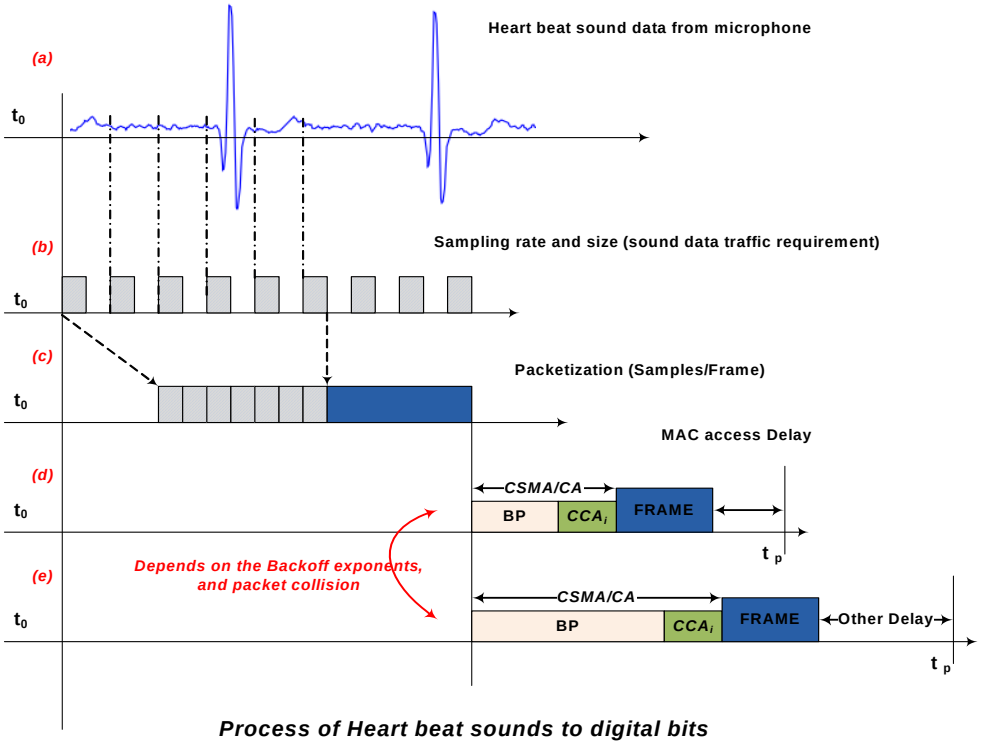


**Figure 7.2** Conversion of heart beat sounds to digital bits.

In this experiment, one coordinator and three network-devices are tested. Only one end-device transmits the sound data continuously and others send the temperature data to the base station periodically. Figure 7.3 shows one whole data packet for heart beat sound transmission. It includes sound data sample (100 bytes), frame control (2 bytes), data sequence number (1 byte), address packet (6 bytes), and 8 bytes for PHY layer packet (preamble, SFD, frame length , and FCS). A temperature or battery check data sample is 5 bytes. Therefore, the total size of a sound data packet is 117 bytes and that of temperature/battery check data packet is 22 bytes.

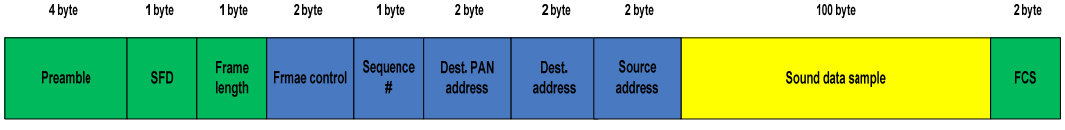


**Figure 7.3** Whole data packet for heart beat sound.

Figure 7.4 shows the results of transmitting and receiving data packets as captured by Packet Sniffer from TI. After a heart beat sound packet is sent to the base station, temperature sensor nodes try to associate and join with the station. Five second packet period is enough to monitor the patient's temperature. To recognize the sound, however, a packet period should be short for real-time communication. This data rate could be up to 64 kbps. For heart beat sound transmission, two options can be applied: acknowledgement (ACK) and non-acknowledgement (NACK). As mentioned in Chapter 4, IEEE 802.15.4 supports an ACK protocol for higher communication reliability. If ACK is applied to communication between the base station and sensor nodes, the higher reliability compared with the NACK option could be achieved. But this option needs

ACK packet transmitting time and receiving time. Therefore, the end-to-end delay increases with the benefit of increasing reliability. To transmit and receive sound data reliably, packet period time should be up to 12 *ms* for ACK and 9 *ms* for NACK from an experimental result. For more data throughput, a short packet interval is needed, but shorter packet interval can increase packet collision or packet loss. Actually measured average packet periods are 20.113 *ms* for ACK and 13.239 *ms* for NACK. These results probably would have been affected by different back-off time based on the CSMA-CA protocol. From the real experiment, we can listen to the heart beat sound from the base station or PC and monitor the heart beat in a real time. Screen capture of heart beat from the real IEEE 802.15.4 module is showed in Figure 7.5. Table 7.1 describes the test results.

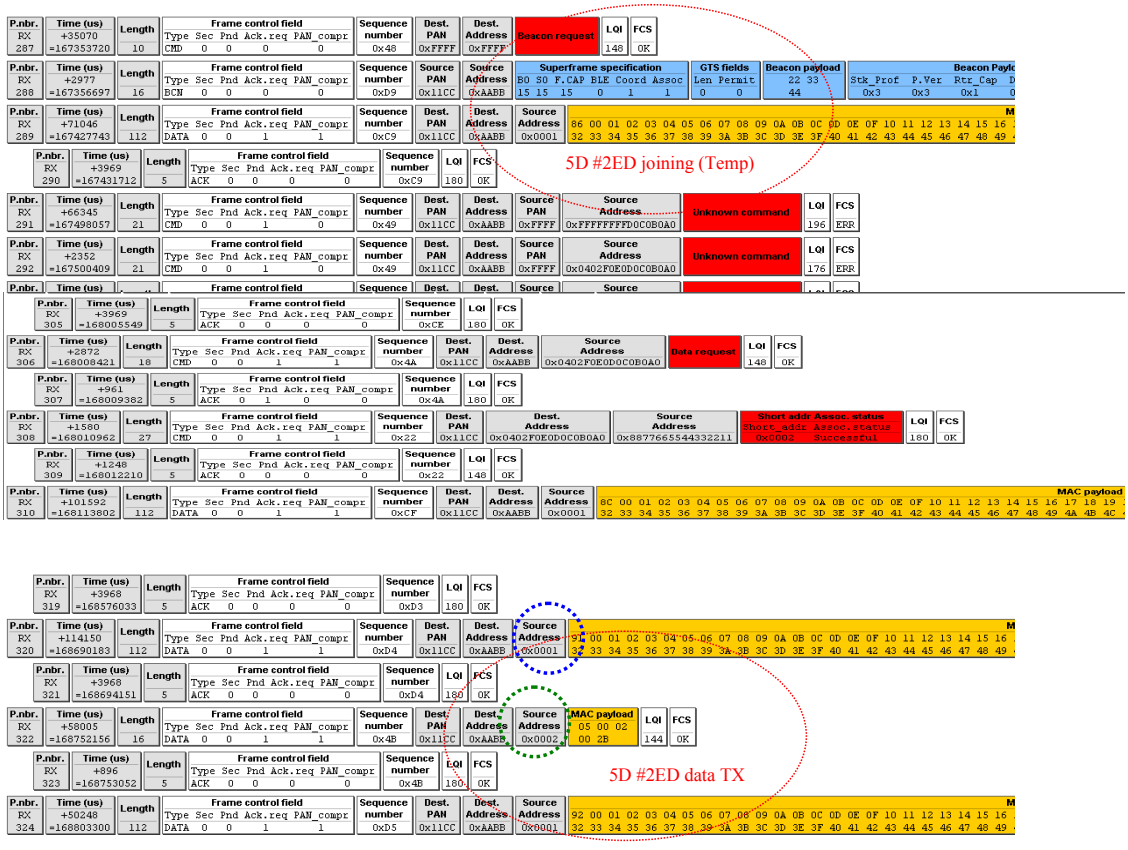


(a) Associating and joining status for multi node communication

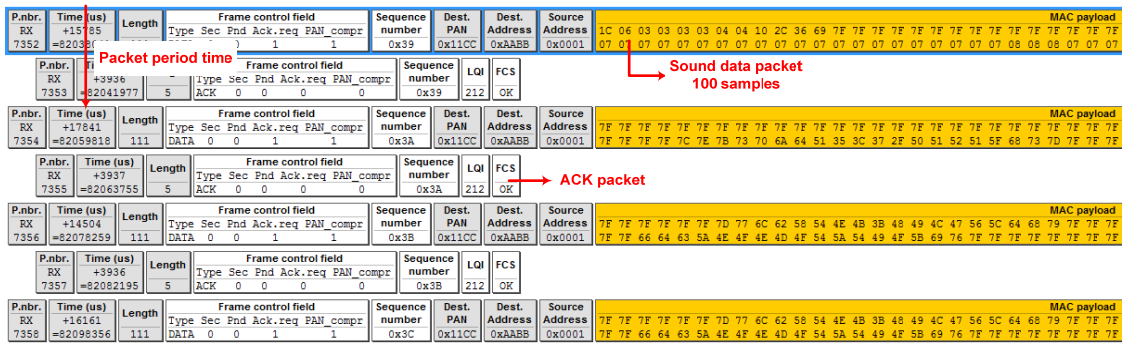


(b) Transmitting sound data packet

**Figure 7.4** Captured data packets on air by Packet Sniffer.

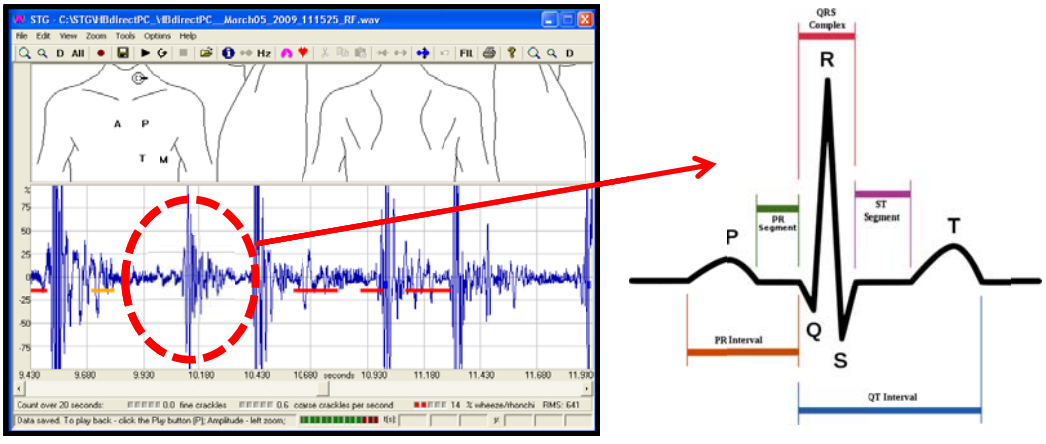


**Figure 7.5** Capture of heartbeat from 802.15.4/Zigbee end device.

**Table 7.1** Summary of the Test Results

| | Heart beat sound | | Temp/Battery check |
|---|---|---|---|
| | With ACK | Without ACK | |
| **Data sample** | 100 bytes | 100 bytes | 5 bytes |
| **One packet** | 117 bytes | 117 bytes | 22 bytes |
| **Packet period (programmed)** | 12 ms | 9 ms | 5 sec |
| **Real measured Ave. packet period** | 20.113 ms | 13.239 ms | 5 sec |
| **Throughput** | 79 kbps | 105 kbps | 27.2 bps |

### 7.2.1 Software Architecture

Figure 7.6 describes the software flow for transmitting and receiving the heart beat sound data. Data from the microphone is captured using ADC. ADC input is read at a frequency of 7.8 kHz and 8-bit samples are taken, thereby leading to a data rate of 64 kbps. The data are then transmitted via the radio in 100-byte packets (data MAC payload, not including

the header). Upon reception by the receiver, the 8-bit data is output on the PWM at a rate of 7.8 kHz.

Note that the transmitter is configured as an end device and the receiver is configured as a coordinator. Either of transmitter and receiver contains two buffers. The buffers of the transmitter are used to store samples from the ADC and the buffers of the receiver are used to store data to be output via the DMA transfer from radio. The use of separate buffers allows the ADC or DAC to use the data in one buffer while the radio uses the other buffer for reception or transmission. For example, data received via the radio is placed into input buffer A. The DMA now outputs the data contained in this buffer. However, before it has finished, more data may arrive via the radio. This time the data is put into input buffer B. Once the DMA transfer completes the output of all data in buffer A, it switches to buffer B.

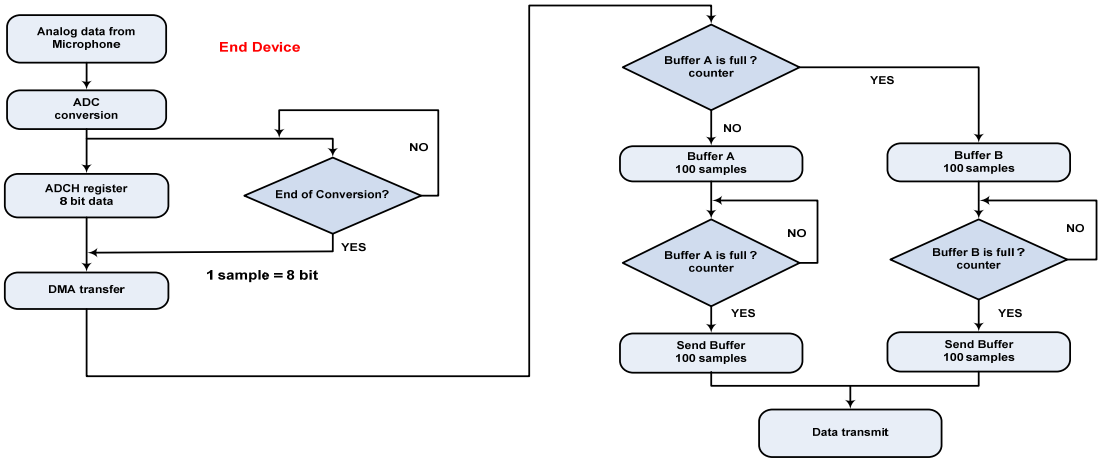


(a) Software for sound packet transmission of an end device

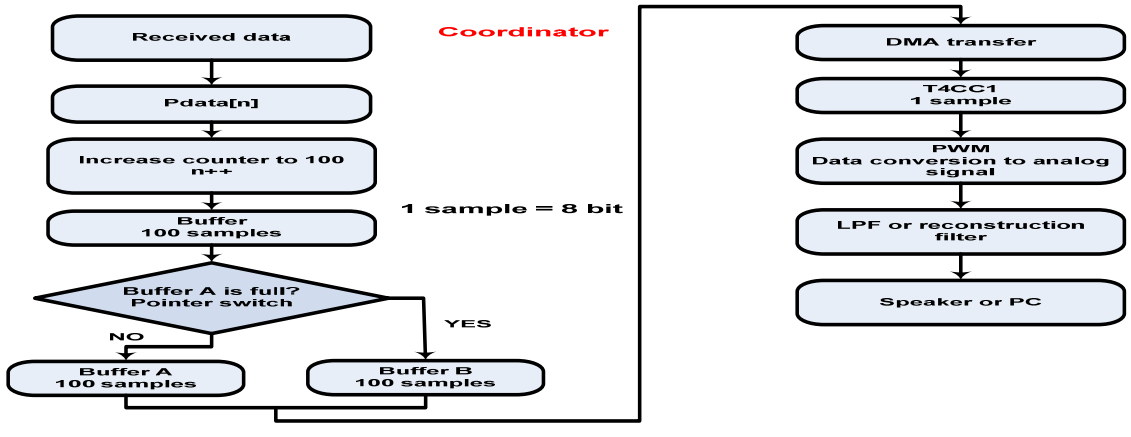


(b) Software for sound packet transmission of a coordinator

**Figure 7.6** Double buffer management for transmitting and receiving data.

### 7.2.2 Hardware Architecture

Table 7.2 describes a CC2430 microcontroller (MCU) and related hardware. The CC2430 MCU by Texas Instruments is an 8-bit ultra-low power MCU with 32k/64k/128k bytes program flash. CC2430 is a system-on-chip (SOC) MCU that includes a processor core and IEEE 802.15.4 RF transceiver. The inner clock is 32 MHz, and the peak power

consumption in operation is 7.0mA. Radio transmission and reception consume 24~27mA, and support a 4 level low power mode. CC2430 provides a low supply voltage range from 2.0 V to 3.6 V. Other features include 12-bit ADC, PWM, 2 USARTs, I2C, and DMA to collect, store, process and transmit data from ADC output. The receiver can interface with a monitoring system using the serial port interface (RS232) through SPI or UART. Network device nodes could use small chip antenna or printed antenna (antenna gain: +0.3dBi) to reduce the size and weight, and a coordinator could use the whip antenna (+1.9dBi).

**Table 7.2** Overview of Hardware

| **Part number** | CC2430 | **RAM [KB]** | 8 | |
|---|---|---|---|---|
| **Type** | SoC | **Max. Clock [MHz]** | 32 | |
| **Package** | QLP48 | **Current CPU [mA]** | 7 | |
| **Supply Voltage [V]** | 2.0~3.6 | **Current Transmit [mA] 0 dBm/Max** | 24.7 | |
| **Sleep Current [µA]** | 0.6 | **Current Receive [mA]** | 27 | |
| **MCU type** | 8051 | **Transmit Power [dBm]** | 0 | |
| **I/O Pins** | 21 | **Receive Sensitivity [dB]** | -94 | |
| **Max. Flash [KB]** | 128 | **Antenna gain** | Whip | +1.9dBi |
| | | | Folded Dipole (Print) | +0.3dBi |

## 7.3 Proposed MAC Protocol for Priority Packet Transmission

From Chapters 4 and 5, it is found that the performance of a CSMA-CA protocol depends on its back-off algorithm and other parameters. Especially, increasing the number of network devices leads to increasing traffic. In a heavy traffic network, many data collisions occur, thereby resulting in long data transmission delay. Especially, network size should be limited to prevent the heavy traffic in the network area of health monitoring. Also, priority data, such as emergency data, should be transmitted more reliably than other normal data. In this section, the modified CSMA/CA MAC protocol is proposed for these two purposes.

### 7.3.1 Proposed Method for Network Devices to be Associated with PAN

Figure 7.7 shows a PAN coordinator starting a non-beacon-enabled network. A coordinator with one PAN ID connects network devices desiring access to the PAN through broadcasting.

An association process starts with an active or passive scan. This scan process allows a device to locate those coordinators transmitting a beacon frame within a PAN area. Note that the beacon request command is not required for a passive scan process. The end device issues an active scan. The active scan selects one channel and transmits a *BeaconRequest* command to the broadcast address (0xFFFF) and broadcast PAN ID (0xFFFF). Then an end device listens to that channel for beacon from any coordinator. Once the defined time expires on that channel, the end device scans another channel and transmits the *BeaconRequest* command again. This active scan process continues until all channels have been scanned. After the scan is complete, the MAC sends a MAC_MLME_SCAN_CNF with the PAN information received during the scan.

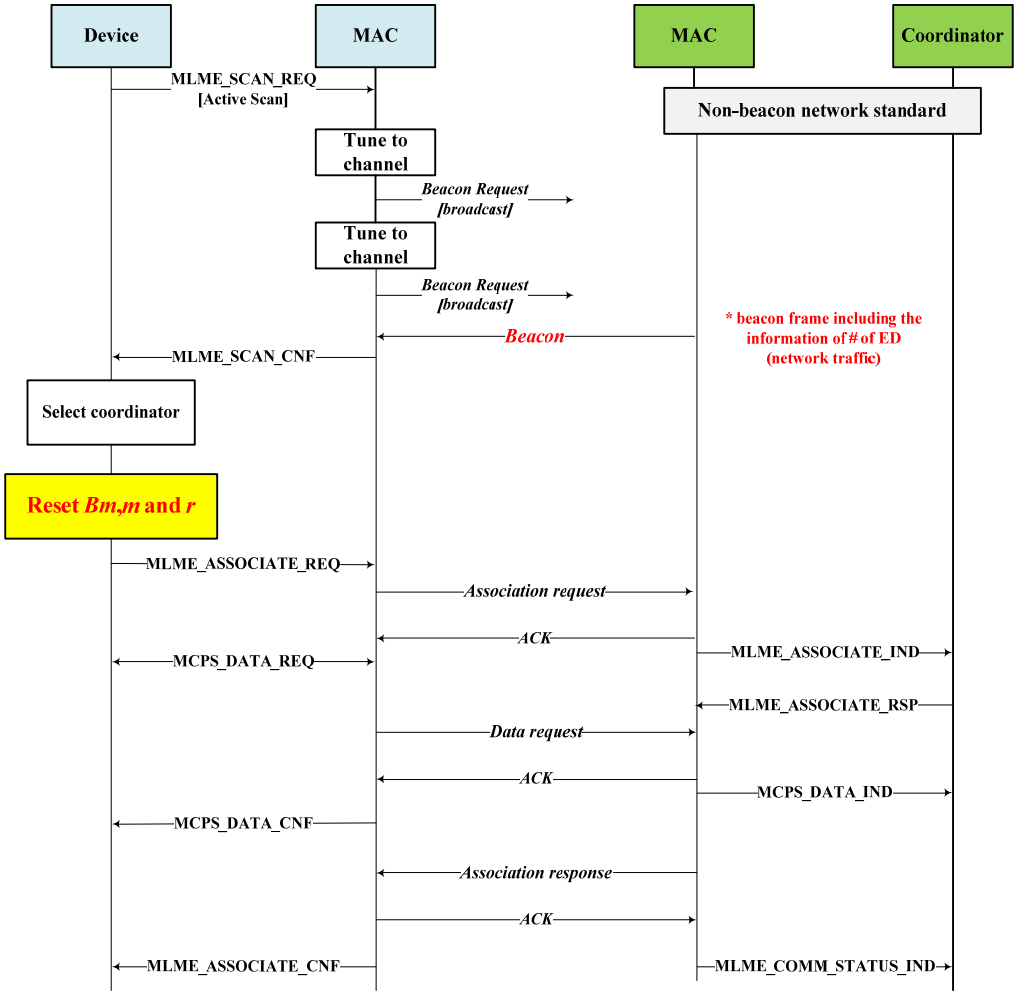


**Figure 7.7** Modified association network flow for priority data transmission.

The higher layer of a device checks the PAN descriptors and selects a coordinator. After choosing the coordinator, a node sends an *Association request* frame to the coordinator. Then the coordinator sends to the currently connected node the information that depends on the network address generated by the network protocol. At this step, the coordinator arranges and gives the short address to the currently connected node. From

these processes, the PAN coordinator can recognize how many devices are associated with it.

Also, during the communication process between a coordinator and nodes, the former can recognize the latter by several communication packet parameters. It can detect the address parameter of each device by MLME_ASSOCIATE and MCPS_DATA process parameter values.

Because a coordinator can know how many nodes join itself, it can estimate the network status. In our proposed scenario, if some nodes request the beacon to join the PAN, the coordinator sends the beacon frame with network status on the frame using the Frame Control Field (FCF) as shown in Figure 7.8.

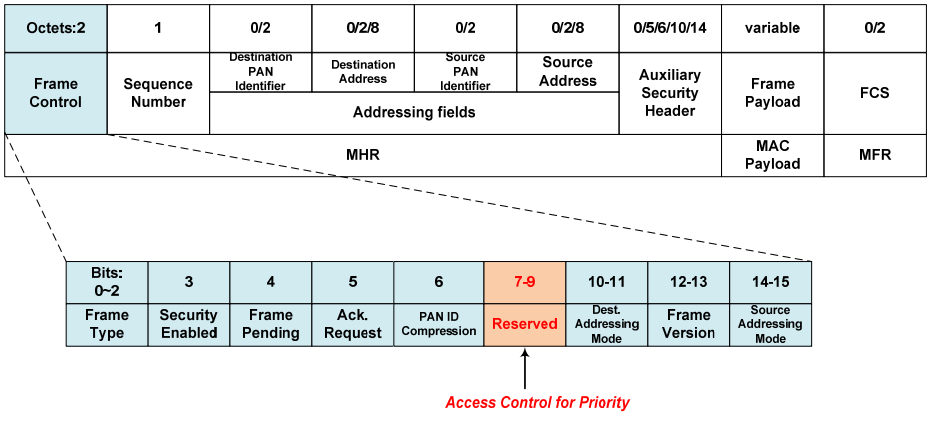


**Figure 7.8** Frame Control Field (FCF).

MAC header's (MHR) Frame Control is 2 bytes long and contains information defining the frame type, addressing field, and other control flags. The reserved field has 3 bits, i.e., bits 7 to 9. The algorithm proposed in this work uses the reserved field to show variable network status. After a node receives a beacon frame from a coordinator about

network status, it can decide to reset its *BE* value to avoid collision; or to associate to that coordinator or scan other available coordinators.

To decide the status of a coordinator, a device checks the reserved field in FCF. These bits predefined by a coordinator indicate the current status. A device sets $B_m$ accordingly.

By setting it differently for network traffic, it can reduce the transmission delay and data packet collision. Note that the IEEE 802.15.4 standard does not consider different network status and set $B_m$ to be 3 for all network devices. Figure 7.9 shows the proposed algorithm for priority packet transmission. It presents two parts of the algorithm. The first part is about realignment parameters (***$B_m$, $B_M$,*** and ***m)*** based on the network status.

Before a device is associated with a coordinator, it can recognize the network status, i.e., the number of devices in a same PAN, by checking the 3-bit reserved field at FCF in a beacon frame from the coordinator. From Table 7.3, the network status information to the 3-bit reserved field at FCF in beacon, i.e., 0x001 as $N < 5$, 0x010 as $5 \leq N < 10$, and 0x011 as $10 \leq N$ is applied.

**Table 7.3** Reserved Fields in FCF

| Command Frame | Nodes in PAN |
|---|---|
| 0x001 | $N < 5$ |
| 0x010 | $5 \leq N < 10$ |
| 0x011 | $10 \leq N$ |

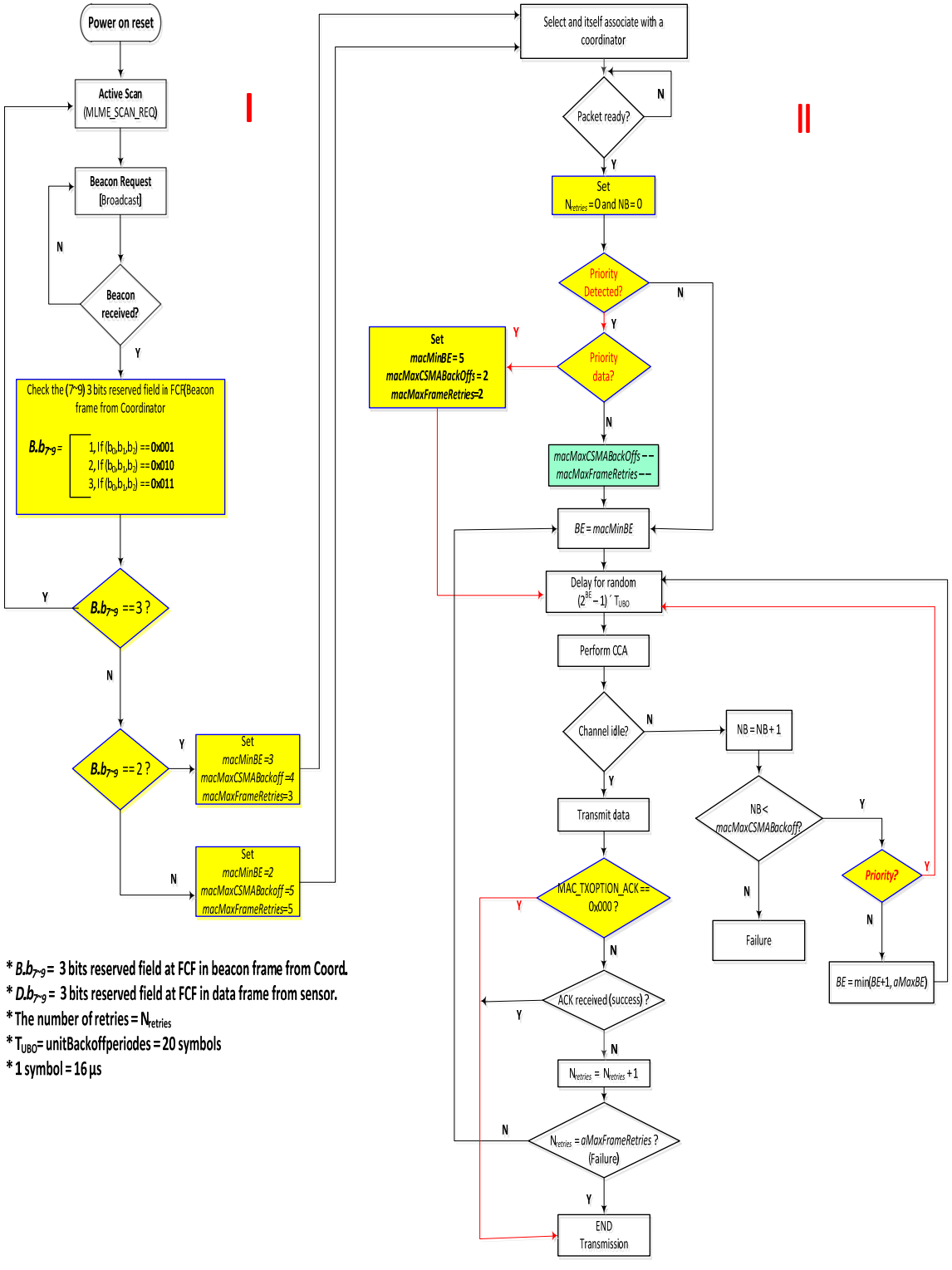


**Figure 7.9** Proposed algorithm for priority packet transmission.

If the current network has a relatively large size, i.e., $N > 10$, or many network devices are already in the PAN, a device would stop associating itself to that coordinator but look for another. If the number of already joined devices is more than 5, but less than 10, a device sets the MAC parameters as default value. If it is less than 5, the device sets adaptive MAC parameters. These different values are considered on the analyzed result from Chapters 4 and 5 for proper network performance.

### 7.3.2 Adaptive MAC Parameter for Priority Data

The second part of Figure 7.9 is about adaptive parameters for priority data in a network device. If a data packet is ready in a network device, MAC initializes *Retries* and *NB* values as "0". Device MAC layer checks FCF to see if the data are of priority or normal. If it is a priority packet, MAC layer sets MAC parameters ($B_m$, $m$, $r$) properly for types of priority packet, and $B_m$ value remains for a priority packet till its whole transmission process is finished.

If a packet is checked as priority data, it sets the MAC parameters to be adapted for their application status. If a certain node is checked as normal data in this network area which has priority data transmission, MAC layer discount their parameters ($m$ and $r$). As decreasing the value of these parameters, back-off attempts after channel access failure and retransmission after packet collision are decreased. Therefore, it helps the node that has a priority packet transmit successfully. Normally, after channel access failure, default CSMA/CA increases the *BE* value. But priority data packet goes back to the next back-off stage without increasing the *BE* value. Keeping this value is better for reliable packet transmission, because this given value is adaptive for this priority packet transmission.

By applying the different parameter to different types of data transmission, i.e., priority or normal data, one can achieve the desired network reliability and real-time monitoring for more valuable data (e.g., real-time heart beat sound) than some periodic data (e.g., human temperature).

## 7.4 Simulation Results and Discussion

In this section the heart beat sound, temperature data and ECG communication under some conditions from a real module is analyzed by using Qualnet 5.0 simulation. For this simulation, the un-slotted CSMA/CA of the IEEE 802.15.4 protocol is developed using Qualnet 5.0. Based on the measurement results in Table 5, 117 bytes packet with 12 *ms* packet period, 22 bytes packet with 5 sec packet interval, and 117 bytes packet with 0.27 sec packet interval are applied to transmit heart beat sound, temperature or battery check data, and ECG data. By considering that people wear a sensor device, it can be decided to coordinate network devices as 1 m away from the floor.

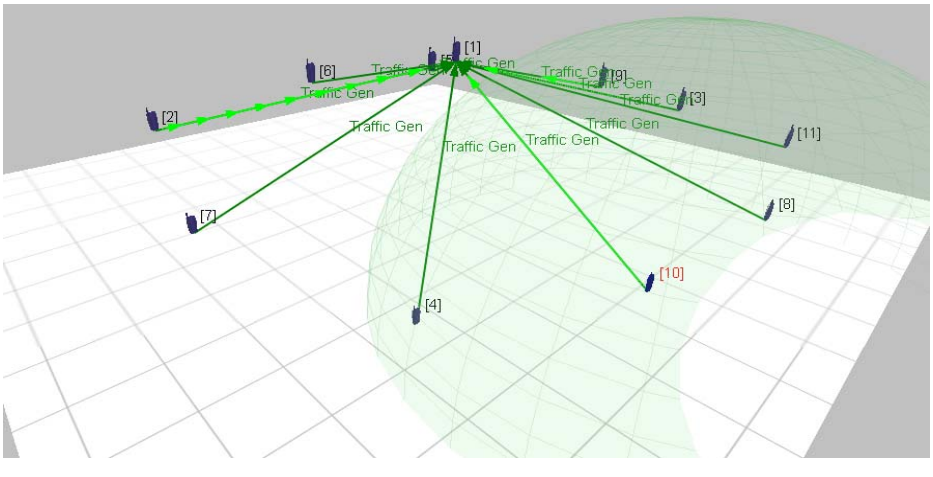


**Figure 7.10** Simulation scenario.

Table 7.4 shows the values of parameter used in this simulation scenario. CBR (constant bit rate) to Node 2, 6 and 7 is applied for continuous heart beat and ECG transmission. Also, Poisson process is applied to Nodes 3, 4 and 5 for temperature data transmission. Two ray path loss model and log normal shadowing are used for this scenario.

Figure 7.11 shows the comparison results of default and adaptive network scenarios. The simulation results of packet delivery ratio (PDR) and average end-to-end delay for priority data transmission are given in Figure 7.11.

From the results of simulation, it can be shown that PDR is below 80% for each node in a default scenario. This is due to packet loss and congestion when receiving packets from all nodes at the same time. Even if nodes 3, 4 and 5 send small data packets (each is 22 bytes long) as 5 sec packet period, their PDRs are just 61% and 70%. It can be realized that nodes 3 and 4 do not have enough chances to acquire the channel because node 2 is sending continuous large sound data and also nodes 6 and 7 are transmitting continuous ECG data to the coordinator. However, PDR of node 2 (heart beat sound) is just around 40%. It is because of that network traffic is heavy because of other nodes' transmission, especially continuous ECG communication. If this heart beat sound is from a patient in an emergency status, a doctor could not receive the correct heart beat sound. For this reason, it is proposed to treat this heart beat sound as a priority packet with the proposed algorithm as mentioned in Figure 7.9. From these simulation results, it can be shown that PDR of heart beat sound is almost doubled, i.e., 73% and average end-to-end delay decrease from 3.2 sec to 2.1 sec. However, other nodes' network performance

decreases based on the proposed algorithm. After emergency data transmission, however, other node's performance can go back to its original status.

**Table 7.4** Simulation Scenario, Setup and Parameters

| **Parameter** | **Value** | |
|---|---|---|
| Num. of nodes | 1 FFD, 6 RFD | |
| Size of area | 50m × 50m × 5m | |
| Channel freq. and data rate | 2.4 GHz and 250kbps | |
| Transmission range | 35 meter | |
| Tx power | 0 dBm | |
| Path loss model | Two Ray Model and Log normal shadowing | |
| PHY and MAC model | IEEE 802.15.4 | |
| Num. of items and payload size | Node 2 | 117 bytes |
| | Node 3~5 | 22 bytes |
| | Node 6,7 | 117 bytes |
| BO, SO | 15/15 | Non-beacon mode |
| Simulation time | 10000 sec | |
| Node start time/ end time | Node2~7 | 5 sec/ until time out |
| Packet interval | Node2 | 12 ms (Heart beat sound) |
| | Node 3~5 | 5 sec (Temp.) |
| | Node 6,7 | 0.27 sec (ECG) |
| Position | Node 2~4 | 10 m from coordinator |
| Traffic type | CBR (Node 2,6,7) | Constant bit rate |
| | Poisson (Node 3,4,5) | Random packet size and interval |

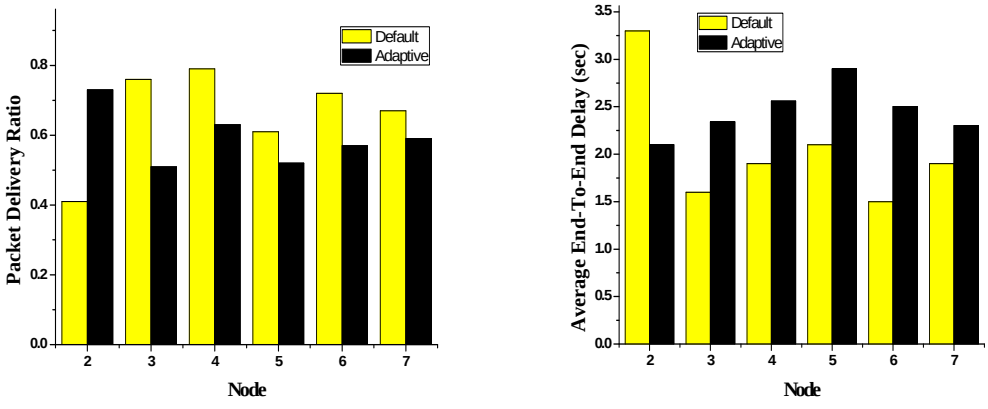


(a) (b)

**Figure 7.11** Comparison of default and adaptive network scenario.

## 7.5 Summary

In this dissertation, the healthcare wireless sensor networks constructed based on IEEE 802.15.4 standard is presented. Healthcare monitoring systems with both experiment and simulation are analyzed. From the simulation results, it can be shown that many data packets drop in each node, which is due to the failure based on CSMA-CA in the sensor to associate with the coordinator of the same network area. This causes nodes to drop the data packets during the transmission. Data size and length of a packet period are two critical factors for packet loss.

Other factors need to be considered. For example, if the transmitted packets are to arrive at the same time at a coordinator, they could create data congestion at the coordinator and may cause lower coordinator throughput and longer delay in transmission time. This can affect energy consumption and packet loss at the sensor nodes.

For a realistic health care monitoring system, its packet loss and end-to-end delay of a packet should be considered. Also the real capacity of a sensor network for patient monitoring and adopt a priority protocol for emergency data processing and transmission should be estimated.

From the proposed algorithm for priority packet transmission, it can be shown that their network performance improves much. This proposed algorithm is helpful for the patients who have emergency situations.

# CHAPTER 8

# CONCLUSIONS AND FUTURE WORK

## 8.1 Conclusions

This doctoral dissertation presents the applications of wireless sensor networks for healthcare applications and investigates the issues and challenges related to the modeling, analysis and performance evaluation of IEEE 802.15.4 wireless communication networks.

In particular, the contributions of this dissertation are presented in four parts. First, the effects of back-off parameters with different network components (the number of network devices and size of data payload) on the performance of un-slotted CSMA/CA operation of a ZigBee MAC protocol are analyzed. Second, an analytical Markov chain model that describes the operation of IEEE 802.15.4 un-slotted CSMA/CA is proposed and analyzed. Third, the QoS parameters such as effective data rate, average end to end delay and packet delivery ratio (PDR) by different network parameters including size of payloads, network devices and data rate with different MAC parameters are simulated, especially, for continuous electrocardiogram (ECG) transmission. Fourth, the continuous heart beat sound and human temperature monitoring system using a TI CC2430 Zigbee module is experimented. The algorithm for priority packet transmission for a health monitoring system is proposed. In this chapter, main contribution of this dissertation is summarized and potential directions of future work are discussed.

## 8.2 Summary of Contributions

The contributions of this dissertation are summarized into the following aspects:

1. It provides a comprehensive survey of the state-of-the art in the area of sensor networks. Current technological advances in sensors, power efficient integrated circuits, and wireless transferring have allowed the development of miniature, lightweight, low-cost, and smart physiological sensor nodes. These sensor nodes have capacity of sensing, controlling, processing, and communication one or more vital signs. Furthermore, they can be used in wireless personal area networks (PANs) or wireless body sensor networks (BSNs) for health monitoring. Many studies were performed and/or are under way in order to develop flexible, reliable, secure, real-time, and power-efficient BSNs suitable for healthcare applications. This work reviews the applications of wireless sensor networks in the healthcare area and discusses the related issues and challenges. Bluetooth is designed for voice application and aims to replace short distance cabling. This kind of applications require just tens of meters network range with a few (1~2) Mbps network speeds. ZigBee intends to meet the needs of sensors and control devices for short message applications. It is designed for small data packet transmission with a lightweight and simple protocol stack in network devices. Because of their small data transmission and multi network devices, ZigBee does not need high network speed. Currently, it provides only 250 kbps data rate. Ultra wide band (UWB) provides high network speeds together with a robust communication using a broad spectrum of frequencies. It best suits for very short range networks. It provides high network speed up to 480 Mbps. Wireless fidelity (Wi-Fi) is very

popular as Wireless local area network (WLAN). It is developed to replace wired Ethernet cable used in a home or office. They provide maximum data rate up to 54 Mbps in an around 50 meter range. Clearly Bluetooth and ZigBee are suitable for low data rate applications with limited power source such as battery-operated sensor nodes or mobile devices. Low power consumption helps prolong a node's life time and reduce its size. On the other hand, UWB and Wi-Fi would be better selections for high data rate applications such as audio/video multimedia appliance. As for power consumption, a ZigBee node can operate at low power for a time period ranging from several months to 2 years from two AA batteries. However, a Bluetooth node running on the same batteries would last just one week. ZigBee networks can support a larger number of devices and a longer range between devices than Bluetooth ones. ZigBee supports the configuration of static and dynamic star networks, a peer to peer network, and mesh network that can provide up to 65000 nodes in a network. Bluetooth allows only eights nodes in a master-slave piconet figure.

2. The effects of back-off parameters with different network environments, such as the number of network devices and size of data payload, on the performance of un-slotted CSMA/CA operation of a ZigBee MAC protocol are in detail analyzed. The back-off exponent *BE* is a critical parameter in the back-off algorithm of CSMA-CA. It is used as an estimate of the random back-off delay before trying to access the channel. The back-off delay time is determined by a random number from 0 ~ ($2^{BE}$ -1) multiplied by *aUnitBackoffPeriod*. Total back-off time for channel access and data transmission is sum of all back-off attempt times. The

number of average back-off attempts under different network environments such as network size, packet size and IEEE 802.15.4 MAC parameters has been derived. From this result, total back-off time periods for different network environments can be predicted.

3. A generalized Markov chain model that describes the IEEE 802.15.4 un-slotted CSMA/CA is proposed. In contrast to the previous work, the presence of limited number of packet retransmissions, acknowledgements, unsaturated traffic and packet generation rate are all considered in the model. Reliability, average end-to-end delay and energy consumption of the network by varying network parameters including payload size, packet arrival rate, and other protocol parameters are analyzed. IEEE 802.15.4 standard recommends default values for different MAC parameters. Originally, IEEE 802.15.4/ZigBee is designed for low-data rate and saturated data communication. Thus, CSMA MAC parameters are specified for such network situations. Since wireless health monitoring systems have characteristics different from the original purpose of IEEE 802.15.4/ZigBee, the configuration of IEEE 802.15.4 MAC parameters should be considered in order to better suit the new network environments. The impact of CSMA/CA MAC parameters is thus studied on the performance of IEEE 802.15.4 MAC layer under different network environments. Health monitoring applications require reliable and correct packet transmission. The network performance is evaluated in terms of the reliability and average delay. A better set of MAC parameters for different network environments are obtained via simulation studies to achieve high reliability and low average packet transmission delay.

4. Simulation-based performance analysis of QoS for a real time ECG monitoring system based on an IEEE 802.15.4 star network is conducted. The impact of different payload size with packet interval up to normal ECG data rate is analyzed and simulated. The best packet interval and MSDU for normal ECG data rate are obtained. It can be found that larger payload size and longer packet interval at the same data rate can improve the network performance. Effective data rate, PDR and end-to-end delay for QoS of ECG transmission are then analyzed and simulated. As an important contribution, we recognize that the default parameters from IEEE 802.15.4 standard are not always suitable for the best QoS. As a result, some CSMA/CA parameters should be changed depending upon the different network scenarios such as periodic and continuous real time monitoring, small or large traffic loads and network size.
5. A continuous heart beat sound and human temperature monitoring system using a TI CC2430 Zigbee module is experimented and simulated. The algorithm for priority packet transmission for health monitoring system is proposed. In this proposed algorithm, two main protocols are introduced. One is that each node can select the base station for data transmission. Normally, if node is turned on for the data transmission, it tries to associate to the base station. However, if many nodes are already associated with one base station, the resulting network would be overflowed. Thus, the network size should be limited for reliable data transmission. As the base station broadcasts their network status, a node can join a less trafficked network. An algorithm is proposed to allow priority data, such as emergency data, to have more chances to transmit than other nodes. Based on this

algorithm, the simulation result in terms of PDR and average End-to-End delay is obtained. It is concluded that the network performance by using the modified CSMA/CA protocol is better than the original CSMA/CA protocol.

## 8.3 Recommendations for Future Research

There are several ways in which this dissertation work can be extended in the future. Some important and promising directions are described as follows:

1. In this work, mobility of sensor nodes and interference from other sources are not considered. Because patients can move around with their bio-sensing units, mobility of sensor nodes can affect the reliable data transmission. Also, if these sensor nodes are used in the hospital, they could be interfered by other medical equipments. For more reliable data transmission for a health monitoring system, these two factors should be researched.
2. In addition to the efforts with performance improvement, future research needs to perform better power management to prolong the entire network lifetime. Power management is a critical issue to most applications of wireless sensor networks for long-term healthcare. Especially, this management is really needed in the cases where continuous real-time monitoring is required for elderly people or critical patients. Some power saving strategies, such as putting a node into a sleep mode, can provide possible solutions for some network situations. However, such sleep mode is not suitable for continuous data transmission. Therefore, rather than using a sleep mode, lightweight MAC protocol or less-power consuming hardware is required. Next research objectives include the investigation of the different platforms that provide an

advanced architecture for a reliable and long-term power source applicable to wireless health monitoring systems.

## REFERENCES


[1] Akyildiz I. F., Su W., Sankarasubramaniam Y., and Cayirci E., “Wireless Sensor Networks: a Survey,” *Computer Networks*, vol. 38, pp. 393-422, 2002.

[2] Bae, D. J., Lee, T. J., Choi, H. K., and Chung, M. Y., “A contention access mechanism based on a partitioned contention access period in IEEE 802.15.4 MAC,” *IEICE TRANS. COMMUN*., vol.E93-B, no.12, Dec 2010.

[3] Barth, A.T., Hanson, M.A., Powell Jr., H.C., and Lach, J., " TEMPO 3.1: A body area sensor network platform for continuous movement assessment," *6th International Workshop on Wearable and Implantable Body Sensor Networks*, *BSN* 2009, Article number 5226915, Pages 71-76 **,** Berkeley, CA, 2009

[4] Bianchi, G., “Performance analysis of the IEEE 802.11 distributed coordination function,” *IEEE Journal on Selected Areas in Communications*, vol.18, no. 3, pp. 535-547, 2000.

[5] Brown L., Grundlhner B., Penders J., and Gyselinckx B., “Body Area Network for Monitoring Autonomic Nervous System Responses,” *2009 3rd International Conference on Pervasive Computing Technologies for Healthcare - Pervasive Health 2009,* Article number 5173603, April 2009.

[6] Burchfield, T. R., Venkatesan, S., and Einer, D., “Maximizing throughput in Zigbee wireless networks through analysis, simulations and implementations,” *In Proc. of the Int. Workshop on Localized Algorithms and Protocols for Wireless Sensor Networks,* pp.15-29, Santa Fe, New Mexico, June 18-20, 2007.

[7] Chai J., and Yang H., “The research of the community healthcare network based on ZigBee technology,” *7th Asian-Pacific Conference on Medical and Biological Engineering*, vol.19, pp. 567-570, Beijing, China,April 2008.

[8] Chen Y., and Wang X., "Design of Distributed Intelligent physiological parameter Monitor System Based on Wireless Communication Technology," *International Seminar on Future BioMedical Information Engineering,* pp.403-406,Wuhan, Hubei, Dec 2008.

[9] Chien R., and Tai C., "A New Wireless-Type Physiological Signal Measuring System Using a PDA and the Bluetooth Technology," *IEEE International Conference on Industrial Technology*, pp.119–120, Mumbai, Dec 2006.

[10] Choi S., Cha H., and Cho S., " A Soc-based Sensor Node: Evaluation of RETOS-enabled CC2430," *4th Annual IEEE Communications Society Conference on Sensor,*

*Mesh and Ad Hoc Communications and Networks, SECON 2007*, Article number 4292825, Pages 132-141, San Diego, CA, 2007.

[11] Choi, Jin Soo and Zhou, Mengchu, "Performance analysis of ZigBee-based body sensor networks," *IEEE International Conference on Systems Man and Cybernetics* (SMC), Istanbul, Turkey, pp. 2427-2433, October 2010.

[12] Choi, Jin Soo and Zhou, Mengchu, "Recent Advances in Wireless Sensor Networks for Health Monitoring," *International Journal of Intelligent Control and Systems*, Vol. 15, No. 4, pp. 49-58, December 2010.

[13] Choi K., and Song J., "A Miniaturized Mote for Wireless Sensor Networks," *International Conference on Advanced Communication Technology, ICACT* ,Vol 1, Article number 4493814, Pages 514-516, Korea, Feb 2008.

[14] Dagtas S., Pekhteryev G., and Sahinoglu Z., "Multi-stage Real Time Health Monitoring via ZigBee in Smart Homes," *Proceedings of the 21st International Conference on Advanced Information Networking and Applications Workshops,* Vol.2, pp. 782-786, Niagara Falls, Ont, May 2007.

[15] Daneshgaran F., Laddomada M., Mesiti F., and Mondin M., "Unsaturated Throughput Analysis of IEEE 802.11 in Presence of Non Ideal Transmission Channel and Capture Effects," *IEEE Transactions on Wireless Communications*, vol.7, pp. 1276-1286, April. 2008.

[16] Estrin D., "Embedded Networked Sensing Research: Emerging System Challenges," *in NSF Workshop on Distributed Communications and Signal Processing for Sensor Networks*, Illinois, USA, 2002.

[17] Feng W., Arumugam N., and Krishna G. H., "Impact of interference on a Bluetooth network in the 2.4 GHz ISM band," *The 8th International Conference on Communication Systems*, Vol. 2, pp. 820 - 823, Singapore, Nov. 2002.

[18] Fensli R., Gunnarson E., and Gundersen T., "A wearable ECG-recording system for continuous arrhythmia monitoring in a wireless tele-homecare situation," *Proc.of the 18th IEEE Symposium on Computer-Based Medical Systems,* pp. 407-412, Ireland, June 2005.

[19] Guo W. W., Healy W. M., and Zhou M., "An Experimental Study of Interference Impacts on ZigBee-based Wireless Communication Inside Buildings," *In Proceedings of 2010 IEEE International Conference on Mechatronics and Automation (ICMA 2010)*, pp. 1982-1987, Xi'an, China, August 4-7, 2010.

[20] Gyselinckx B., Penders J., and Vullers R., "Potential and challenges of body area networks for cardiac monitoring," *J. Electrocardiology*, vol. 40, pp. S165–S168, Nov, 2007.

[21] Heart Attack http://www.medicinenet.com , accessed date: Jan 2010

[22] Hande A., Polk T., Walker W., and Bhatia D., "Indoor solar energy harvesting for sensor network router nodes," *Microprocessor and Microsystems*, Volume 31, Issue 6, Pages 420-432, Sept. 2007.

[23] Howitt I., "WLAN and WPAN coexistence in UL band," *IEEE Transactions on Vehicular Technology*, Vol. 50, No. 4, pp. 1114 - 1124, July 2001.

[24] Hauer J., Handziski V., and Wolisz A., "Experimental Study of the Impact of WLAN Interference on IEEE 802.15.4 Body Area Networks," *Proceedings of the 6th European Conference on Wireless Sensor Networks*, pp, 17-32, Cork, Ireland, February 2009.

[25] Hackmann G. 2006 "*802.15 Personal Area Networks*," Department of Computer Science and Engineering, Washington University. http://www.cse.wustl.edu/~jain/cse574-06/wpans.htm accessed date: Feb 2010.

[26] Hyun L. *et al*., "Issues in data fusion for healthcare monitoring," *Proceedings of the 1st International Conference on Pervasive Technologies Related to Assistive Environments,* Vol.282, pp.1-8, Athens, Greece, July 2008.

[27] IEEE, Wireless medium access control (MAC) and physical layer (PHY) specifications for low-rate wireless personal area networks (WPANs)," *IEEE Std. 802.15.4-2006*, 2006.

[28] Ilyas, M., and Mahgoub, I., *Handbook of Sensor Networks: Compact Wireless and Wired Sensing Systems*, Boca Raton, CA: CRC, 2005.

[29] Jovanov E., Milenkovic A., Otto C., Groen P. D., Johnson B, Warren S, and Taibi G, "A WBAN System for Ambulatory Monitoring of Physical Activity and Health Status: Applications and Challenges," *IEEE-EMBS 2005, 27th Annual International Conference*, pp. 3810 - 3813, Shanghai, China, Jan 2005.

[30] Jo J.H., and Jayant N., "Performance Evaluation of Multiple IEEE 802.11b WLAN Stations in the Presence of Bluetooth Radio Interference," *IEEE Journal on Communications*, vol. 2, pp. 1163-1168, May 2003.

[31] Jung, C. Y., Hwang, H. Y., Sung, D. K., Hwang, G. U., "Enhanced Markov chain model and throughput analysis of the slotted CSMA/CA for IEEE 802.15.4 under unsaturated traffic conditions," *IEEE Transactions on Vehicular Technology*, 58(1):473-478, 2009.

[32] Juyng J., and Lee J.,"ZigBee Device Access Control and Reliable Data Transmission in ZigBee Based Health Monitoring System," *10th International Conference on*

*Advanced Communication Technology,* Vol. 1, 17-20, pp.795 – 797, Gangwon, Korea, Feb. 2008.

[33] Kang M. *et al*., "Adaptive Interference-Aware Multi-Channel Clustering Algorithm in a ZigBee Network in the Presence of WLAN Interference," *Proc. of the International Symposium on Wireless Pervasive Computing,* pp.5-7, San Juan, Puerto Rico, Feb. 2007.

[34] Khemapech I., Duncan I., and Miller A., "A Survey of Wireless Sensor Networks Technology," *Proceedings of the 6th Annual PostGraduate Symposium on the Convergence of Telecommunications, Networking & Broadcasting*, Liverpool John Moores University, Liverpool, 2005.

[35] Kim, E. J., Shon, T., Park, J., and Jeong, Y.S., "Throughput Fairness Enhancement Using Differentiated Channel Access in Heterogeneous Sensor Networks," *Sensors* 2011, *11*(7), 6629-6644; doi:10.3390/s110706629.

[36] Kim, T. O., Park, J. S., Chong, H. J., Kim, K. J, and Choi, B. D., "Performance Analysis of IEEE 802.15.4 Non-beacon Mode with Unslotted CSMA/CA," *IEEE Communications Letters*, pp.238-240, April 2008.

[37] Kim S. M., Chong J. W., Jung C. Y., Jeon T. H., Park J. H., Kang Y. J., Jeong S. H., Kim M. J., and Sung D. K., "Experiments on Interference and Coexistence between Zigbee and WLAN Devices Operating in the 2.4 GHz ISM Band," *Proc. NGPC*, pp. 15 - 19, Nov 2005.

[38] Kohvakka, M., Kuorilehto, M., Hannikainen, M., and Hamalainen, T.D., "Performance analysis of IEEE 802.15.4 and ZigBee for large-scale wireless sensor network applications," *Proc. 3rd ACM Int. Workshop on Performance Evaluation of Wireless Ad Hoc, Sensor, and Ubiquitous Networks*, Terromolinos, Spain, Page 48-57, 2006.

[39] Lee, B. H, Lai, R. L., Wu, H. K., and Wong, C. M., "Study on Additional Carrier Sensing for IEEE 802.15.4 Wireless Sensor Networks," *Sensors* 2010, *10*(7), 6275-6289; doi:10.3390/s100706275.

[40] Lee J. S., Su Y. W., and Shen C. "A comparative study of wireless protocols: bluetooth, uwb, zigbee, and wi-fi," *Proceedings of The 33rd Annual Conference of the IEEE Industrial Electronics Society (IECON)*, pp. 46-51,Taipei, Nov. 2007.

[41] Lee D.S., Lee Y.D., Chung W.Y., and Myllyla R., "Vital Sign Monitoring System with Life Emergency Event Detection using Wireless Sensor Network," *5th IEEE Conference on Sensors*, Daegu, South Korea, pp. 518-521, 2006.

[42] Malan, D., Fulford-Jones, T., Welsh, M., and Moulton, S., "Codeblue: an ad-hoc sensor network infrastructure for emergency medical care," *in Proc. of the 1st Int. Workshop on Wearable and Implantable Body Sensor Networks*, London, UK, 2004.

[43] Mangharam, R., Rowe, A., Rajkumar, R., and Suzki, R., "Voice over sensor networks," In *Proc. of the 27th IEEE Int. Real-Time Systems Symposium*, Rio de Janeiro, Brazil, 2006.

[44] Milenkovic A., Otto C., and Jovanov E., "Wireless sensor networks for personal health monitoring: Issues and an implementation," *Computer Communications*, vol. 29, pp. 2521-2533, 2006.

[45] Miller M.J., and Vaidya N.H., "A MAC protocol to reduce sensor network energy consumption using a wakeup radio," *IEEE Transactions on Mobile Computing,* 4(3), Page(s):228 – 242, May-June 2005.

[46] Misic, J., and Misic, V. B. "Access delay for nodes with finite buffers in IEEE 802.15.4 beacon enabled PAN with uplink transmissions," *Comput. Commun.*, vol. 28(10), pp. 1152-1166, Jun. 2005.

[47] Misic, J., Shafi, S., and Misic, V. B., "Performance of a Beacon Enabled IEEE 802.15.4 Cluster with Downlink and Uplink Traffic," *IEEE Transactions on Parallel and Distributed Systems*, pp. 361-376, April 2006.

[48] Monton E., Hernandez J. F., Blasco J. M., Herve T., Micallef J., Grech I, Brincat A, and Traver V, "Body area network for wireless patient monitoring," *Telemed. E-Health Commun. Syst.*, vol. 2, issue 2, pp. 215–222, Feb. 2008.

[49] Ning X., Rangwala, S., Chintalapudi, K. K., Ganesan, D., Alan Broad, Govindan, R, and Estrin, D., "A wireless sensor network for structural monitoring," *Proceedings of the 2nd international conference on Embedded network sensor systems SenSys 04*, Vol.20, Issue:7, pp.12-24, Baltimore, MD, USA, Nov. 2004.

[50] Omeni O., Eljamaly O., and Burdett A., "Energy Efficient Medium Access Protocol for Wireless Medical Body Area Sensor Networks," *Proc. IEEE-EMBS Symposium on Medical Devices and Biosensors*, pp. 29-32, Cambridge, UK, Aug 2007.

[51] Oliver N., and Flores Msngas F., "HealthGear: A real-time wearable system for monitoring and analyzing physiological signals," Microsoft Res., Tech. Rep. MSR-TR-2005-182, Apr. 2006.

[52] Pakzad, S. Z., Fenves, G. L., Kim, S., and Culler, D. E., "Design and Implementation of Scalable Wireless Sensor Network for Structural Monitoring," *Journal of Infrastructure Systems*, Vol. 14, Issue:1, pp. 89-101, 2008.

[53] Paradiso J.A., and Starner T., "Energy scavenging for mobile and wireless electronics," *Pervasive Computing, IEEE 2005*, Volume 4, Issue 1, Pages: 18-27, 2005.

[54] Park, T. R., Kim, T. H., Choi, J. Y., Choi, S., and Kwon, W. H., "Throughput and energy consumption analysis of IEEE 802.15.4 slotted CSMA/CA," *Electron. Lett.*, vol. 41, pp. 1017, 2005.

[55] Park, P., Di Marco, P., Soldati, P., Fischione, C., and Johansson, K.H., "A Generalized Markov Chain Model for Effective Analysis of slotted IEEE 802.15.4," *Mobile Adhoc and Sensor System*, *IEEE 6th International Conference*," Macau, pp. 130-139, 2009.

[56] Pollin S., Ergen M., Ergen S. C., Bougard B., Perre L.V., Moerman I., Bahai A., Varaiya P. and Catthoor F., "Performance Analysis of Slotted Carrier Sense IEEE 802.15.4 Medium Access Layer," *IEEE Transactions on Wireless Communication*, vol. 7, no. 9, pp. 3359-3371, 2008.

[57] Pollin S., Ergen M., Ergen S. C., Bougard B., Catthoor F., Bahai A., and, Varaiya P., "Performance Analysis of Slotted Carrier Sense IEEE 802.15.4 acknowledged uplink transmissions," *in Proc. of IEEE WCNC*, pp. 1559-1564, Las Vegas, NV, March, 2008.

[58] Razvan Musaloiu-Elefteri, Andreas Terzis, "Minimizing the effect of WiFi interference in 82.15.4 wireless sensor networks," *IJSNet* 3(1), p.p. 43-54, 2008.

[59] RFID Handbook: Fundamentals and Applications in Contactless Smart Cards and Identification 2nd Edition, Wiley, 2003, Hoboken, NJ.

[60] Roundy S., and Wright P.K., "A Piezoelectric Vibration Based Generator for Wireless Electronics," *Smart Materials and Structures*, 13, pp. 1131–1142, 2004.

[61] Ramakrishnan S., Huang H., Balakrishnan M., and Mullen J., "Impact of sleep in wireless sensor MAC protocol," *IEEE Vehicular Technology Conference*, vol. 7, pp. 4621-4624, Los Angeles, CA. September 2004.

[62] Rajiv C., "Mobicare: A Programmable Service Architecture for Mobile Medical Care," *4th Annual IEEE International Conference on Pervasive Computing and Communications Workshops, PerCom Workshops 2006*, Vol. 2006, pp. 532-536, Pisa, Italy, March 2006.

[63] Sahoo, P. K., and Sheu, Jang. P., "Modeling IEEE 802.15.4 based Wireless Sensor Network with Packet Retry Limits," *Proceedings of the 5th ACM symposium on Performance evaluation of wireless ad hoc, sensor, and ubiquitous networks*, pp. 63-70, ACM, NY, 2008.

[64] Sakal I., and Simunic D., "Simulation of interference between Bluetooth and 802.11b systems," *EEE International Symposium on Electromagnetic Compatibility*, Vol. 2, pp. 1321 - 1324, Istanbul, Turkey, May 2003.

[65] Stark I., "Invited Talk: Thermal Energy Harvesting with Thermo Life," *Proceedings of the International Workshop on Wearable and Implantable Body Sensor Networks, BSN 2006*, pp. 19-22, Boston, USA, April 2006.

[66] Tony S., Ling C., Chih H., Guang Y., and Mario G., "Measuring Effective Capacity of IEEE 802.15.4 Beaconless Mode," in *Proc. of IEEE Wireless Communications and Networking Conference*, Volume 1, pp. 493-498, Las Vegas, NV, April, 2006.

[67] Tijs van Dam, and Koen Langendoen, "An adaptive energy-efficient MAC protocol for wireless sensor networks," *Proceedings of the 1st international conference on Embedded networked sensor systems*, Pages: 171 – 180, Los Angeles, CA, Nov. 2003.

[68] U.S. Census Bureau, Projections of the Population by Selected Age Group and Sex for the United States: 2010 to 2050. www.census.gov/population/www/projections/summarytable.html , accessed date: May 2010.

[69] Varshney U., "Pervasive healthcare and wireless health monitoring," *Mobile Networks and Application*, 12(2-3), pp.113-127, 2007.

[70] Wang, F., Li, D., and Zhao, Y., "Analysis and Comparison of Slotted and Unslotted CSMA in IEEE 802.15.4," in *Proc. of 2009 Int. Conf. on Wireless Communications, Networking and Mobile Computing*, pp. 1-5, Beijing, China, Sept. 2009.

[71] Wang, F., Li, D., and Zhao, Y., "On Analysis of the Contention Access Period of IEEE 802.15.4 MAC and its Improvement," *WIRELESS PERSONAL COMMUNICATION*, DOI: 10.1007/s11277-011-0321-8.

[72] Wang B., *et all*., "A Body Sensor Networks Development Platform for Pervasive Healthcare," *3rd International Conference on Bioinformatics and Biomedical Engineering*, Volume , Issue ,11-13, pp.1 – 4, Beijing, China, June 2009.

[73] Wijetunge, S., Gunawardana, U., and Liyanapathirana, R., "Wireless Sensor Networks for Structural Health Monitoring: Considerations for communication protocol design," *IEEE 17th International Conference on Telecommunications (ICT)*, pp.694-699, Doha, Qatar, April. 2010.

[74] Willig A., Matheus K., and Wolisz A., "Wireless technology in industrial networks," *Proc. of the IEEE*, 93(6), pp. 1130-1151, June 2005.

[75] Yang G., and Yu Y., "ZigBee networks performance under WLAN 802.11b/g interference," *Proceedings of the 4th international conference on Wireless pervasive computing,* pp.337-340, Melbourne, VIC, Feb. 2009.

[76] Yan, C., and Chung, W.Y., "IEEE 802.15.4 Wireless Mobile Application for Healthcare system," *International Confer-ence on Convergence Information Technology, ICCIT 2007*, Article number 4420456, pp.1433-1438, Gyeongju, Korea, Nov. 2007.

[77] Zhai H., and Fang Y., "Physical Carrier Sensing and Spatial Reuse in Multirate and Multihop Wireless Ad Hoc Networks," *In Proceedings of the 25th IEEE International Conference on Computer Communications*, pp. 1-12, Barcelona, Spain, April. 2006.

[78] Zhang J., Li W., Xia Z., Wang G., and Wan Z., " The Implementation of Communication for CC2430-Based wireless Sensor Network Nodes," *5th International Conference on Wireless Communications, Networking and Mobile Computing, WiCom '09*, pp. 1-4, Beijing, China, Sept. 2009.

[79] Zheng, T., Radhakrishnan, S., Sarangan, V., "PMAC: an adaptive energy-efficient MAC protocol for wireless sensor networks," *Proceedings of the 19th IEEE International Parallel and Distributed Processing Symposium (IPDPS'05) - Workshop 12,* Page(s):8 pp, Denver, Colorado, April 04-08, 2005.

[80] Zixue Qiu, Jian Wu, and Shenfang Yuan, "A wireless sensor network design and evaluation for large structural strain field monitoring," *Measurement Science and Technology (IOP Science),* Volume 22, Number 7, 075205, 2011.